Electric Technology U.S.S.R.

ЭЛЕКТРИЧЕСТВО

Volume 4, 1961

Selected papers from
Elektrichestvo Nos. 10, 11 and 12, 1961

olished by

RGAMON PRESS NEW YORK LONDON OXFORD PARIS

for Pergamon Institute, Washington and Oxfor

Published May 1962

ELECTRIC TECHNOLOGY, U.S.S.R.

PERGAMON INSTITUTE

A DIVISION OF PERGAMON INTERNATIONAL CORPORATION, OPERATED IN THE PUBLIC SERVICE FOR THE FURTHERANCE AND DISSEMINATION OF SCIENTIFIC KNOWLEDGE

President of the Scientific Advisory Council:
Sir Robert Robinson, O.M., F.R.S.

Executive Director: Captain I. R. Maxwell, M.C.

122 *East 55th Street New York* 22, *N.Y.* (*Telephone No. Plaza* 39651).

Headington Hill Hall, OXFORD. (*Telephone No. Oxford* 64881)

Pergamon Institute can occasionally use additional translators for science and engineering material to assist with this programme of translation from Russian and other Slavonic languages.

Scientists and engineers who have a knowledge of Russian, and who are willing to assist with this work, should apply to the Administrative Secretary of the Institute. They should write to New York or Oxford for rates of payment and other details.

Four volumes per annum. Approximately 700 pages per annum.
Annual Subscription Rate £20 ($60).
Single volumes may be purchased for £6 ($14).

Orders should be sent to the distributors at either of the following addresses

Headington Hill Hall, Oxford
122 East 55th Street, New York 22, N.Y.

PUBLISHED BY

PERGAMON PRESS LTD.

NEW YORK · LONDON · OXFORD · PARIS

May 1962

CONTACTLESS CONTROL OF ELECTRIC COACHES*

I.B. BASHUK and A.I. KHOMENKO

(Moscow Institute of Railway Transport Engineers)

(Received 24 June 1961)

A disadvantage of electric drives controlled by relays and contactors is the unreliability of the contacts, due to their wear, oxidation, contamination etc. This disadvantage is particularly marked if the contacts are opened and closed with great frequency. It can however be overcome if contacts are completely eliminated from the control system. Until now this problem has only been solved by using magnetic amplifiers as relays. Yet these cannot always be used owing to the relatively large dimensions of the amplifiers.

The dimensions of control circuit elements can be considerably reduced for independent or group drives if the apparatus is "interlocked" by means of transistors which are controlled by electrical pickups (transducers) that produce output voltages as a function of the position of the control object.

Even the relays can be made quite small without contacts, and only small magnetic amplifiers are required for isolating the power circuit and control circuits and feeding the signals of trigger circuits to the transistors.

This allows the production of improved control systems for electric coaches based on principles which have not hitherto been used. The new units also improve the reliability and performance of a control system.

Electrical circuits can be switched on and off by transistors acting either as switches or as trigger circuits. Transistors can be controlled by signals from transducers without the use of contacts.

---

* *Elektrichestvo*, 10, 24-29, 1961.

In 1957 the authors of this paper patented [1] a contactless interlooking system which combined a transistor with a transducer. The rectified output voltage of the transducer was fed to the input to the transistor (see Fig. 1). The moving core of the transducer was mechanically coupled with the control object in such a way that in one working position the output voltage of the transducer was zero, whilst in the other position it was sufficient to change the "non-conducting" triode into the saturated state. The transistor switched the particular section of the control circuit "on" or "off" accordingly, and took the place of a normally closed or normally open blocking contact.

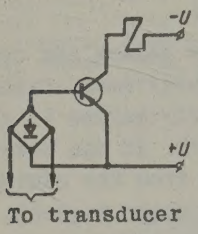

Fig. 1.

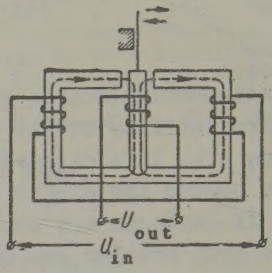

Fig. 2.

An alternative method is to use a trigger or "flip-flop" circuit to switch the circuit "on" and "off" by means of a signal from a transducer or some circuit element. Various types of design system are possible and these will now be considered.

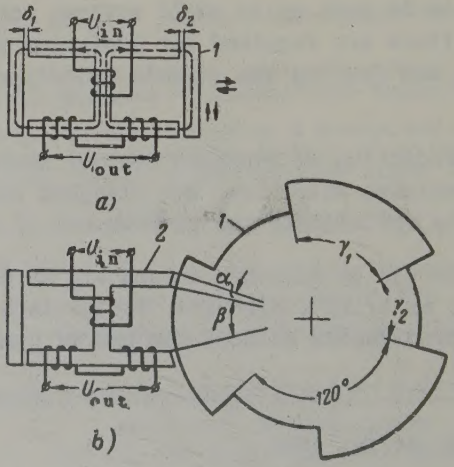

Fig. 3.

Different types of transducer can be used for controlling the transistor or trigger circuit. A differential inductive transducer is illustrated in Fig. 2. In the middle position of the moving core the resultant magnetic flux there is zero and the output voltage is likewise zero. A variable voltage is produced at the output of the transducer when the moving core deviates from its middle position. This transducer can be made highly sensitive so that the triode can be changed from "on" to "off" (or vice versa) by the core moving tenths of a millimetre.

Figure 3*a* illustrates the circuit of a transducer which produces a zero output voltage if the air gaps δ_1 and δ_2 are the same. If the core *1* is moved in any of the directions indicated in Fig. 3*a*, the two gaps cease to be equal and a voltage is then produced at the output of the transducer. The merit of this device is the absence of "hinges".

The transducers shown in Figs. 2 and 3*a* are convenient for controlling contactors. For apparatus with a group drive, use may be made of the recently patented transducer circuit shown in Fig. 3*b*. Here the moving core *1* is a shaped steel disc with projections. This disc is coupled to the camshaft of the apparatus [2]. If one of the projections is opposite the fixed core 2, the output voltage of the transducer is zero. But if one of the recesses is opposite this fixed core, a voltage is produced at the output of the transducer.

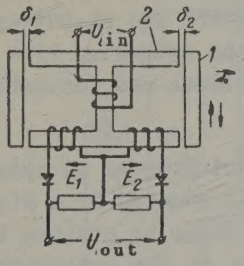

Fig. 5.

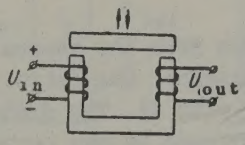

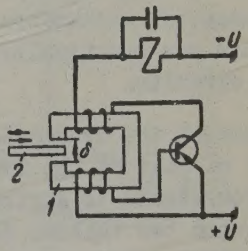

Fig. 6.

The number of projecting sections depends on the design of the group apparatus. The necessary relationship between the transducer output voltage and the angle of rotation of the disc (moving core) can be obtained by an appropriate choice of the angles α, β, γ_1 and γ_2.

If it is required to produce an output voltage which reverses polarity, use may be made of the device shown in Fig. 4. This is made so that δ_1 is greater than δ_2 if the moving core *1* is opposite the fixed core 2. The e.m.f. E_2 of the output winding then becomes greater than E_1 and the rectified output voltage is the same in polarity. The polarity of the output voltage is reversed when the e.m.f. E_2 decreases on movement

of core *1*.

An alternating input voltage can be obtained from a transistorized inverter for such transducers.

The device shown in Fig. 5 may be used to control a trigger circuit. Movement of the core produces a voltage pulse at the output. The polarity of this pulse depends on the direction in which the core moves. However, the amplitude of the output voltage of this particular device depends on the speed with which the core moves. If the control object changes position at a reduced speed for one reason or another, the trigger circuit cannot be "changed over".

Figure 6 illustrates the circuit of a device which generates relaxation oscillations provided that the gain feedback factor is positive and much greater than one. The core *1* is made from ferrite material. When disc 2, which is made of conducting material, enters the air gap δ, the oscillations are damped and the current in the load circuit is reduced to zero. Unfortunately it is a complicated matter to ensure sharply defined attenuation of the oscillations and to resume oscillations under all operating conditions.

The system of contactless interlocking shown in Fig. 1 (employing a P4-P-type transistor and the transducer illustrated in Fig. 2) has been tested on PK-301A-type electro-pneumatic contactors and PK-504-type electromagnetic contactors. From test results the switching time of the contactors was practically the same for conventional and contactless control circuits.

To protect the transistors from the surges which occur on opening the coil circuit of the contactor, the latter is shunted by a diode with a resistance in series with it. The diode tends to prolong the time between the initial decrease in the current in the contactor coil and the final complete opening of the contacts. It has, however, been established by tests that the total increase in time is very small, so that the use of this contactless interlocking system does not alter the operating conditions of the contactors.

However, the combined use of contactless interlocking and logical circuits "and", "or", etc provides all the relationships enjoyed in existing control systems.

It is obvious that contactless interlocking is advisable wherever existing electro-mechanical interlocking systems are unsatisfactory.

On suburban and Underground coaches the interlocking systems under the greatest strain are those controlling the drive of the rheostat controller which is the main apparatus controlling the starting of the

train.

Using the foregoing principles, the rheostat controller (with the existing acceleration relays) can be controlled by a transistorized contactless interlocking system. As regards trains using pneumatic drives, the use of transistors is facilitated in that the necessary currents for controlling the electro-pneumatic valves are only a fraction of an ampere and so are much less than the maximum permissible currents of such triodes as the P4 model. It can also be arranged that the effective voltage is within permissible limits.

The solution of the problem rests on the substitution of three appropriate contactless interlockings for the three blocking contacts which control the two valves of the controller and the "lift" coil of the acceleration relay. But this requires three inductance-type transducers. It is, however, possible to dispense with one of them if only one is used for controlling the trigger circuit (for switching the two valves of the controller), and one other for controlling the lift coil of the acceleration relay.

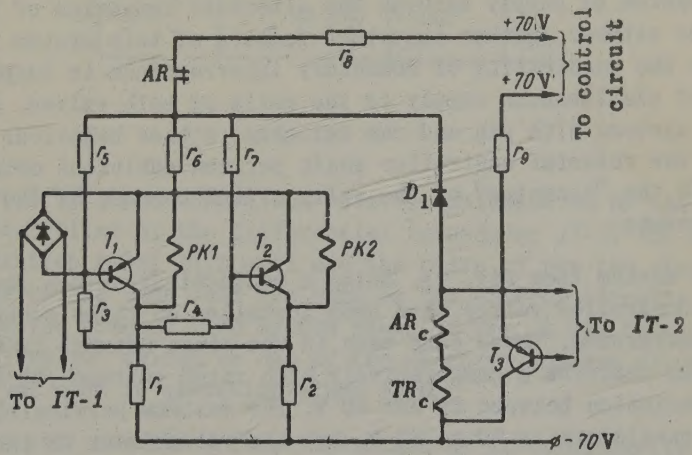

Fig. 7.

This method is illustrated in Fig. 7 in reference to electric coaches on the Underground. The trigger circuit, employing transistors T_1 and T_2, controls the alternate supply to the rheostat controller valves *PK1* and *PK2*. The trigger circuit is controlled by the inductance-type transducer *IT-1* which is similar to the system shown in Fig. 3*b*. When a projecting section of the disc comes to the core, the output voltage is reduced to zero and the triode T_1 is "off" whilst T_2 is "on", since the resistance r_5 is less than the resistance r_7. Therefore, when

the contacts of the acceleration relay *AR* are closed, the coil of *PK1* is disconnected and that of *PK2* is connected.

The output voltage of the other inductance-type transducer *IT-2* (see Fig. 4) is supplied to the triode T_3 and makes it "conducting" or, near certain positions, "fixed" of the controller. The lift coils of the acceleration relay AR_c and time relay TR_c are therefore short-circuited. Between certain "fixed" positions of the controller the output voltage of the transducer *IT-2* changes polarity so that triode T_3 is made "non-conducting" and the lift coils of the acceleration relay and time relay are therefore switched "on". In this case the trigger circuit and coil of one of the rheostat controller valves are supplied via resistance r_9 and diode D_1.

When the shaft of the controller reaches the next "fixed" position, there will be a disc recess opposite the fixed core of the transducer *IT-1* and not a projection, and the rectified output voltage of the transducer is applied to the emitter-base circuit of the triode T_1. This "changes over" the trigger circuit, disconnects the valve *PK1* and connects *PK2*.

This system of supply ensures the alternate connexion of the rheostat controller valves. Another important feature of this system is that it precludes the possibility of momentary interruptions in supply as well as that of simultaneous supply to the coils of both valves. However, in existing systems with pin and cam switches, either behaviour can occur and lock the rheostat controller shaft between positions owing to changes in the "scanning" of the valve switch because of the wear of the components.

Such a system (see Fig. 7), using a contactless switch for the rheostat controller valves, has been installed on three coaches of the Moscow Underground. These have been in use since October 1960. The control system features a comparatively high rated voltage (70 V) and voltage variation between 60 and 90 V. The maximum permissible voltage for the transistors is 50 to 60 V, but the reliability of the transistors is safeguarded by an appropriate choice of the resistances r_1, r_2, r_8 and r_9. The voltage across the transistors never exceeds 35 V even when the control circuit voltage is 90 V.

The disadvantage of this system (Fig. 7) is its high power consumption since the valves are disconnected by short-circuiting their coils. It is only advisable to use this type of system when the control-circuit voltage is much greater than the permissible transistor voltage.

The control-circuit voltage in suburban coaches is 50 V and its variation is much less than that of coaches on the Underground. Use may

therefore be made of the system illustrated in Fig. 8 for the rheostat controller valves of electric suburban coaches. It incorporates two differential transducers similar to the one shown in Fig. 4. The introduction of the controlling triode T_1 not only allows a considerable reduction in the dimensions and power of the transducer, but also reduces the current to zero in the valve coils when they are switched "off". This is impossible when using conventional triggers with loads connected in the collector circuits, owing to the presence of feedback resistance.

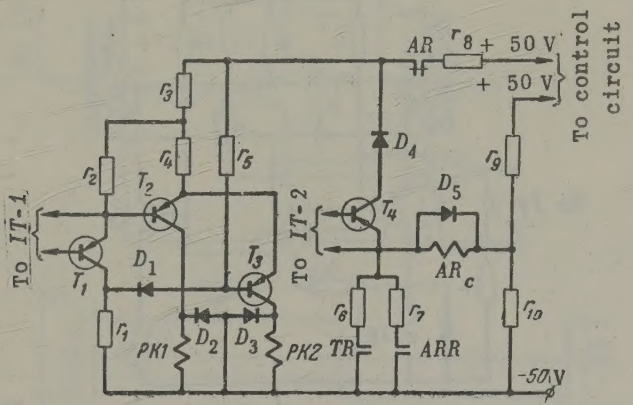

Fig. 8.

The lift coil of the acceleration relay is switched on by the triode T_4. This is controlled by the differential transducer *IT*-2. The supply of the acceleration relay lift coil and the coils of the two rheostat controller valves has been left the same as for control circuits of ER-1 type electric coaches. The system shown in Fig. 8 has been used for a contactless "valve" switch on one of the electric coaches of October Railways. It has been in operation since 1960.

It is known that sharply defined operation by electromagnetic acceleration relays depends to a great extent on the duration of the supply to the lift coil. This only takes about 0.05 sec. Such a short period of time for the coil to be under voltage is explained by the fact that voltage is only supplied to the coil after the camshaft of the rheostat controller has been partially revolved. Unless the relay armature is attracted during this time, the shaft of the rheostat controller jumps through the next "fixed" position. In principle this drawback can be overcome by using the system shown in Fig. 9*a* for supplying the lift coil.

Besides the main windings *1* and 2, auxiliary windings *3* and *4* are mounted on the magnetic circuits of the electro-pneumatic valves. An

impulse voltage is then produced in the windings in question whenever one of the valves is connected or disconnected. This voltage can be used for "changing over" the trigger circuit; as the result of a signal, triode T_1 is made "conducting" and the lift coil AR_c of the acceleration relay is switched "on". In this case the controlling triode T_3 is "off", since the output voltage of *IT*-2 (a device similar to that in Fig. 4) makes the base potential of this triode higher than the emitter

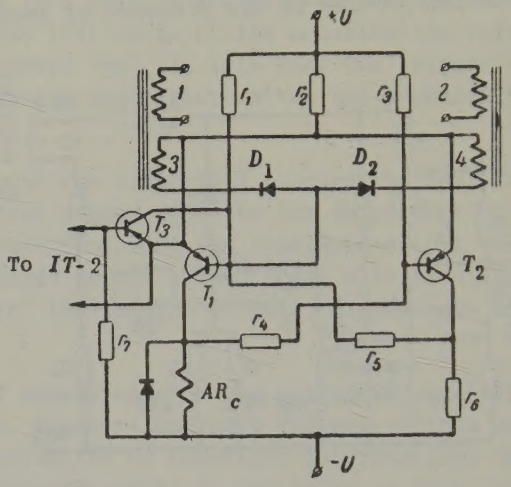

a)

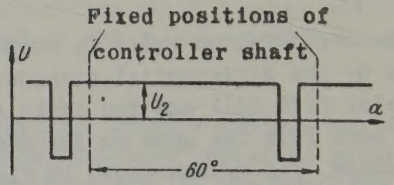

b)

Fig. 9.

potential. Figure 9b illustrates the relationship between the output voltage of *IT*-2 and the angle of rotation α of the rheostat controller shaft. This relationship can be produced by six projections and six recesses on the moving core of the transducer and an appropriate choice of the angles α, β, γ_1 and γ_2.

The lift coil of the acceleration relay is switched off slightly before the camshaft of the controller reaches a "fixed" position. The triode T_1 becomes "off" when the controlling triode T_3 becomes "on" at

the instant the output voltage of *IT-2* changes sign. The triode T_3 again becomes "off" when the controller shaft is in the fixed position.

If the system shown in Fig. 9*a* is used to control the lift coil of the acceleration relay, the valves can be switched by the circuit in Fig. 10*a*.

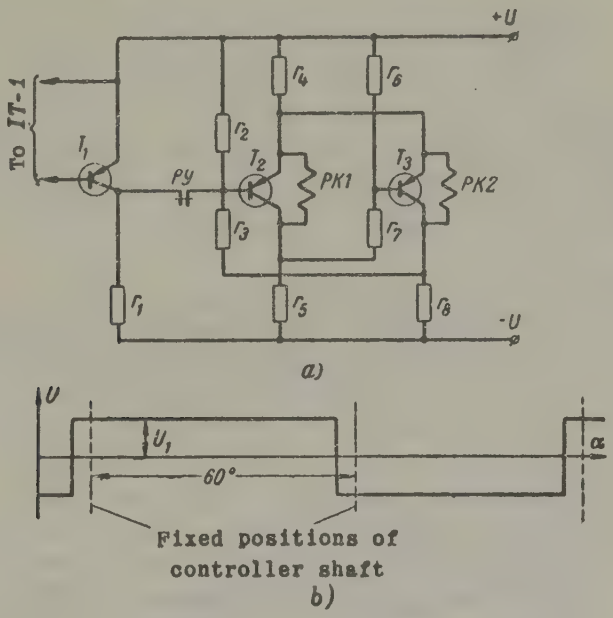

Fig. 10.

In the closed position of the acceleration relay contacts, the state of the trigger depends on the sign of the signal of the *IT-1* transducer (here the system shown in Fig. 4 is used). The relationship between the output voltage U_1 of this transducer and the angle α of the controller shaft is illustrated in Fig. 10*b*. On transition of the controller to the next "fixed" position, the acceleration relay contacts open, but the trigger still remains in the same state. This maintains the continuity of supply to the valve coils in the interim periods between "fixed" positions. For several degrees before the next position is reached, the sign of the transducer output voltage becomes such as to change over the trigger into the new state which sets in after the acceleration relay contacts close. The merit of this system is the absence of electrical coupling between the supply of the acceleration relay lift coil and the valve-switching circuit.

Transistorized contactless interlocking systems such as those

described above can also be used in two-position group apparatus such as reversers, brake switches, etc.

However, the relays of electric coach control systems can also be made without contacts. Here it is advisable to use a magnetic amplifier, the control winding of which receives a signal from the power circuit. The output of the magnetic amplifier can be connected to the transistor circuit which switches "on" a certain part of the control circuit when the control criterion deviates from the desired magnitude. For this purpose use may for instance be made of a trigger circuit with a controlling triode or other trigger circuit. The design of contactless relays allows the control and power circuits to be kept separate, ensures the necessary operating speed of the relays and reduces the power and dimensions of the magnetic amplifier, since it is only required for controlling the transistorized control circuit.

A contactless acceleration relay is illustrated in Fig. 11 (a minimum current relay). The relay consists of a differential magnetic amplifier *MA* which is made up of two conventional irreversible magnetic amplifiers *A1* and *A2*. The loads of the two amplifiers are the resistances r_1 and r_2.

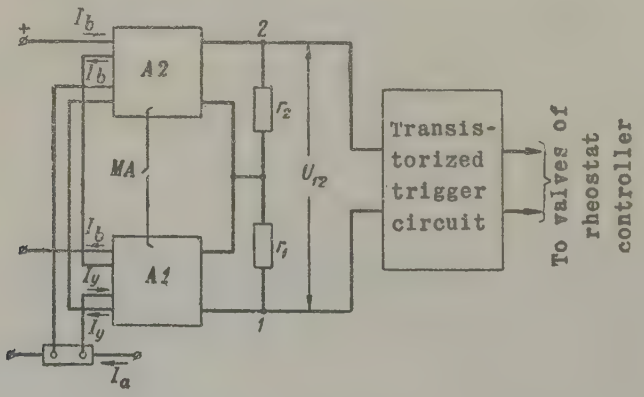

Fig. 11.

If the bias windings of the magnetic amplifier are connected to an external source, then its characteristic, which passes through the origin at zero bias, is shifted to the left by an amount which depends on the bias current. Thus, in the absence of a control signal, the voltage across r_1 and r_2 is proportional to the bias current. Its direction is such that the potential at point *1* (see Fig. 11) is positive and that at point *2* negative.

On supply of the control signal I_y, if the magnetic flux produced by it is in the opposite direction to that produced by the bias current in the respective cores, then the resulting voltage U_{12} is reduced at the output of the magnetic amplifier. If the two fluxes are equal, the resulting voltage U_{12} is zero and if I_y increases further the output voltage reverses polarity.

A transistorized trigger circuit can be made such that "changeover" takes place at zero input voltage. Then, if the current I_a in the armature of the traction motors is less than the current setting of the relay, the first triode of the circuit will be "off" and the circuit will be in a stable state. A reduction of the voltage at the input of the trigger circuit to zero, due to an increase in the control current I_y, results in an abrupt increase in the current at the output of the circuit.

The magnetic amplifier of such an acceleration relay has been made with permalloy cores 7 × 20 × 28 mm. The re-setting ratio was 0.99. The variation of the relay setting was ± 2 per cent of nominal values in the presence of variations ± 10 per cent in the supply voltage at an ambient temperature of 50° C; at an ambient temperature of 20° C the relay setting variation was + 3 to − 0.8 per cent of nominal values. Variations within these limits are no greater than those occurring on existing electromagnetic acceleration relays. The proposed acceleration relay has been made insensitive to variation of the supply voltage by the use of a balance circuit which maintains the voltage difference across r_1 and r_2 constant.

The relay setting is regulated by varying the bias current, but since the relay operates when the m.m.f.'s in the bias and control windings are equal, the operating point of the amplifier remains unchanged when the setting is adjusted. The relay setting can be regulated automatically by providing the relay with several control windings which alter its setting when the load varies or slipping occurs, etc.

From tests on an electronic simulator for a coefficient of non-uniform starting K = ± 10 per cent, a supply frequency of 400 c/s and adequate acceleration time, the operating time of the relay is about 0.03 to 0.05 sec.

The use of contactless acceleration relays in conjunction with contactless valve switches similar to that in Fig. 10 simplifies the whole system of control over the rheostat controller, since only one transducer is required.

The same principle can also be used to produce maximum current

relays such as overload relays and contactless maximum and minimum voltage relays.

In conclusion, it should be noted that the foregoing contactless control circuits and relays can also be used throughout industry in electric drive control systems, particularly when the gear has to be switched on and off with great frequency.

Translated by O.M. Blunn

REFERENCES

1. I.B. Bashuk and A.I. Khomenko; Auth. Cert. No. 113115, dated 12 September 1957.

2. I.B. Bashuk and A.I. Khomenko; Auth. Cert. No. 137136, dated 5 April 1960.

THE DESIGN OF REACTOR-CONTROLLED SEMICONDUCTOR RECTIFIERS*

G.P. MOSTKOVA and F.I. KOVALEV

(Krzhighansk Electrical Engineering Institute)

(Received 2 June 1961)

There is now a need for a simple and accurate method of designing reactor-controlled semiconductor rectifiers in view of the growing demand for this type of equipment. The design problem is two-fold in that attention must be paid to the system of reactor control as well as to the performance of the rectifier.

One of the most promising reactor-controlled three-phase bridge rectifiers in illustrated in Fig. 1. It has satisfactory operating characteristics, and the reactors meet requirements as regards minimum control power, weight and size [1.3].

It must however be borne in mind that the modes of operation of *reactor-controlled* rectifiers (RC rectifiers) depend on the condition of reactor magnetization and not on the number of alternately conducting "valves", as is the case with *conventional* rectifiers with "controlled" valves. The following four modes of operation can be distinguished at loads for which the duration of actual commutation γ does not exceed 60°:

1. The next valve (rectifier) is triggered at the instant the e.m.f.'s of the two phases become equal. From this instant onwards the reactor is re-magnetized. Its main winding is connected in series with the "conducting" valve. In the interval ωt from 0 to α the induction of the reactor varies from B_0, which depends on the magnitude of the magnetizing current, to the saturation induction B_s. The start of actual commutation of the operating current is delayed by the angle α which is equal to the duration of the period of reactor re-magnetization. The

* *Elektrichestvo*, 10, 38-46, 1961.

rectified voltage is similar in shape to that of conventional rectifiers with the control angle α. The first mode of operation is characteristic of loads for which $\alpha + \gamma = 60°$.

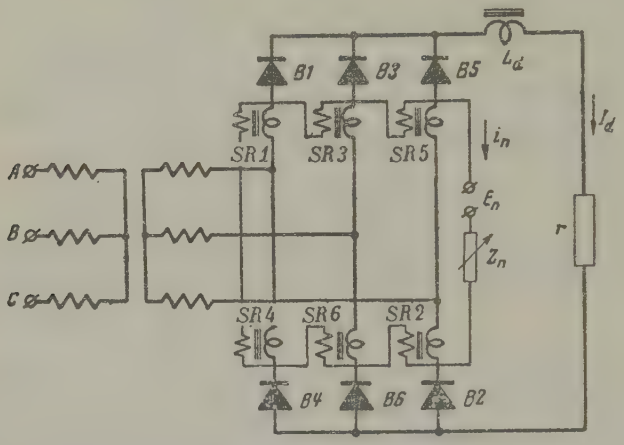

Fig. 1. Main circuit of a reactor-controlled three-phase bridge rectifier:

SR1 – SR6 – saturable reactors;
B1 – B6 – silicon rectifiers;
I_d – load current.

2. The triggering of the next valve is retarded by the angle α_0. The magnitude of this angle depends on the load current. With increasing rectified current the angle α_0 increases from zero to a certain angle α_0^* depending on the time constant of the particular rectifier. The reactor is re-magnetized in the period α_0 to α', where α' is the actual control angle of the rectifier. Under these conditions α' is greater than the duration of reactor re-magnetization and greater than α.

This second mode of operation changes into the third or fourth modes of operation at loads for which α_0 attains particular values, i.e. the third mode sets in when $\alpha_0 = \alpha_0^*$ and $\alpha' + \gamma = 60 + \alpha_0^*$, whereas the fourth mode sets in when $\alpha_0 = \alpha_0^{(k)}$.

3. The triggering of the valves takes place with an angle of lag α_0^* which is independent of the load current. In this mode of operation the control angle α' exceeds the angle α and the duration of reactor re-magnetization. The boundaries of the third mode are: $\gamma < 60°$ and $\alpha' < \alpha'_{k3}$.

4. The next valve is triggered at the instant $\omega t = 0$. The

TABLE 1

Mode	Formulae for α' and α_0	Mode boundaries	Formulae for limiting angles
1	$\cos\alpha' = \cos\alpha$	$(\alpha' + \gamma)_{12} = 60°$	
2	$\cos\alpha' = \sin(30° - \alpha_0) + \frac{2I_d x_\Sigma}{E_{max}}$; $\sin(30° + \alpha_0) = 1 - \cos\alpha + \frac{2I_d x_\Sigma}{E_{max}}$	$(\alpha' + \gamma)_{23} = 60° + \alpha_0^*$; $(\alpha_0)_{24} = \alpha_0^{(k)}$	$\cot\alpha_0^* = \frac{4x_\Sigma - x'_p}{\sqrt{3}x'_p}$; $\cos\alpha_0^{(k)} = \frac{(2-A)(1-A\cos\alpha) \pm \sqrt{3A[(A^2-A+1)-(1-A\cos\alpha)^2]}}{2(A^2-A+1)}$, where $A = \frac{x'_p}{2x_\Sigma + x'_p}$.
3	$\cos\alpha' = \frac{2x_\Sigma}{2x_\Sigma - x'_p}(\cos\alpha_0^* - 1 + \cos\alpha) - \frac{x'_p}{2x_\Sigma - x'_p}\left[\cos(60° + \alpha_0^*) + \frac{2I_d x_\Sigma}{E_{max}}\right]$	$\gamma_{35} = 60°$; $(\alpha')_{34} = \alpha'_{k3}$	$\cos\alpha'_{k3} = \frac{2x'_\Sigma}{x'_p}(1 - \cos\alpha_0^*) + \cos(60° + \alpha_0^*)$
4	$\cos\alpha' = \cos\alpha - \frac{x'_p}{x_\Sigma}\frac{I_d x_\Sigma}{E_{max}}$		$\cos\alpha_{k2} = \left(1 + \frac{2x_\Sigma}{x'_p}\right) - \sqrt{1 + \frac{2x_\Sigma}{x'_p} + \left(\frac{2x_\Sigma}{x'_p}\right)^2}$

N.B. The commutation equation $\cos\alpha' - \cos(\alpha' + \gamma) = 2I_d x_\Sigma / E_{max}$ and the equation $1 - \cos\alpha = Q\nu_m\omega \cdot 10^{-8}/E_{max}$ hold for all modes of operation.

TABLE 2

Mode	Equation of sections of operating characteristic	Mode boundaries
1	$U_d^* = \cos\alpha - \frac{I_d x_\Sigma}{E_{max}}$	1—2 modes $U_d^* = \frac{1}{2} + \frac{I_d x_\Sigma}{E_{max}}$
2	$U_d^* = \sin(30° - \alpha_0) + \frac{I_d x_\Sigma}{E_{max}}$, $\sin(30° + \alpha_0) = 1 - \cos\alpha + 2\frac{I_d x_\Sigma}{E_{max}}$	2—3 modes $U_d^* = \cos(60° + \alpha_0^*) + \frac{I_d x_\Sigma}{E_{max}}$
3	$U_d^* = \frac{2x_\Sigma}{2x_\Sigma - x'_p}\cos\alpha - \frac{2x_\Sigma + x'_p}{2x_\Sigma - x'_p}\cdot\frac{I_d x_\Sigma}{E_{max}} - \frac{x'_p}{2x_\Sigma}\cos\alpha'_{k3}$	3—4 modes $U_d^* = \cos\alpha'_{k3} - \frac{I_d x_\Sigma}{E_{max}}$
4	$U_d^* = \cos\alpha - \frac{x_\Sigma + x'_p}{x_\Sigma}\cdot\frac{I_d x_\Sigma}{E_{max}}$	2—4 modes $U_d^* = \sin(30° - \alpha_0^{(k)}) + \frac{I_d x_\Sigma}{E_{max}}$; $\sin(30° + \alpha_0^{(k)}) = 1 - \cos\alpha + \frac{2I_d x_\Sigma}{E_{max}}$

N.B. 1. At large loads ($\gamma > 60°$) modes of operation occur with double "overlaps" (5th mode) which are not considered in this paper. The boundary between the third and fifth modes is represented by the arc of an ellipse and described by the equation $[(2/\sqrt{3})U^*]^2 + [(2x_\Sigma/E_{max})I_d]^2 = 1$.

2. The angles $\alpha_0^{(k)}$, α_0^* and α'_{k3} and found by the formulae in Table 1.

re-magnetization of the reactor takes place by a linear voltage, but the reactor voltage decreases in the interval of actual commutation of the valve in the opposite arm of the phase in question. Re-magnetization is therefore prolonged. The control angle α' is equal to the duration of reactor re-magnetization, but greater than α.

A detailed analysis of the modes of operation of reactor-controlled rectifiers (with "non-controlled" valves and non-linear anode inductances) has already been published in Russian [1]. The main formulae for each mode of operation are reproduced in Table 1. Reference should also be made to the comprehensive glossary of notation at the end of the paper.

These formulae were derived on the following assumptions. The self-capacitances and resistances of the circuit were ignored. It was assumed that the characteristics of the individual rectifiers were ideal and that the rectified current was ideally smooth. The inductance of the reactor on re-magnetization was assumed to be slightly greater than the leakage inductance of the transformer. The current in the main winding of the reactor on re-magnetization was regarded as negligible compared with the mean value of the rectified current. Finally it was assumed that no ripple occurred in the current in the reactor magnetization windings.

Rectifier performance

The main operating characteristic of a rectifier is that which represents the mean value of the rectified voltage as a function of the mean rectified current at a given control current.

An analysis has already been made of electromagnetic phenomena in reactor-controlled rectifiers. It was found that the equation for the relationship between the mean value of the rectified voltage on the one hand and the control and actual commutation angles on the other is exactly the same for reactor-controlled rectifiers as for conventional rectifiers:

$$U_d = U_{d0} \frac{\cos \alpha' + \cos (\alpha' + \gamma)}{2}. \qquad (1)$$

Since the commutation equation is the same for all modes of operation (see Table 1), equation (1) can be written in the form

$$U_d = \cos \alpha' - \frac{I_d x_\Sigma}{E}, \qquad (2)$$

where

$$U_d^* = \frac{U_d}{U_{d0}}.$$

Substituting in (2) the values $\cos \alpha' = f(B_0, I_d)$ or $\cos \alpha' = f(\alpha, I_d)$ from Table 1, it is possible to form equations for individual sections of an operating characteristic corresponding to the various modes of operation (see Table 2).

Each of these modes of operation is possible over a particular range of values of the load current and angle α, i.e. there is a corresponding section of the characteristic $U^*_d = f(I_d)$ for each mode of operation.

Figure 2 shows the operating characteristics and mode boundaries as calculated by the formulae in Table 2. Each curve corresponds to a particular initial value of B_0.

For illustrative purposes and in order to compare RC rectifiers with conventional systems, the corresponding angles α of B_0 are plotted instead of B_0.

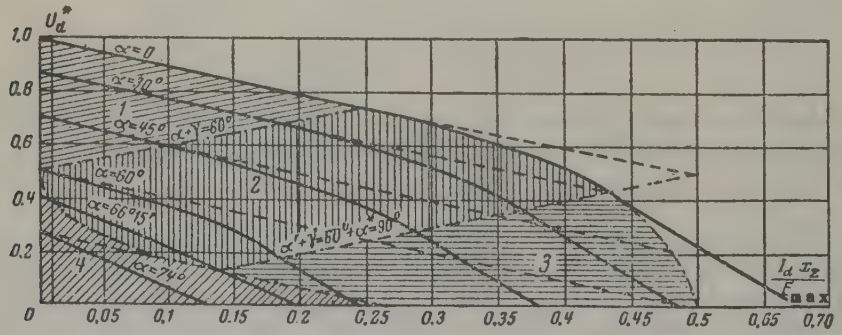

Fig. 2. The operating characteristics of a rectifier for $x'_p/x_\Sigma = 1$ (continuous line) and $x'_p/x_\Sigma = 0$ (broken line); (-.-.-.- mode boundaries).

It will be seen from Table 2 and Fig. 2 that the rectified voltage can be regulated within wide limits in RC rectifiers by varying the magnetization current. Here the shape of the curves depends to a considerable extent on the relationship between the reactances of the valve and phase circuits. If the phase reactance x'_p is much less than the "valve" reactance x_r (see glossary at end of the paper), the characteristics of RC rectifiers will be the same as those of conventional

rectifiers. If $x'_p \gg x_r$, this will only be the case in the first mode of operation (i.e. when $\alpha + \gamma < 60°$). In the other modes of operation (with large load currents and a large degree of control of the rectified voltage) there will be a marked difference in the characteristics of the rectifiers.

These formulae have been checked by tests on silicon rectifiers and saturable reactors with toroidal cores of permalloy-type material. The calculations and tests were both made for $x'_p/x_\Sigma = 0.905$. A smoothing inductance was included in the load circuit.

The calculated curves and test results are shown in Fig. 3. It will be seen that quite good agreement is obtained. The error is within 15 per cent as regards the voltage. Similar results were obtained for reactors with magnetic circuits made from cold-rolled steel.

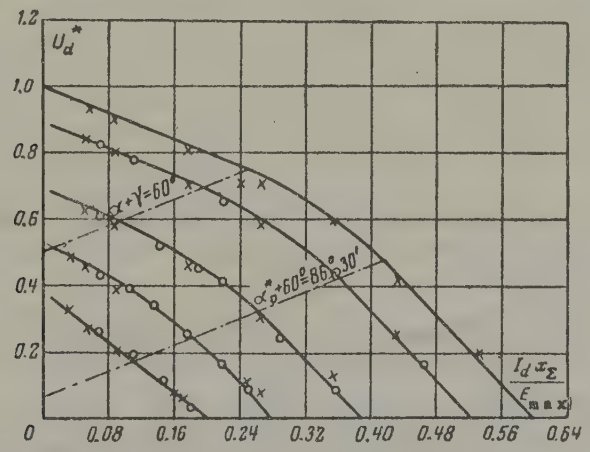

Fig. 3. Operating characteristics of a silicon rectifier: ——— - calculated characteristics; × - experimentally determined points (rectified current smoothed); ° - experimentally determined points on active load).

The proposed formulae can also be used for the design of large three-phase rectifiers with active loads. Figure 3 shows that the error is still of the same order even with a smoothing inductance in the load circuit. However, it is the purpose of this paper to consider the performance of the equipment under conditions of forced reactor magnetization, i.e. when the current harmonics of the magnetization circuit are suppressed. But even if no large resistance is present in the control circuit, only multiples of the sixth harmonic can occur there, and therefore the rectifier in practice operates as if even harmonics were

suppressed [4]. Consequently, the proposed formulae are equally applicable to cases when the resistance in the magnetization circuit is small. Tests have confirmed that the only error occurs in the third mode of operation (i.e. on overload) when the slope of the actual characteristics is less than that obtained by the calculations.

The control characteristic

The control characteristic represents the relationship between the mean value of the rectified current (or output voltage of the rectifier) and the magnetization current for a given load impedance.

The equation of the control characteristic is obtained by substituting $I_d r/U_{d0}$ for U^*_d in formula (2)

$$I^*_d = -\frac{r}{r + \frac{3}{\pi} x_\Sigma} \cos \alpha', \tag{3}$$

where

$$I^*_d = \frac{I_d}{I_{d0}}; \qquad I_{d0} = \frac{U_{d0}}{r}.$$

The equation of the control characteristic for each mode of operation is formed by substituting the appropriate value of cos α' in equation (3) (see Table 3).

The value of cos α depends on the initial induction B in the cores of the reactor and therefore depends on the magnetization current.

This relationship can be found graphically by defining various values of the magnetization current and using the hysteresis loop and the equation $\cos \alpha = (1 - Qw_z\omega/E_{max} \times 10^8)(B_s - B_0)$. The control characteristics are then plotted from the formulae in Table 3.

But if the hysteresis loop of the core material can be represented approximately by short straight-line sections, the magnetization current can easily be expressed analytically:

$$B_s - B_0 = \frac{\Delta B_{max}}{2(1+\nu)} [\nu - (2+\nu) I_m].$$

The coefficient $\nu = H_k/|H_c|$ defines the intensity of the magnetic field corresponding to the bend in the hysteresis loop. Thus, for a linear approximation of the hysteresis loop, the formula for cos α takes the form

$$\cos\alpha = 1 - \frac{k}{2(1+\nu)}[\nu - (2+\nu)I_{\text{л}}^*],$$

where

$$k = \frac{Qw_{\text{л}}\omega}{E_{\max}\cdot 10^8}\Delta B_{\max}.$$

Analytical expressions are then found for the sections of the control characteristic corresponding to the different modes of operation by substituting the expression cos $\alpha = f(I_{\text{л}}^*)$ in the formulae in column 1 of Table 3. The equations in column 2 are the result. The third column shows the relative values of the load currents at which one mode of operation changes into another.

It will be seen from the curves in Fig. 4 (rectifier operating characteristics and load lines for limiting resistances at rectifier output) that the control characteristics do not always pass successively through all four modes of operation. The sequence depends on the load resistance and the design of rectifier. The limiting loads are calculated as the ratio of the output voltage to the current at particular points on the boundaries between modes.

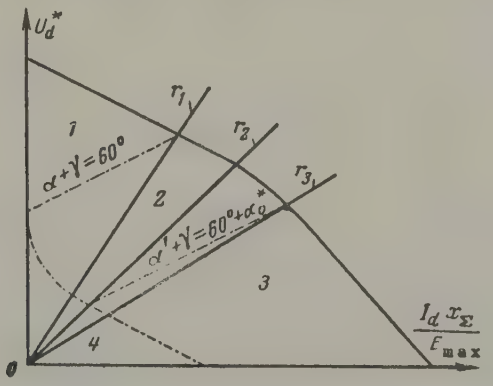

Fig. 4. The domain of the rectifier operating characteristics.

Figure 5 illustrates the formulae in Table 3 by a number of calculated control characteristics. The curves are plotted for $x_p/x_\Sigma = 1$ and a linear approximation of the hysteresis loop ($\nu = -0.5$).

Figure 6 shows the calculated control characteristics of the rectifying system in Fig. 1. The continuous curves have been plotted by the graphical-analytical method from the actual hysteresis loop of the core

TABLE 3

Mode	Equations of the sections of control characteristics		Value of currents at mode boundaries
	In general form	For linear approximation of hysteresis loop	
1	$I_d^* = \frac{r}{r - \frac{3}{\pi} x_\Sigma} \cos\alpha$	$I_d^* = \frac{r}{r + \frac{3}{\pi} x_\Sigma} \times$ $\times \left\{1 - \frac{k}{2(1+\nu)} [-I_{\blacksquare}^*(2+\nu) + \nu]\right\}$	$(I_d^*)_{12} = \frac{1}{2} \cdot \frac{r}{r - \frac{3}{\pi} x_\Sigma}$
2	$I_d^* = \frac{r}{r - \frac{3}{\pi} x_\Sigma} \sin(30° - \alpha_0)$ $\sin(30° + \alpha_0 - \varphi) =$ $= \frac{1 - \frac{3x_\Sigma}{\pi r}}{\sqrt{1 + 3\left(\frac{3x_\Sigma}{\pi r}\right)^2}} (1 - \cos\alpha)$	$I_d^* = \frac{r}{r - \frac{3}{\pi} x_\Sigma} \sin(30° - \alpha_0);$ $\frac{k}{2(1+\nu)} [-I_{\blacksquare}^*(2+\nu) + \nu] =$ $= \frac{\sqrt{1 + 3\left(\frac{3}{\pi} \cdot \frac{x_\Sigma}{r}\right)^2}}{1 - \frac{3}{\pi} \cdot \frac{x_\Sigma}{r}} \sin(30° + \alpha_0 - \varphi)$	$(I_d^*)_{23} = \frac{r}{r - \frac{3}{\pi} x_\Sigma} \times$ $\times \sin(30° - \alpha_0^*)$
	$\tan\varphi = \frac{3\sqrt{3}}{\pi} \cdot \frac{x_\Sigma}{r}$		$(I_d^*)_{2i} = \frac{r}{r - \frac{3}{\pi} x_\Sigma} \times$ $\times \sin(30° - \alpha_0^{(k)})$

3	$I_d^* = \frac{r}{r\left(1-\frac{x'_{p_1}}{2x_\Sigma}\right)+\frac{3}{\pi}\left(x_\Sigma+\frac{1}{2}x'_{p_1}\right)} \times \left[\cos\alpha - \frac{x'_{p_1}}{2x_\Sigma}\cos\alpha'_{k3}\right]$	$I_d^* = \frac{r}{r\left(1-\frac{x'_p}{2x_\Sigma}\right)+\frac{3}{\pi}\left(\frac{2x_\Sigma+x'_p}{2}\right)} \times \left\{1-\frac{x'_p}{2x_\Sigma}\cos\alpha'_{k3} - \frac{k}{2(1+\nu)} \times [-I_*^*(2+\nu)+\nu]\right\}$	$(I_d^*)_{34} = \frac{r}{r+\frac{3}{\pi}x_\Sigma} \times \cos\alpha'_{k3}$
4	$I_d^* = \frac{r}{r+\frac{3}{\pi}(x_\Sigma+x'_{p_1})}\cos\alpha.$	$I_d^* = \frac{r}{r+\frac{3}{\pi}(x_\Sigma+x'_p)} \times \left\{1-\frac{k}{2(2+\nu)}[-I_*^*(2+\nu)+\nu]\right\}$	

N.B. In determining $(I_d^*)_{24}$, the angle $\alpha_0^{(k)}$ should be calculated by the formula

$$\sin(x-\alpha_0^{(k)}) = \frac{1}{\sqrt{1+B+B^2}}, \text{ where } x = \arctan\frac{2+B}{\sqrt{3B}} \text{ and } B = \frac{\frac{3}{\pi}x'_p}{r-\frac{3}{\pi}x_\Sigma}.$$

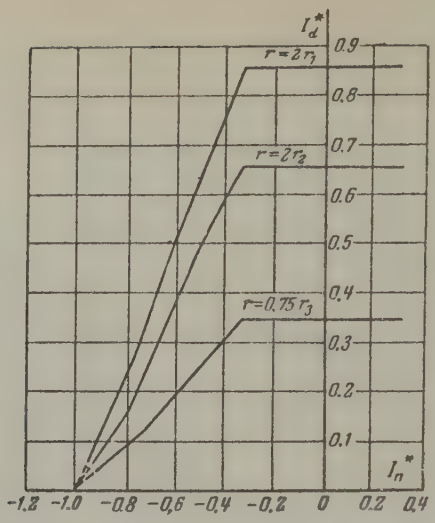

Fig. 5. The control characteristics of the rectifier.

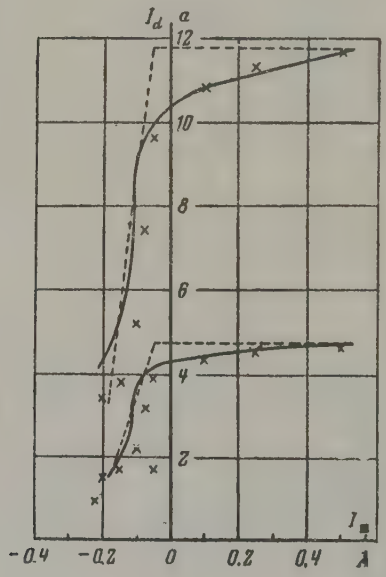

Fig. 6. Control characteristics of a silicon rectifier: - - - - calculated curves with linear approximation of the hysteresis loop of the reactor cores; ———— - characteristics plotted by a graphical analytical method from the actual hysteresis loop; × - test points (the upper ones correspond to $r = 10\ \Omega$ and the lower ones to $r = 50\ \Omega$).

materials. The broken curves are from the expressions in Table 3 using the linear approximation of the hysteresis loop. Experimentally-determined points are also marked on the diagram. The discrepancies are due to the use of the maximum dynamic hysteresis loop in the calculations. In fact, the re-magnetization of saturable reactors follows special loops which are narrower than the maximum loops, so that the calculated values of the control current are higher than those found experimentally.

The minimum load current

In analysing the various modes of operation and plotting the operating characteristics it was assumed that the current in the operating windings of the reactors on re-magnetization was zero. But, in fact, currents do flow in these windings, and their magnitude depends mainly on the slope and width of the dynamic hysteresis loop. Since the reactor cores are made from high-quality materials with practically ideal magnetization curves, it follows that these currents are small and have a negligible effect if the load current is greater than a certain minimum value $I_{d.min}$. But if the load current I_d is less than $I_{d.min}$, the electromagnetic phenomena and shape of the operating characteristics are affected accordingly. The loads for which $0 < I_d < I_{d.min}$ (see the thin vertical line in Fig. 2 [sic]) are non-operational.

To determine the magnitude of $I_{d.min}$ it is necessary to consider the performance of the rectifier for $r = 0$. In this mode of operation the current through the load only depends on the reactor re-magnetization currents. It will be seen from the curves in Fig. 7 that in this case the six rectifiers have a constant mode of operation. The rectified current is therefore equal to the sum of the currents in the operating windings of the three reactors in one arm of the bridge. The magnetization of one of the reactors (e.g. SR1) is finished at the instant $\omega t = \alpha$. Partial magnetization of the reactor (SR3) in the next phase of the same arm is "completed" at the same time [1]. Since a mode of operation is under consideration with the rectifier completely regulated and $r = 0$, the magnetization of the reactor (SR5) of the preceding phase begins at the instant $\omega t = \alpha$. The magnetic states of the reactors at the instant under consideration have been marked on the hysteresis loop in Fig. 7. (The various reactors SR1 to SR6 are indicated by subscripts 1 - 6 in the notation for the magnetizing currents):

$$i_{\mu 1} = (2 + \nu) I_c;$$

$$i_{\mu 3} = [1 + (1 - \sqrt{3})(1 + \nu)] I_c;$$

$$i_{\mu 5} = \nu I_c,$$

where

$$I_c = \frac{H_c l_\mu}{1.25 w_z}.$$

Reference should be made to the glossary of notation at the end of the paper for other symbols.

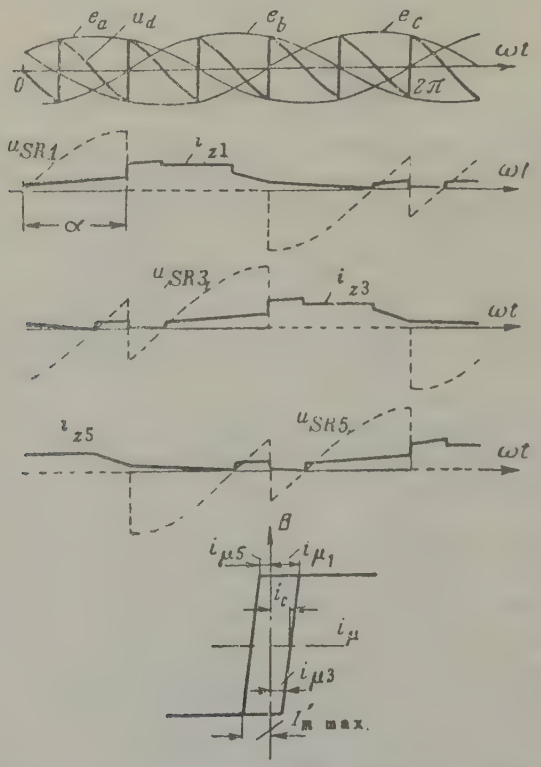

Fig. 7. The rectified voltage, the currents in the operating windings of the reactors, the voltages on the reactors and the hysteresis loop of the reactor cores for $r = 0$.

The current in the operating winding of the reactor is

$$i_z = i_\mu - \frac{w_R}{w_z} I_R.$$

The minimum rectified current $I_{d.min}$ is then found by adding the currents in the operating windings of the three saturable reactors in one arm of the bridge (i.e. SR1, SR3 and SR5):

$$I_{d\,min} = i_{z1} + i_{z3} + i_{z5} = i_{\mu 1} + i_{\mu 3} + i_{\mu 5} - 3\frac{w_m}{w_z} I_m.$$

It is obvious that for a completely regulated rectifier

$$I_m = -\frac{w_z}{w_m}(2+\nu) I_c.$$

By definition

$$I_{d\,min} = 8.27(1+0.52\nu) I_c = 6.6(1+0.52\nu)\frac{l_\mu}{w_z} H_c. \qquad (4)$$

The minimum rectified current of large rectifiers is about 2 to 6 per cent of its rated value*.

Design of the reactors

The voltage drop on re-magnetization of the reactors depends on the value of ΔB_{max} in the cores, the number of turns in the operating windings and the cross section of the core. The degree of regulation of the rectified voltage likewise depends on these factors. Knowledge of the relationship between the maximum degree of regulation and the voltage on each reactor is necessary for design purposes. Strictly speaking, this relationship can be found if the modes of operation of the rectifier covered by the "domain of regulation" (see Fig. 8) are known. But this implies that the operating characteristics of the rectifier are known, whereas they can only be constructed from the design of the reactor. The problem of reactor design can, however, be solved with sufficient accuracy for practical purposes if it is assumed that all the operating characteristics are a set of straight lines within the control domain described by the equation $U_d = U_{d0} \cos \alpha - 3/\pi\, x_\Sigma I_d$. The operating characteristics are obviously straight lines described by this equation if the control domain only covers the first mode of operation and if $x_r \gg x'_p$. However, if x_r is commensurate with x'_p and the control domain covers other modes of operation besides the first, then the stated assumption slightly over-states the reactor criteria. The error can, however, be adjusted later in the calculations.

The formula for the rectified voltage is obtained by the expression which links the control angle with changes in induction $\Delta B = B_s - B_0$:

---

* When operating into an active load $I_{d.min}$ is slightly less.

$$U_d = U_{d0} - \frac{3}{\pi} Qw_{\text{ж}} \Delta B \cdot 10^{-8} - \frac{3}{\pi} I_d x_{\Sigma} = \\ = U_{d0} + \Delta U_{d\alpha} - \Delta U_{d\gamma}, \quad (5)$$

Hence it follows that the variation of the voltage at the output of the rectifier $\Delta U_d = U_{d0} - U_d$ depends on the voltage drop in the reactor $\Delta U_{d\alpha}$ and the commutation voltage drop $\Delta U_{d\gamma}$. The quantity $\Delta U_{d\alpha}$ represents the degree of regulation of the rectified voltage. The variation of induction is a maximum if the degree of regulation is also a maximum. The formula for Qw then takes the form

$$Qw_{\text{ж}} = \frac{\pi}{3} \cdot \frac{(\Delta U_{d\alpha})_{\max} \cdot 10^8}{\omega \Delta B_{\max}}. \quad (6)$$

This expression is the main formula for designing the reactor according to the desired degree of regulation of the rectified voltage.

The quantity $\Delta B_{\max}$ depends on the quality of the core material and the construction of the core. The best magnetic properties are possessed most consistently by "interleaved" solid cores with "strengthened" yokes which have been [literally in the Russian] "charged in the well"* [5]. It is advisable to select the operational range of variation of the induction of the reactor in large rectifiers so as to make full use of the hysteresis loop. This makes for the highest possible power factor. But the increase in $\Delta B_{\max}$ is restricted by the requirement of minimum control power. Quite good results can be obtained by taking $\Delta B_{\max} = 2B_k$, where B_k is the induction at the intersection of the descending and ascending portions of the dynamic hysteresis loop. In this case $\Delta B_{\max}$ is about 30,000 to 32,000 G for grade E-330 cold-rolled electrical steel.

The maximum degree of regulation which the reactors must ensure is sometimes known beforehand. This quantity is then entered in formula (6). If however the rectifier has to meet requirements regarding the stability of the output voltage or current under varying load or supply voltage conditions, or if particular operating characteristics are required, the value of $(\Delta U_{d\alpha})_{\max}$ can then be calculated by the formula (see Fig. 8)

$$(\Delta U_{d\alpha})_{\max} = (U_{d0})_{+\Delta U_c} - U_{d\min} - \\ - \frac{e_{\kappa\Sigma}\%}{100} \cdot \frac{I_{d\min}}{I_{d\,\text{nom}}} U_{d\,\text{nom}} \quad (7)$$

---

* Possibly a reference to annealing in a soaking pit.

The quantity $e_{k\Sigma}$ % has to be estimated first, and its value checked later after analysis and rough drawings have been made. If necessary, the reactor must be designed for a new value of $e_{k\Sigma}$ %.
cent.

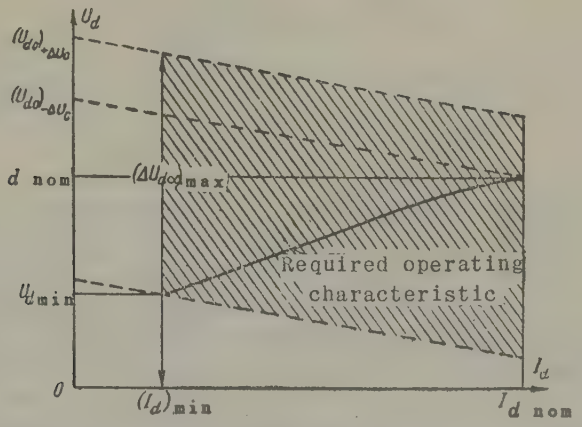

Fig. 8. The requisite operating characteristic and the domain of regulation (the shaded area).

The cross section of the magnetic circuit Q and the number of turns in the operating winding w_z depend on the requirements to be met as regards minimum loss, weight and dimensions.

The following equation can be used for the number of turns in the control winding:

$$I_{m.max} = \frac{H_{max} l_\mu}{1{,}25 w_m}. \qquad (8)$$

Here it must be borne in mind that wide variation of the magnetization current is required between $+I_{m.max}$ and $-I_{m.max}$ in order to make full use of the hysteresis loop. If, however, a change in the direction of the current in the magnetization winding is undesirable or impossible, the magnetization winding can be divided into two windings, namely, a control winding and a bias winding, which is supplied by current $+I_{m.max}$. In this case the current in the control winding varies between 0 and $-2I_{m.max}$. The value of H for "interleaved" solid cores of grade E-330 electrical steel is 2 to 3 oersted.

Another factor in the design of the control winding is the voltage induced in it during re-magnetization of the reactor:

$$u'_{SR} = u_{SR} \frac{w_m}{w_z} = \frac{w_m}{w_z} E_{max} \sin \omega t. \qquad (9)$$

This voltage attains its maximum value under conditions of maximum regulation, i.e. when $I_{\text{н}} = I_{\text{н. max}}$ and $\alpha = \alpha_{\text{max}}$. The maximum value of the control angle is given approximately by the expression

$$\cos \alpha_{\text{max}} \approx \frac{U_{d\,\text{min}}}{(U_{d0})_{+\Delta U_c}}.$$

Then, by definition

$$(u'_{SR})_{\text{max}} = \frac{w_{\text{н}}}{w_{\text{з}}} E_{\text{max}} \sin \alpha_{\text{max}}. \qquad (10)$$

Strictly speaking, the angle $(\alpha' + \gamma + \delta)$ should be substituted for ωt in formula (9) in order to determine the maximum voltage on the magnetization windings. But this can only be done after constructing the operating characteristics and determining the control zone (see Fig. 8). For draft projects use may be made of formula (10). The value of $(u'_{SR})_{\text{max}}$ can be stated more precisely later.

Thus the number of turns in the magnetization windings can be found by formulae (8) and (10) according to the desired control current or maximum permissible voltage on the magnetization windings.

Reactor power

The weight and dimensions of saturable reactors inevitably depend on the equivalent rating of the reactors, as well as on the maximum voltage and the effective value of the rated current in the reactor windings. In its turn the equivalent rating depends on the shape and operating time of the voltage in the reactor windings and is defined (by analogy with conventional transformers) as the average of the products of the effective value of the current of each winding, times the equivalent e.m.f. [6]. The equivalent e.m.f. is that sinusoidal voltage which, on being applied to a particular reactor, will cause its complete re-magnetization (from $-B_k$ to $+B_k$) during a half-period. It is calculated by the formula

$$E_0 = \frac{1}{2\sqrt{2}} \int_0^{\alpha} u_{SR}\, d\omega t.$$

Here, in order to determine the reactor voltage, it is necessary to use an expression for it at load currents close to the minimum value of the rectified current (practically on no load of the rectifier). In this case the reactor voltage can be represented in the following form at any magnetization current:

$$u_{SR} = E_{\text{max}} \sin \omega t,$$

where

$$0 \leqslant \omega t \leqslant \alpha.$$

Then

$$E_{\vartheta} = \frac{1}{2\sqrt{2}} E_{max} (1 - \cos \alpha_{max}).$$

Considering that

$$E_{max}(1 - \cos \alpha_{max}) = \frac{\pi}{3} (\Delta U_{d\alpha})_{max},$$

the formula for the equivalent e.m.f. is

$$E_{\vartheta} = \frac{1}{2\sqrt{2}} \frac{\pi}{3} (\Delta U_{d\alpha})_{max}.$$

In calculating the effective value of the current in the main winding of a reactor it can be assumed that the current flowing through the rectifier is rectangular in shape, even though this tends to over-state the calculated values of the current and equivalent rating by 4 to 5 per cent. For the circuit under consideration in this article, the current in the main winding of the reactor is

$$I_z = \frac{1}{\sqrt{3}} I_d.$$

The maximum value of the magnetization current, referred to the main winding, does not exceed 5 per cent of the current in the main winding for large rectifiers using a circuit with internal feedback. It can therefore be assumed in the derivation of the formula for the equivalent rating of a saturable reactor that $I'_m = 0.05\ I_d$.

The equivalent rating of the six reactors as a percentage of the power of the supply transformer is

$$P^*_{6\vartheta} = \frac{9}{\pi} \cdot \frac{E_{\vartheta}}{U_{d0}} \cdot \frac{I_{z1} + I'_m}{I_{d.nom}} \cdot 100\%.$$

Substituting the expressions for E_{ϑ}, I_z and I'_m in this formula:

$$P^*_{6SR} = 1.05 \frac{\sqrt{3}}{2\sqrt{2}} \cdot \frac{(\Delta U_{d\alpha})_{max}}{U_{d0}} \cdot 100\%.$$

The quantity

$$\frac{(\Delta U_{d\alpha})_{max}}{U_{d0}} \cdot 100\% = (\Delta U^*_{d\alpha})_{max}$$

is the maximum degree of regulation of the rectified voltage as a

percentage of the no-load voltage of the rectifier. Consequently, the equivalent rating of the six reactors in the rectifier system under consideration is a linear function of the desired degree of rectified voltage regulation.

If 100 per cent regulation of the rectified voltage is required over a wide range of load currents (from $I_{d.min}$ to $I_{d.nom}$), the equivalent rating of the saturable reactors is a maximum and is about 65 per cent of the supply transformer rating.

Glossary of notation

ΔB_{max} – the maximum change in induction in the reactor core

E_{max} – the amplitude of the line voltage in the LT winding of the transformer

$e_k\Sigma\%$ – the total rectified voltage drop as a percentage of its rated value

U_d – the mean value of the rectified voltage

U_{d0} – the mean value of the rectified voltage on no load

$U_{d.nom}$ – the rated rectified voltage

$(U_{d0}) + \Delta U_c$ – the no-load voltage of the rectifier with an increase in supply voltage

u_{SR} – the voltage on the main winding of the reactor (instantaneous value)

u'_{SR} – the instantaneous value of the voltage on the magnetization winding of the reactor

H_k – the intensity of the magnetic field corresponding to the kink in the linear approximation of the hysteresis loop

H_c – the coercive force of the dynamic hysteresis loop of the reactor cores

H_{max} – the intensity of the magnetic field corresponding to the maximum magnetization current

I_z – the effective value of the current in the main winding of the reactor

I'_m – the mean value of the current in the magnetization winding referred to the main winding

I_d – the mean value of the rectified current

$I^*_m = I_m/I_{m.max}$ – the magnetization current in relative units

$I_{m.max}$ – the maximum value of the magnetization

$I_{d.nom}$ – the rated rectified current

$I_{d.min}$ – the load current corresponding to the minimum desired value of the rectified voltage

i_z – the instantaneous value of the current in the main winding of the reactor

l_μ – the length of the middle magnetic line of the reactor core

w_m – the number of turns in the magnetization winding

w_z – the number of turns in the main winding of the reactor

Q – the active cross section of the reactor core, cm^2

r – the load resistance

$x_\Sigma = x'_p + x_r$ – the total reactance

x'_p – the referred phase reactance, including the leakage reactance of the transformer and system

x_r – the reactance of the reactor in the saturated state

α – the duration of the magnetization of the reactor on condition that the winding voltage varies according to the law $E_{max} \sin \omega t$ in the interval from 0 to α

α_0 – the angle of delay in triggering the alternate valve

α_0^* – the angle of delay at which the third mode of operation begins

α' – the control angle of the rectifier

α'_{k3} – the control angle at which the third mode of operation changes into the fourth

$a_0^{(k)}$ – the angle of delay at the boundary of the second and fourth modes

γ – the actual commutation angle

Translated by O.M. Blunn

REFERENCES

1. G.P. Mostkova and F.I. Kovalev; Izd. Akad. Nauk SSSR, *Elektroenergetika*, No. 4 (1961).

2. H.F. Storm and C.W. Flairty; *Communication and Electronics*, No. 1 (1960).

3. W.H. Moore; *New techniques in designing three-phase magnetic amplifiers*. Amer. Inst. elect. Engrs. (1957).

4. M.A. Rozenblat; *Magnetic amplifiers* (*Magnitnye usiliteli*), Part II. Sov. Radio (1960).

5. P. Kratz and A. Lang; *AEG Mitt.*, No. 8/9 (1959).

6. Yu.G. Tolstov; *The use of saturable reactors in installations for d.c. transmission* (*Primeneniye nasyshchayushchikhsya drosselei v ustanovkakh dlya peredachi energii postoyannym tokom*). Izd. Akad. Nauk SSSR (1951).

HOW THE POST-BREAKDOWN VOLTAGE ON AN ARRESTER DEPENDS ON THE LENGTH OF THE CURRENT WAVEFRONT*

V. I. PRUZHININA-GRANOVSKAYA and V. A. VOL'KENAU

(Lenin All-Union Electrical Engineering Institute)

(Received 28 March 1961)

Recent improvements in the performance of valve arresters have resulted in lower insulation levels on transformers and other gear.

The surges which follow lightning strokes differ in duration and may be very short. The insulation is accordingly designed for voltage wavefronts of approximately 1 to 2 μsec.

But the "standard" post-breakdown voltages of valve arresters have been calculated for current wavefront lengths of about 10 μsec owing to the relative simplicity and accuracy of the measurements, even though the arrester may be affected by current wavefront lengths τ_w of less than 10 μsec in operation [1]. This situation has been recognized in the regulations governing surge protection where post-breakdown voltages are specified for τ_w of 3 to 5 μsec.

Use is at present made of two types of non-linear resistors in Soviet valve arresters. "Vylite"** resistors are used in lightning arresters and "tervite"** resistors in "combined" arresters for protection from

---

* *Elektrichestvo*, 10, 53-54, 1961.

** These types of arrester are considered in an article translated in this journal from *Elektrichestvo* No. 4, 1961. Vylite is a ceramic material which consists of SiC + clay and graphite. Tervite is another special type of material used for non-linear arresters (Translation Editor).

internal surges as well as lightning strokes. The electrical characteristics of these two types of resistor are quite different, and the same applies to the relationship between their post-breakdown voltage and the current wavefront.

The effect of the current wavefront on the post-breakdown voltage is essentially as follows. At a given current the voltage on the resistor depends on the temperature of the inter-grain contacts owing to the high temperature coefficient of resistance of carborundum. This relationship determines the looped shape of the dynamic voltampere characteristic of operating resistors and the relationship between the post-breakdown voltage and the length of the current wavefront. Since the temperature coefficient of resistance of carborundum is negative, it follows that the post-breakdown voltage decreases with increasing length of the wavefront.

The variation of the post-breakdown voltage U' with a reduction in the length of the wavefront depends on the "density" of the impulse current as well as on the properties of the resistor. For arresters made by the American firm of Westinghouse [3], the residual voltage at 10 kA for τ_w of 3 μsec is 12 per cent greater than that for $\tau_w = 10\,\mu$sec. For the Swedish 380 kV arrester, the post-breakdown voltage at 8 kA is 10 per cent higher for a current wavefront slope of 3 kA/μsec than for 1 kA/μsec. The post-breakdown voltage at 10 kA on the vylite resistors of Russian RVS arresters in production up to 1950 was increased 6 to 7 per cent by a reduction in the length of the current wavefront from 10 to 5 μsec [5].

For the RVS arresters now in production, the post-breakdown voltage U' is 4 and 6 per cent higher respectively for $\tau_w = 5$ and 3 μsec than for $\tau_w = 10\,\mu$sec.

This paper presents the results of investigations into the relationship between the post-breakdown voltage and the length of the current wavefront for tervite and vylite arresters in modern Soviet lightning arresters. The measurements were taken on tervite and vylite discs 70 mm in diameter and 20 mm thick for $\tau = 3$, 5 and 10 μsec at 2.5 and 10 kA. The changes in the post-breakdown voltage $\Delta U'$ for $\tau_w < 10\,\mu$sec are expressed as percentages of the post-breakdown voltage U'_{10} at $\tau_w = 10$ μsec:

$$(\Delta U'/U'_{10})\ \% = (U'_\tau - U'_{10}/U'_{10}) \times 100$$

The figure is about 2 to 3 per cent, especially at low currents. This requires great accuracy in measuring U'. The error depends on the slope of the impulse current and must be minimized.

The figure is about 2 to 3 per cent, especially at low currents. This requires great accuracy in measuring U'. The error depends on the slope of the impulse current and must be minimized.

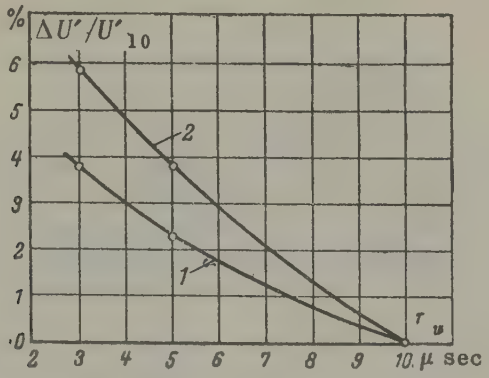

Fig. 1. The post-breakdown voltage on an arrester with vylite resistor discs 70 mm in diameter and 20 mm thick as a function of the length of the current wavefront:

$1 - I_{max} = 2.5$ kA; $2 - I_{max} = 5$ kA.

To achieve an acceptable degree of accuracy, use was made of compensation for the main part of the voltage to be measured so that a voltage of about 15 per cent of U_{max} was recorded on the oscillogram. Thus the oscillogram sensitivity was about 20 V/mm at values U_{max} equal to 3-5 kV. An impedance voltage divider was set up at the oscillograph, but its resistance was sufficiently low to avoid errors due to the capacitance connected in parallel with the lower arm of the divider (the time constant of this circuit did not exceed 3×10^{-8} sec).

Figure 1 shows the ratio $\Delta U'/U'_{10}$ as a function of τ_w for vylite discs. The experimentally-determined values of $\Delta U'/U'_{10}$ agreed satisfactorily with previous results. Thus, a reduction in length of the current wavefront from 10 to 5 μsec at 5 kA resulted in a 3.8 per cent increase in the post-breakdown voltage on the discs 70 mm in diameter (this is equivalent to a 10 kA current through resistors 100 mm in diameter for RVS arresters).

Figure 2 shows the curves for $\Delta U'/U'_{10} = f_2(\tau_w)$ in respect of tervite discs 70 mm in diameter and 20 mm thick at 2.5, 5 and 10 kA. It will be seen from a comparison of Figs. 1 and 2 that the variation of the post-breakdown voltage is greater on vylite discs than on tervite discs given the same current density. There is only a comparable change

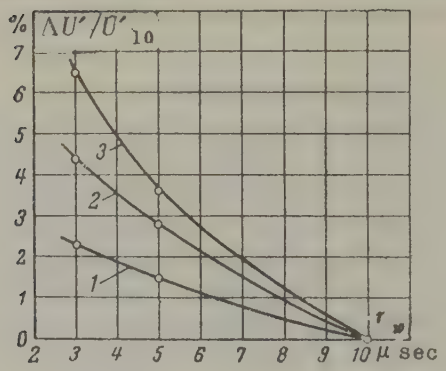

Fig. 2. The post-breakdown voltage on an arrester with tervite resistor discs as a function of the length of the current wavefront:

1 – I_{max} = 2.5 kA; 2 – I_{max} = 5 kA; 3 – I_{max} = 10 kA.

in U' on both types of disc if the current density is approximately halved on one of them. The increase in $\Delta U'/U'_{10}$ with an increase in the length of the current wavefront adversely affects the non-linearity

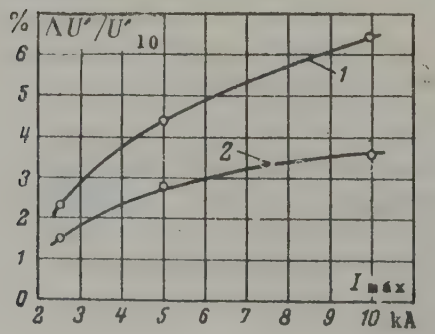

Fig. 3. The post-breakdown voltage on an arrester with tervite discs 70 mm in diameter and 20 mm thick as a function of I_{max}:

1 – τ_w = 3 μ sec; 2 – τ_w = 5 μ sec.

a of the resistor at large currents if τ_w is decreased. The corresponding data for tervite discs at 2.5 to 10 kA is given below.

τ_w μsec	a
3	0.208
5	0.190
10	0.173

Figure 3 illustrates the relationship between the post-breakdown voltage and the amplitude of the current impulse. These curves provide and estimate of $\Delta U'/U'_{10}$ in combined arresters in which tervite discs are used. Thus, for example, the post-breakdown voltage changes about 3 per cent on a 500 kV arrester at standard impulse current density if the length of the current wavefront is reduced from 10 to 3 μsec.

Translated by O.M. Blunn

REFERENCES

1. E. Beck; *Trans. Amer. Inst. elect. Engrs.* 70, pt. II, 1134 (1951).

2. *Regulations for the surge protection of electrical a.c. equipment 3-220 kV (Rukovodyashchiye ukazaniya po zashchite ot perenapryazhenii elektrotekhnicheskikh ustanovok peremennogo toka 3-220 kv).* Gosenergoizdat (1954).

3. A.M. Opsahl and N.K. Osmundsen; *Westinghouse eng.*, 3, 88 (1957).

4. A. Rusck and B.G. Rathsman; *ASEAJ*, 26, No. 3-4, 67 (1953).

5. A.I. Piryazeva; *Proceedings of the scientific conference on overvoltages (Trud. nauchno-tekh. sessii po perenapryzheniyam)*, p. 185, Gosenergoizdat (1950).

DISCRIMINATIVE EARTH-FAULT INDICATION*

V.V. SHUT'

(Odessa)

(Received 10 August 1960)

No device has hitherto been perfected for discriminative earth-fault indication in compensated three-phase high-voltage networks. Previous attempts to develop such a device have not produced satisfactory results.

In 1936 Neigebauer [1] proposed an electronic device which determined the fault direction from the sign of the first half-wave of the transient current. The device was not reliable in operation owing to the rapid ageing of the valves as a result of the permanently heated state of the cathodes. It was also necessary to re-adjust the circuit when replacing valves. Maranchak [2] improved this system in 1955 and evolved a method of designing its individual parts, but the main disadvantages remained.

In 1956 Darchenko and Stepnov [3] proposed the use of an electromagnetic relay which used a restraint winding which took the sign of the first half-wave of the earth current into account. This method can be employed successfully at remote points from supply sources where the frequency of the transient current is low. But experience has shown that it is unsuitable for power stations and large substations since the device is non-selective when the frequency of the transient current is high.

In 1958 Raik [4] developed a "manually-operated" device for determining the direction of the fault in which the sign of the active component of the earth current was tested and compared alternately. This device did not satisfy elementary requirements.

In 1959 Kalendo proposed the use of a system of polarized relays but

---

* *Elektrichestvo*, 10, 68-71, 1961.

none have as yet been made which will operate after the first half-wave of the transient current (a fraction of a millisecond).

In this paper a description is given of a device, proposed by the author, which has been tested in the Odessa power system. The device uses the transient currents in the system during the first few instants after an earth fault.

Earth faults may occur because of a gradual deterioration or sudden rupture of the insulation. In either event the rate of voltage build-up at 50 c/s exceeds the rate at which the earthed object "approximates" the phase, so that in the overwhelming majority of cases the breakdown occurs at an instantaneous value of the phase voltage which is 70 per cent or more of maximum, i.e. the capacitance of the network under fault conditions is almost completely charged at the instant the breakdown occurs.

The discharge of this capacitance after the earth fault is a decaying oscillatory process. Numerous tests have shown that the decay time constant in modern networks is approximately $0.285\ \omega_0$.

In designing the system of protection it is important to know the frequency f_0 of the oscillations in the discharge process. It can be found from the following formula

$$f_0 = \frac{1}{2\pi}\sqrt{\frac{1}{LC} - \left(\frac{R}{2L}\right)^2},$$

where L is the inductance across which the capacitance of the fault phase is discharged, C the phase capacitance, and R the resistance into which the discharge takes place.

Ignoring the resistance and assuming that the inductance L is equal to the inductance of the reactor, and that the voltage on the bus bars is not reduced during the short circuit, then

$$L = \frac{U}{\omega I_k}$$

and, furthermore

$$C = \frac{I_C}{\omega U}.$$

Consequently

$$f_0 = f\sqrt{\frac{I_k}{I_C}},$$

where I_k is the steady-state short-circuit current at the earth point

(easily determined by a network analyser, an analogue of the network or by analysis); I_C is the earth-fault current in the absence of compensation, defined as the sum of the earth and arc-quenching coil currents for under-compensation, or as the difference between those currents for over-compensation; and f is the supply frequency.

Oscillograms taken in numerous experiments have shown that formula (1) produces accurate results in spite of its simplification.

The current discharges from the capacitance of the non-faulted connexions across a zero-sequence current transformer $ZSCT$ into the bus bars, and then across another zero-sequence current transformer in the direction of the actual point of the earth fault. The discharge current across this second transformer is in the opposite direction to that across the first transformer, regardless of the sign of the charge in the phase where the fault has occurred. The direction of the discharge current across the transformers in any half-wave can be used to determine the faulty connexion. The most convenient half-wave for this purpose is the first one, since it is in this half-wave that the amplitude of the current is greatest. The filter illustrated in Fig. 1 is a very convenient device for isolating this half-wave.

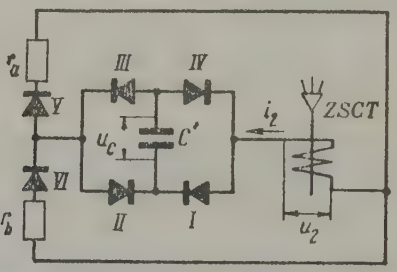

Fig. 1.

On flow of the decaying sinusoidal oscillatory discharge current through the zero-sequence current transformer, the capacitor C' is so connected that the voltage to the secondary winding of the transformer is always the same in sign.

At the first instant after the earth fault, u_2 is greater than u_C and the capacitor is charged from the transformer ($ZSCT$) via the resistance r_a and rectifiers *I*, *III* and *V*, or via resistance r_b and the rectifiers *II*, *IV* and *VI*, depending on the sign of the discharge current. The current across either of these resistances is quite large in the first instant and the potential difference between their

terminals is comparatively large. This process continues until $u_2 = u_C$.

As soon as $u_2 < u_C$, a rather small current flows into r_a (or r_b) which depends on the difference between u_2 and u_C, the large resistance of the three series-connected rectifiers and the output resistance r_a (or r_b). In this situation the capacitor is slightly discharged and its voltage is reduced, so that in the second half-wave the voltage u_2 may again be greater than u_C. But this difference will be very small and the current through r_a (or r_b) will also be small accordingly (see Fig. 2).

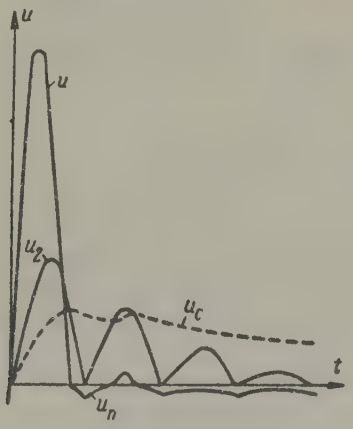

Fig. 2.

Tests have shown that a voltage surge occurs in the first half-wave at the output of r_a (or r_b) which in amplitude is equal to

$$U = \sqrt{2}U_2 \frac{f_0}{f_T} K,$$

where U_2 is the effective value of the voltage across the secondary winding of the transformer, found experimentally by passing a current I_C at a frequency f_T (close to f_0) through the secondary winding of the current transformer; K is the characteristic of the filter:

$$K = \vartheta[e^{-\tau t}(\eta \cos \omega_0 t + \rho \sin \omega_0 t) - \lambda e^{-\mu t}],$$

where

$$\vartheta = \frac{1}{\omega_0^2 + \left(\frac{1}{rC'} - \tau\right)^2}; \quad \tau = 0.285\omega_0;$$

$$\lambda = -\frac{1}{rC'}\left(\frac{1}{rC'} - \tau\right); \quad \eta = \left(\frac{1}{rC'} - \tau\right) - \omega_0;$$

$$\mu = -\frac{1}{rC'}; \quad \rho = \frac{\omega_0}{rC'}.$$

The filter characteristic K is between 0.35 and 0.25 at the frequency f_0 if $r = 1000\ \Omega$ and $C' = 0.5\ \mu F$. When $u_2 < u_C$, the "noise" voltage at the output is

$$U_n \leqslant \sqrt{2}U_2 \frac{f_0}{f_T} \cdot \frac{r}{2nr_0},$$

where r_0 is the back resistance of one rectifier, and n the number of series-connected rectifiers in one arm of the bridge.

Tests have shown that the filter reliably isolates the first half-wave of the non-decaying voltage as well as the decaying voltage.

In the presence of an earth fault a voltage is seen instantaneously across r_a or r_b depending on the sign of the first half-wave of the capacitor discharge current through the zero-sequence current transformer. This voltage does not appear across the same resistance in the direction of the fault as in the opposite direction. The voltage across either of the output resistances is supplied to the cathode and ignitor of one of the non-filament thyratrons in which there is always a voltage between the anode and cathode (see Fig. 3).

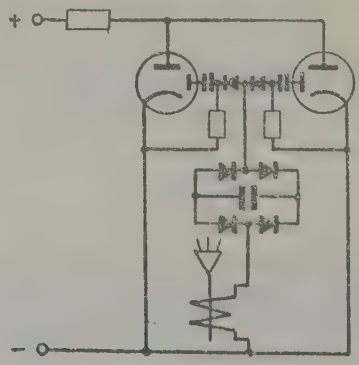

Fig. 3.

One version of the indication device is intended for use in conventional substations in which personnel are on duty. The device has a number of "cells" such as that illustrated in Fig. 3. The thyratron

itself is quite a good indication device. The thyratrons are arranged in two rows (Fig. 4), two thyratrons for each direction (one in each row). An upper thyratron lights up during the first half-period if the discharge current is away from the bus bars. A lower one lights if the current is towards the bus. The thyratrons light in different rows depending on the direction of the discharge current. The signal is acknowledged manually by the duty personnel.

Fig. 4.

The signal may also be transmitted from fully automatic substations to a central despatcher point by television. However, in this case the signal cannot be repeated indefinitely until acknowledged unless the system illustrated in Fig. 5 is adopted. This system is also able to transmit signals by conventional telecommunication equipment as well as by television.

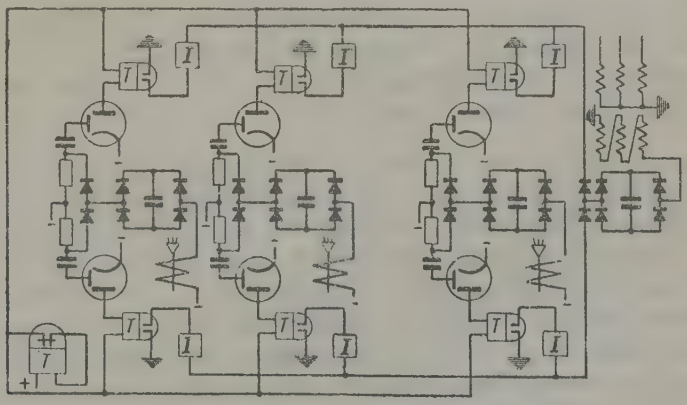

Fig. 5.

In this system the discharge current i in the first period is compared with the zero sequence voltages u_0, which are always identical in the direction towards the fault.

The zero sequence voltage comes to the upper or lower row of

indicator relays depending on its sign. The indicator relays only operate in the row to which u_0 is applied and only for that direction for which one of the thyratrons has fired. If the outgoing zero sequence voltage leads of the filter are correctly connected, this combination of events will only occur at the faulted connexion.

All the anode circuits are supplied via a common relay which has normally closed contacts which only open after a time lag. This relay disconnects the thyratrons for sufficient time to allow the indicator relays to operate and the capacitors of the filters to discharge. Repeated operation is therefore possible in the event of intermittent faults.

Only the earth-fault signal of a particular substation can be transmitted to the central despatcher point. On receipt, service engineers are sent to restore the supply, disconnect the section with the fault and to carry out the necessary inspection and repairs. Use is made of indicator relays with signal flags which drop down and cannot return of their own accord.

Operating experience has shown that simultaneous intermittent earth faults in different directions are highly improbable, so that the simpler and more reliable system illustrated in Fig. 3 should be used wherever possible. But even the system shown in Fig. 5 is not particularly complicated. It consists of ordinary electromagnetic relays. No special requirements have to be satisfied as regards operating, since they only have to operate in a quarter of a period of the operating frequency (50 m sec). Numerous relays such as the ET, ES and ESh types operate three to four times as fast.

The proposed earth-fault systems differ from the earlier system of Neigebauer and Maranchak in that the first half-wave of the transient current is isolated by a special filter and not by "cutting off" the circuit. The proposed systems differ from those put forward by Darchenko and Stepnov in that they react to the direction of the current in the first half-wave and are practically independent of amplitude so that the effective range is much wider. Performance is independent of the operating speed of mechanical relays, which is not the case with the systems proposed by Kalendo, Darchenko and Stepnov.

Ordinary batch-produced items and economical non-filament thyratrons, semiconductor diodes, etc, are used.

The author has thoroughly tested the systems and all that has been written about them in this paper is authentic. The equipment has shown itself to be simple, selective and completely reliable.

Translated by O.M. Blunn

REFERENCES

1. Kh. Neigebauer; *Energet. obozrenie*, No. 8 (1936).

2. V.M. Maranchak; *Elektrichestvo*, No. 11 (1955).

3. V.E. Darchenko and T.V. Stepnov; *Elektrichestvo*, No. 2 (1956).

4. M.N. Raik; The protection of generator-transformer units from earth faults (Zashchita ot zamykanii na zemlyu blokov generator-transformator). *Energetika za rubezhom, ser. rel. zashchita*, No. 3 (1960).

5. Yu.I. Kalendo; A device for indicating earth faults in compensated networks (Ustroistvo dlya signalizatsii o zamykanii na zemlyu v kompensirovannykh setyakh). *Byull. izobretenii*, No. 23 (1959).

ABSTRACTS FROM PAPERS PUBLISHED IN ELEKTRICHESTVO No. 10, 1961.

Editorial

The great programme for building communism, (pp. 1-5).

The article defines communism from the party programme and briefly considers the next twenty years of development. The role of the communist party is discussed along with the part to be played by science in forming the material-technical basis of communism.

Automatic control

Charging a capacitor from an a.c. circuit through a valve. S.M. Smirnov, (pp. 60-64).

A study is made of the process of charging a filter capacitor by sinusoidal voltage pulses. Cases of purely capacitive and capacitive-active loads of rectifiers connected in half-wave and full-wave rectifying systems are considered.

Transforming Grey's code into a binary code. V.A. Kougiia, (p. 74).

The direct use of Grey's parallel code for control devices in servo systems (e.g. for determining the angle of rotation of shafts) is not considered convenient in programme control systems based on potential logical elements. Accordingly a system of transforming Grey's code into a parallel binary code is suggested.

Control engineering

Fundamentals for constructing a standard series of automatic motor drives for multi-cable mine hoists. V.S. Tulin, (pp. 12-19).

A study is made of the regulations and standards governing mine hoisting and lifting equipment with a view to forming a theoretical

basis for standardization and greater efficiency in electrical drives.

An instrument for measuring active power. Ia.I. Stiop, (pp. 65-66).

A description is given of a device for measuring power in which the main part, used to square the sum and difference of the input quantities (current and voltage), uses thyrite elements as the non-linear resistors with a load resistance to adjust the voltampere characteristic.

A controllable d.c. drive. A.I. Ioffe, (pp. 71-73).

A study is made of a new variable d.c. drive with a simple converter. The drive is based on a typical d.c. motor with independent excitation with its speed controlled by varying the voltage applied to the armature from the converter. The converter consists of a three-phase transformer with primary windings connected in star and connected to the a.c. network. The secondary windings have different numbers of turns so that the e.m.f. is different in each winding. Rectified voltages can be fed to several drive motors at different speeds.

Power systems

Appraising electric power costs in designing industrial plants. D.S. Stepanov, (pp. 6-11).

The estimation of the cost of electrical energy in planning industrial undertakings is considered in the light of socialist methods of planning without resort to existing tariffs.

Relays and protection

The behaviour of overcurrent relays during out-of-step conditions in a power system. S.E. Stepurin, (pp. 55-60).

Investigations have confirmed that overcurrent relays may operate incorrectly during out-of-step conditions of the generators. It is proposed to overcome this by adjusting the reset time of the relay or using a voltage starting relay with a particular voltage setting. The method of analysis is also applicable to other types of voltage and current relay.

The relationship between the Curie point and the composition of copper-zinc ferrites. A.I. Andriyevskii *et al.*, (pp. 66-68).

An account is given of investigations into copper-zinc ferrites of various compositions corresponding to values of the Curie point between the boiling point of liquid nitrogen and 460°C. The Curie points of the compositions were determined to within 4 to 6°C by a method which is described. Particular compositions are used for thermal relays which are also described.

Rotating machines

The maximum torque of coal-cutter induction motors connected in mine networks. E.S. Traube, (pp. 19-23).

In order to ensure the necessary conditions for a highly efficient performance from coal-cutting combines, the author seeks to elucidate the maximum possibilities of mine networks by finding the general laws which govern the variation of the actual torque of induction motors. Test results appear to confirm the theoretical propositions.

Locus diagrams for synchronous generator control devices with phase compounding. V.N. Breev *et al.*, (pp. 29-34).

The properties of the various control devices in the steady-state excitation circuit of generators with phase compounding are described by a single diagram so that the effect of the parameters of individual circuit elements on the excitation current can be established and so that a preliminary selection can be made of requisite initial coefficients depending on the regulation and forcing of the excitation current.

A new way of mounting brushes in electrical machines. V.G. Gurin, (pp. 47-48).

An account is given of tests and calculations which indicate that the most efficient position of "reactive" brushes in electrical machines is that with trailing brushes at angles greater than 10 or 15° to the radial direction except when vibration is excessive.

The performance of a three-phase induction motor having an unequal number of turns i the stator phases. I.M. Kamen', (pp. 48-52).

General equations are formed for the analysis of the operating conditions of non-salient pole machines having a three phase winding with identical phase zones, but with different numbers of turns in the phases.

Synchronous machine damper winding losses due to voltage time harmonics. Iu.A. Kulik, (pp. 34-37).

A study is made of the effect of voltage harmonics on the currents of the damper winding and the resultant losses. The distribution of the currents in the damper winding is analysed and the total losses caused by higher time harmonics are determined by the mean square value of the current in the conductor of the damper winding.

THE MERCURY-ARC RECTIFIER DRIVE*

B. M. GUTKIN

(Vniiem)

(Received 21 August 1961)

The MAR drive is a complex electromechanical system. In the past the control system of the rectifier has not been regarded as an integral part of the whole system of regulation, and no account has been taken of the requirements which rectifier control systems should satisfy.

As a result it has not been possible to take full advantage of the many valuable features of mercury-arc rectifiers in all applications, and this is especially the case with the electrical drive.

The extensive use of MAR drives in industry during the past 10 to 15 years has not only stimulated progress in the design of new rectifiers, but it has also brought about a rather new approach to the development of drives in which the rectifier is regarded as one element of the whole automatic control system, and in which the control system of the rectifier is regarded as the main element on which the whole system of regulation depends.

Much has been written about such drives in the Soviet and foreign press [1,2,3 *et al.*]. The control system elements of actual rectifiers and drives have already been considered as a whole [4]. In this paper attention is confined to pressing problems which, if solved, could be instrumental in the production of highly reliable MAR drives with a great dynamic Q-factor.

There is a great variety of drive control circuits, but they can be classified as follows, independently of the power circuits of the rectifiers and control systems:

1. Circuits in which control is effected by varying the voltage

---

* *Elektrichestvo*, 11, 14-22, 1961.

applied to the motor armature.

2. Circuits in which control is effected by varying the excitation current.

3. Circuits in which control is effected by varying the excitation current as well as the voltage applied to the armature. Such circuits will be referred to as "hybrid" circuits.

In order to simplify the study, it is proposed to consider irreversible and reversible systems separately.

MAR drives range from 0.05 to 10,000 kW. Small and medium drives are widely used in general engineering, particularly in machine tools. Large drives are used in the iron and steel industry and in mining.

Irreversible systems

Figure 1 shows the circuits of small and medium irreversible drives. The system illustrated in Fig. 1a uses a semi-controlled single-phase bridge system. If hot cathode bulbs are utilized, this system can be used for powers varying from 0.3 to 2 kW. Since no transformer is employed, the motor voltage is non-standard and it must be matched with the supply grid voltage. The system shown in Fig. 1b can be recommended for use in drives up to 200 kW depending on the type of rectifier bulbs, hot cathode bulbs being used up to 20 kW and pool cathode bulbs for larger outputs.

Systems without transformers are very promising for small drives, since their weight and cost can be reduced and they are a better economic proposition.

For large outputs it is advisable to employ transformers. Power circuits of large irreversible drives are illustrated in Fig. 2.

Here the current cannot change direction owing to the unidirectional conductance of the bulb. When the motor e.m.f. becomes greater than the converter rectifier voltage, the current in the main circuit is zero and the motor starts to "coast". Additional apparatus is therefore required in these systems to provide electrical braking.

All irreversible drive systems can accordingly be classified by the method of braking into those with dynamic braking and those with regenerative braking.

Dynamic braking is employed in the circuits illustrated in Figs. 1 and 2. When the motor e.m.f. becomes greater than the rectifier voltage, the current in the main circuit is zero, and this can be used as a

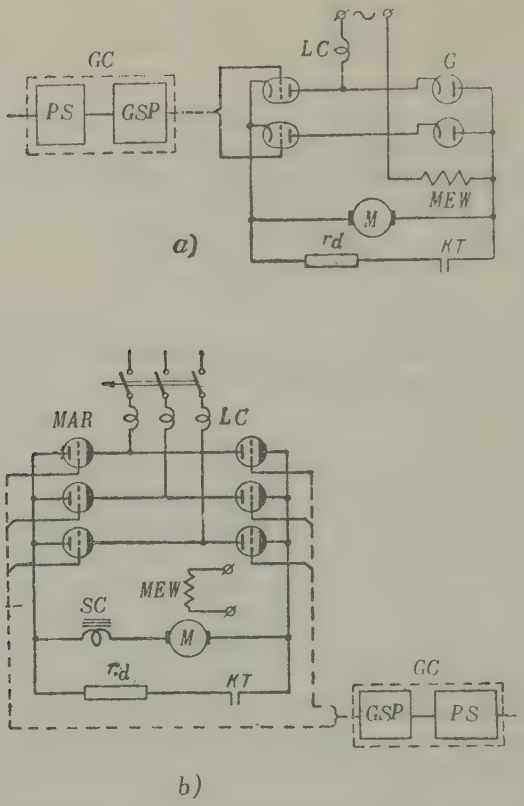

Fig. 1. Small and medium non-reversible MAR drives.

a – semi-controlled single-phase bridge circuit; *b* – three-phase bridge circuit; *PS* – phase shifting system; *GSP* – grid supply panel; *GC* – grid control system; *T* – thyratron; *G* – gas-filled rectifier (gazotron); *MAR* – mercury-arc rectifier; *M* – motor; *MEW* – motor excitation winding; *LC* – limiting choke; *SC* – smoothing choke; *KT* – brake contactor.

control signal for operating the dynamic braking contactor *KT* (Fig. 1). The motor and rectifier are then connected to the dynamic braking resistance r_d where the energy from the rectifier and the kinetic energy stored by the drive is dissipated. This is a widely used method of braking, but though it may be acceptable for small and medium drives, it cannot be regarded as satisfactory for large drives with special braking conditions.

An alternative method of dynamic braking employs a special measuring

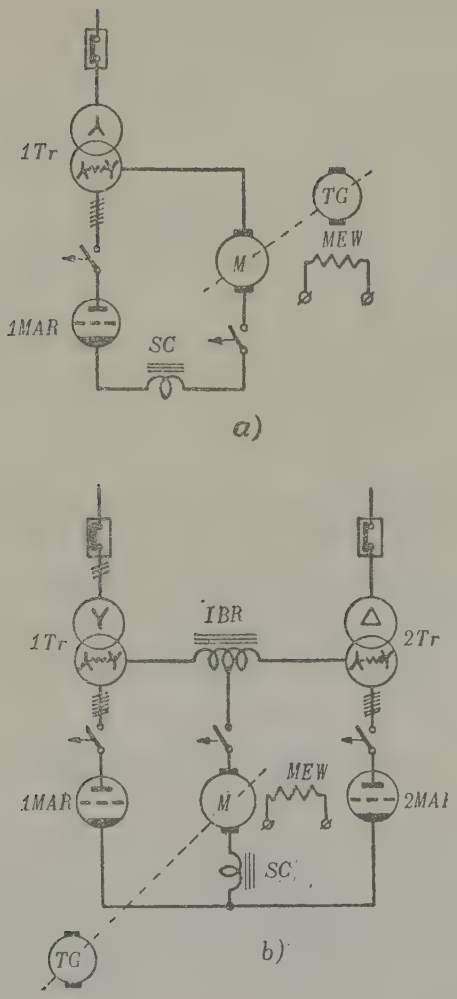

Fig. 2. Large non-reversing MAR drives.

a – six-phase circuit; *b* – twelve-phase circuit; *1 MAR*, *2 MAR* – mercury-arc rectifiers; *1 Tr*, *2 Tr* – anode transformers with built-in balancing reactors; *BR* – type-2 balancing reactor; *SC* – smoothing choke; *M* – motor; *TG* – tachometer generator.

device which operates on the cessation of current in the main circuit. It then either acts on the grid circuits of the rectifier and turns the rectifier "off", or else disconnects the rectifier from the load by special apparatus. Neither method provides smooth control over the

current whilst braking, and it becomes necessary to switch the resistance r_d. If it is decided to use such switching apparatus, it is advisable to follow the system illustrated in Fig. 3.

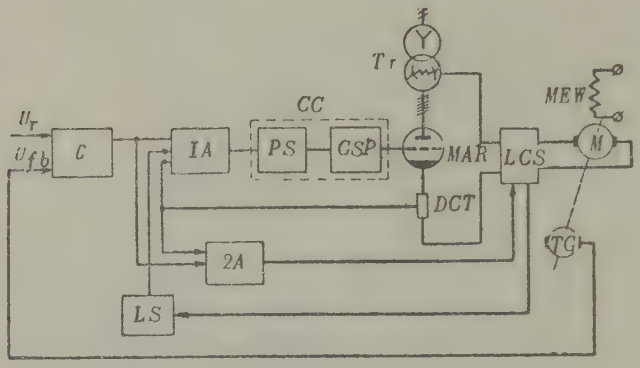

Fig. 3. Functional block-diagram of MAR drive with a switch in the armature circuit.

Tr – anode transformer; *MAR* – mercury-arc rectifier; *LCS* – load circuit switch; *M* – motor; *DCT* – d.c. transformer; *PS* – phase shifting system; *GSP* – grid supply panel; *GC* – grid control system; *C* – comparison circuit; *LS* – limiting system; *1A* – amplifier of regulating device; *2A* – switch amplifier; U_r – reference voltage; U_{fb} – feedback voltage; *TG* – tachometer generator.

Here the armature circuit is switched by a special switching amplifier which receives a control signal at its input, whilst the windings of the armature circuit switch are connected at its output.

Speed control in a closed system is governed by a law which may be written in the form

$$U_c = \mu (U_r - K_{fb} U_{fb}), \tag{1}$$

where U_c is the control signal at the input to the governor, U_r the reference voltage, K_{fb} the feedback factor, U_{fb} the feedback voltage, and μ the amplification factor of the amplifier.

A change in sign of the control signal determines the required mode of operation of the converter. If $U_r > K_{fb} U_{fb}$ and $U_c > 0$, the rectifier operates as a rectifier, but if $U_r < K_{fb} U_{fb}$ and $U_c < 0$, braking is necessary and the rectifier must act as an inverter. For switching the armature circuit without interruption of the current, it is necessary

to employ interlocking which allows switching only if $I_d = 0$. It will be seen from a consideration of the regenerative braking system that systems with a switch in the load circuit can also be used in reversing drives, in which case the rectifier acts as a rectifier in clockwise and anti-clockwise rotation in different positions of the switch. The rectifier characteristics are then in quadrant *I* and those of the inverter are in quadrant *IV*.

Reversing systems

The reversing drive has a switch in the armature circuit, but in some cases, and especially for drives with a short time cycle and servo systems with zero mis-match, it is necessary to arrange for continuous control without a switch in the armature circuit. It is then advisable to use systems with two sets of bulbs. It should be noted that for a long period of time articles have been published in the foreign press on reversing drives with a switch in the armature circuit, but recently there has been a tendency to change over to systems with two sets of rectifier bulbs for large drives. The power circuits of mercury-arc rectifiers with two sets of bulbs have been somewhat improved in recent years and they have become a better economic proposition since the "counter-parallel" system has been adopted. The "cruciform" system is rarely used.

"Mercury-arc exciters"

For a long time, relay-contactor systems were used for the excitation of electrical machines in controlled d.c. drives. Contactless systems of excitation have since been developed and amplidyne systems in particular. For large machines, amplidyne excitation systems represent a multi-stage system in which an amplidyne with a longitudinal or transverse field is used as the first stage.

The amplidyne allows adequate stabilization of the transient behaviour, but reductions in the duration of transient behaviour and their associated increase in productivity are limited by the inertia of the stage system of excitation. A mercury-arc rectifier is a delay-free apparatus, and therefore its use in excitation systems for large d.c. drives opens up new possibilities both as regards higher productivity and new flexible and reliable static systems of excitation.

It is proposed to refer to mercury-arc rectifiers which are used for electrical machine excitation as *mercury-arc exciters*. Mercury-arc exciters are not only used when the amplidyne system of excitation is a multi-stage one, but whenever high-speed super-quality control is

required.

Mercury-arc exciters may be reversible or irreversible exactly like their rectifier counterparts.

Mercury-arc exciters which maintain the same direction of current at the output can be used for excitation of generators and the motors of non-reversing drives. Those which do provide for the reversal of current can be used for the excitation of generators and motors in reversible drives.

The power P_r of the rectified output of a mercury-arc exciter depends on the forcing factor which is required for minimizing transient behaviour and is given by the expression

$$P_r = k_f U_d I_d 10^{-3} \text{ [kW]}, \tag{2}$$

where U_d is the rated voltage of the excitation winding of the electrical machine, I_d the rated excitation current of the electrical machine, and k_f the forcing coefficient.

Under rated conditions a mercury-arc rectifier operates with large control angles, which ensures large amplification factors and eliminates the effect of variations in the supply voltage on the generator voltage if the control system is correctly designed. With forcing, the control angle is considerably reduced and the rectified voltage at the output of a mercury-arc exciter reaches 100 per cent, which in relation to the rated voltage of the excitation winding of the electrical machine is $k_f U_d$. On extinction of the field the mercury-arc exciter acts as an inverter ($\alpha > \pi/2$) and the electromagnetic energy stored in the excitation winding of the generator is returned to the network.

The power circuits of mercury-arc exciters can be made like those of mercury-arc rectifiers used for controlling the armature voltage. Since the inductance of the excitation winding of an electrical machine is considerable, mercury-arc exciters could utilize a minimum of phases, i.e. use could be made of a full-wave system of rectification, but three-phase systems are used for the sake of reliability. If one of the bulbs is out of order in the full-wave system, the electrical machine may practically lose its excitation, since the excitation current is then equal to $2U/\omega L$ and it is small if L is considerable.

In the general case the number of phases on the rectified current side depends on the design of the electrical machine and the bulbs used in the mercury-arc rectifier. Use may sometimes be made of hot cathode bulbs for the excitation of large generators. Pool cathode bulbs are generally used in mercury-arc exciters for the low-speed motors used in

the iron and steel industry and mining, owing to their considerable excitation currents.

If the direction of rotation of the motor is changed by reversing the field, then in order to obtain an acceptable reversing time for certain equipments, the power of each set of rectifier bulbs in a mercury-arc exciter is about 10 to 15 per cent of the power of the set of bulbs in the armature circuit. The further increase in power that might otherwise be obtained by forcing, or a shorter reversing time, is limited by the conditions of commutation. If machines with a laminated yoke are used, the field can be reversed in 0.2 to 0.7 sec depending on the power of the motor. Reversing drives can be produced for plant with a considerable time cycle in which the motor excitation field is reversed.

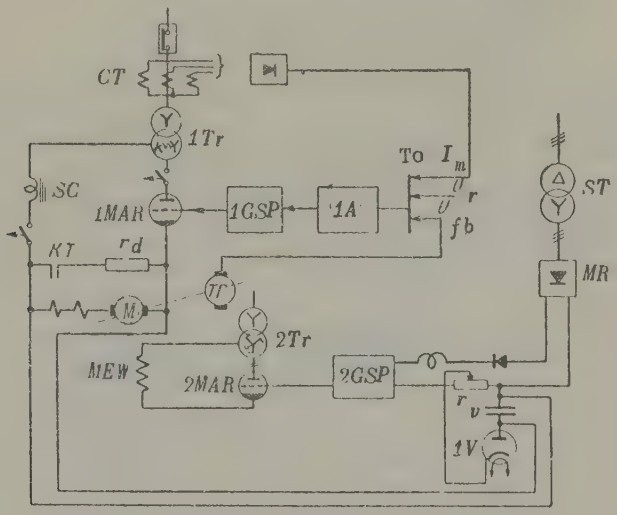

Fig. 4. Simplified circuit diagram of a non-reversing MAR drive of a light-section 350 rolling mill.

1 Tr – anode transformer of armature circuit switch; *2 Tr* – anode transformer of mercury-arc exciter; *1MAR, 2MAR* – mercury-arc rectifiers; *M* – motor; r_d – dynamic braking resistance; *SC* – smoothing choke; *MEW* – motor excitation winding; *KT* – braking contactor; *CT* – current transformer; *1GSP, 2GSP* – grid supply panels; *MR* – main voltage rectifier; *ST* – supply transformer of main voltage rectifier; *1V* – gas-filled rectifier (gazotron); r_v – variable resistance; *1A* – amplifier of armature voltage control system.

Hybrid control

In blooming mill drives speed is controlled up to fundamental speed by varying the armature voltage and at higher speeds by varying the excitation current of the motor. The presence of controlled mercury arc rectifiers in two circuits (i.e. the armature and excitation circuits) implies that the control system has to satisfy certain requirements which if left unfulfilled would result in sudden changes in current, flashover and other fault conditions.

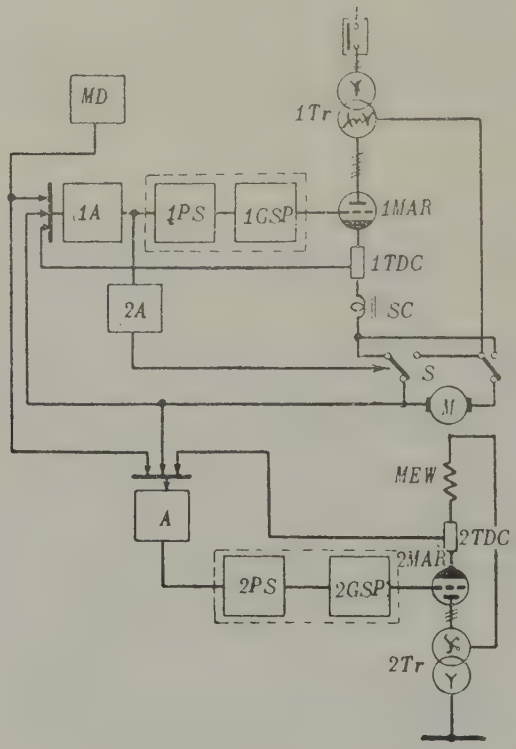

Fig. 5. Functional block-diagram of a hybrid control system for a reversing drive.

1 Tr, *2 Tr* – anode transformers; *1 TDC*, *2 TDC* – d.c. transformers; *1 MAR*, *2 MAR* – mercury-arc rectifiers; *1A* – regulator for voltage applied to armature circuit; *A* – regulater for excitation current; *1 PS*, *2 PS* – phase shifting systems; *1 GSP*, *2 GSP* – grid supply panels; *MD* – master device; *M* – motor; *MEW* – motor excitation winding; *SC* – smoothing choke; *S* – switch.

By way of illustration Fig. 4 shows a simplified fundamental circuit diagram for the drive of a 350 light section rolling mill using this type of hybrid control. The speed of the roll motor is controlled at first by varying the armature voltage. Afterwards, when the armature voltage reaches a pre-determined level, the "gazotron" (gas-filled rectifier) *1V* fires and the resistance in the magnetization winding circuits of the peak transformers is shorted, which alters the control angle of the mercury-arc rectifier in the excitation circuit of the motor and weakens the field.

Figure 5 shows a functional block-diagram of the hybrid control system of a reversing drive with a switch in the armature circuit. Both in this circuit and in those of non-reversing drives, a system of interlocking is used which only allows the field to be weakened at a predetermined value of the armature voltage.

The control of MAR drives

An MAR drive control system is defined as the complex of apparatus which participates in forming the control law. In accordance with this definition, that whole range of contact and contactless apparatus which is widely used in industrial drives for protection and starting, etc, is of no concern here. The control system elements under consideration in this paper are the amplifying and shaping devices and the electrical pickups.

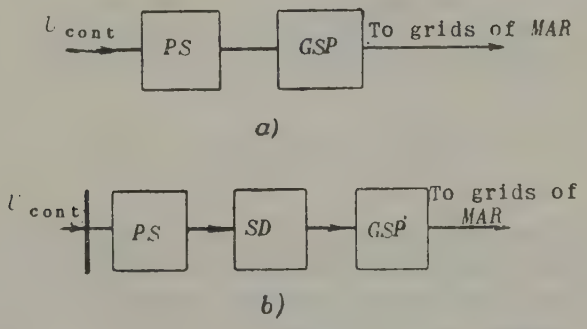

Fig. 6. Functional block diagram of a grid control system with controlled semiconductor rectifiers.

a – system with transistors in grod supply panel; *b* – system with transistors in the grid supply panel and phase shifting; *PS* – phase shifting system; *SD* – shaping device; *GSP* – grid supply panel; *MAR* – mercury-arc rectifier.

Increases in machine productivity are associated with larger drive outputs and faster operating speeds. An increase in speed makes exacting demands on the quality of the control system and its individual elements. In recent years there has been a tendency to replace electromagnetic apparatus by transistors in MAR control systems. All kinds of transistorized circuits have been developed, but functionally they all fall into either of two categories (see Fig. 6).

In the functional block-diagram in Fig. 6*a* the conversion of a sinusoidal voltage into a trigger pulse of given amplitude, width and slope is performed by transistors. The presence of active elements in the grid supply panel *GSP* allows a considerable reduction in the power of the static phase-shifting device *PS* and an improvement in the *Q*-factor of the control system, since low-power static phase shifters with a variable (alternating) active arm are then practicable. The method of varying the resistance of the active arm was originally proposed by Shipillo [5].

The majority of rectifier control systems fit the block-diagram in Fig. 6*b*. The principle of sawtooth voltage cut-off is used in the phase-shifting system. A control voltage is connected counter to the output of the sawtooth voltage generator and if these voltages are equal, the output voltage of the phase-shifting system is zero. The instant in time when the output voltage of the phase-shifting system is zero is moved in phase relative to the supply voltage on variation of the control voltage. This method of control has been referred to elsewhere as the "vertical" method. Sometimes a sinusoidal voltage is connected counter to the control voltage of the phase-shifting system and the instant of zero output voltage of the phase-shifter is then given by the expression

$$\omega t = \vartheta = \sin^{-1} \frac{U_{cont}}{U}. \qquad (3)$$

The instant of zero output voltage of the phase shifter is precisely the moment when the shaping process begins in the shaping device *SD*, which consists of a transistor and differentiating "cell"; and the moment when the positive trigger pulse is supplied.

Transistorized rectifier control systems are practically instantaneous and it is natural to require that the quality of all the other control elements should be equally as good.

Magnetic amplifiers are now widely used in MAR drive control systems. To improve the *Q*-factor of control systems using magnetic amplifiers, it is necessary to employ high-frequency amplifiers which require special supply sources.

Fig. 7. Block-diagram of a device with magnetic amplifiers and an independent supply source.

DCS – d.c. supply; *FC* – frequency converter; *MA* – magnetic amplifier.

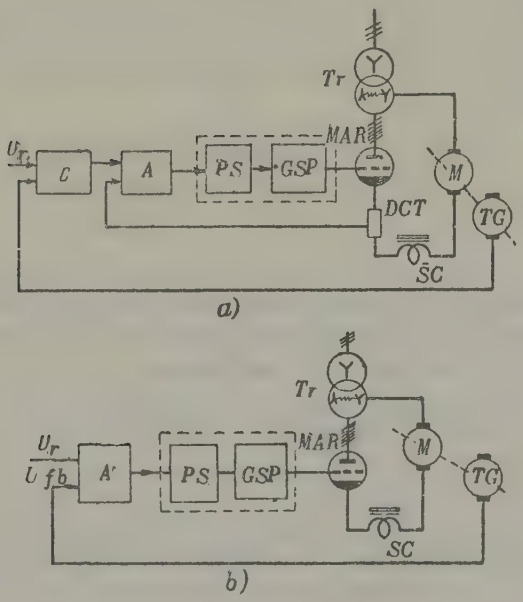

Fig. 8. Block-diagram of speed control system.

a – system with "electrical" comparison and negative current feedback; *b* – system with "magnetic" comparison; *Tr* – anode transformer; *MAR* – mercury-arc rectifier; *DCT* – d.c. transformer; *M* – motor; *TG* – tachometer generator; *C* – comparison circuit; *A* – amplifier of regulator; *PS* – phase shifting system; *GSP* – grid supply panel.

To dispense with special supply sources it is expedient to supply the magnetic amplifiers from an independent h.f. source in the form of a blocking oscillator or symmetrical transistorized multi-vibrator. It

should be pointed out that the frequency of such sources can be chosen in the light of constructional considerations. Various magnetic amplifier circuits with independent supply sources have been devised, but they all contain the elements indicated in Fig. 7.

A number of functional block-diagrams will now be considered to illustrate the design of MAR drive control systems.

Figure 8 shows functional block-diagrams of a system of speed control. In Fig. 8*a* the first element compares the desired speed with the actual speed as measured by a tachometer generator. The element is, as it were, a speed governor whose output defines the magnitude of the armature current. The second element compares the desired armature current, as obtained at the output of the first element, with the actual armature current as measured by a d.c. transformer or simple transformer in the a.c. circuit. Current feedback provides a simple means of stabilizing the system.

The system in Fig. 8*b* is not provided with current feedback and all the control signals are added, shaped and amplified in the first element of the control circuit.

Tachometer generators measure the speed in speed-control systems. These generators have to satisfy exacting demands if the demands made on the control system as a whole are stringent. The simplest form of speed-control law is that represented by expression (1).

The terminal voltage of an "ideal" tachometer generator is

$$U_{fb} = c_e \omega.$$

The terminal voltage of a real tachometer generator can be written in the form

$$U_{fb} = U_s + U_n, \tag{4}$$

where U_s is the useful signal voltage which is proportional to the speed, and U_n the voltage of the non-attenuated noise signal for the particular speed.

The expression for the noise signal is

$$U_n = m_1 \sin k_1 \omega t + m_2 \sin k_2 \omega t + m_3 \sin k_3 \omega t, \tag{5}$$

where

$$m_1 = \frac{\Delta U_{cp}}{K_{fb} U_{fb}}; \quad m_2 = \frac{\Delta U_{rp}}{K_{fb} U_{fb}};$$

$$m_3 = \frac{\Delta U_{mp}}{K_{fb} U_{fb}}; \qquad (6)$$

and ΔU_{cp} is the voltage amplitude of the collector oscillations, ΔU_{rp} the voltage amplitude of the reverse oscillations, ΔU_{mp} the voltage amplitude caused by oscillation in speed owing to eccentricity in the coupling of tachometer generator to the driven shaft, and $k_1\omega$, $k_2\omega$ and $k_3\omega$ the frequencies of the collector, reverse and "mechanical" oscillations respectively.

When considered with (4) and (5), expression (3) [sic] takes the form

$$U_c = \mu [U_r - K_{fb} U_{fb} (1 + m_1 \sin k_1 \omega t + \\ + m_2 \sin k_2 \omega t + m_3 \sin k_3 \omega t)]. \qquad (7)$$

A speed law of type (7) in a delay-free control system results in variation of the current in the main circuit and in speed variation if the moment of inertia of the motor and driven device is low. For partial elimination of such variation, use may be made of negative current feedback, but this reduces the amplification factor of the system, or alternatively powerful stabilizing feedback, although this adversely affects the dynamic properties of the system. High-frequency oscillations of the noise signal can be filtered out without difficulty if the degree of speed control is "light"; but it is a different matter with reverse oscillations and mechanical speed oscillations and the dynamic properties of the system suffer accordingly. This case has been specially considered in order to show that exacting demands have to be met by all the elements of the entire control system if an instantaneous rectifier control system with a high dynamic Q-factor is required. There is no justification for a delay-free rectifier control system on its own.

Figure 9 shows the functional block-diagram of a reversible MAR drive in which use is made of a mercury-arc rectifier with two sets of bulbs. The "counter-parallel" system is employed for the rectifier. A special circuit is used to limit the balancing current which arises in a mercury-arc rectifier with two sets of bulbs. The d.c. transformers *1TDC* and *2TDC* are included in the circuit for each set of bulbs. They are magnetic amplifiers with series-connected load windings.

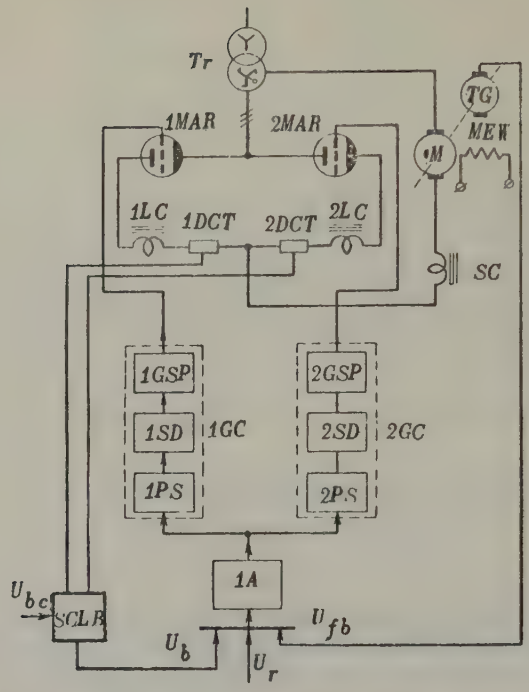

Fig. 9. Block-diagram of reversing MAR drive with two sets of bulbs.

Tr – anode transformer; *1 MAR*, *2 MAR* – mercury-arc rectifiers; *1 LC*, *2 LC* – limiting chokes; *SC* – smoothing choke; *1 DCT*, *2 DCT* – d.c. transformers; *1 GSP*, *2 GSP* – grid supply panels; *1 SD*, *2 SD* – shaping devices; *1 PS*, *2 PS* – phase shifting systems; *1A* – regulator amplifier; *SCLB* – special circuit for limiting balancing current; *1 GC*, *2 GC* – grid control systems for rectifiers; *M* – motor; *MEW* – motor excitation winding; *TG* – tachometer generator, U_r – reference voltage; U_{bc} – setting for magnitude of balancing current; U_b – voltage regulating the magnitude of the balancing current; U_{fb} – speed feedback voltage.

The balancing current and operating currents of the main circuit flow through the control windings of the d.c. transformers. The voltages in the secondary windings of the d.c. transformers will be different depending on the magnitude of the operating current and balancing current. This voltage is "rectified" in the special circuit (*SCLB*)

for limiting the balancing current, and it is compared in the amplification circuit with the "desired magnitude" of the balancing current. The deviation of the actual balancing current from the desired magnitude automatically alters the control angles of both sets of bulbs.

In a number of cases a control system with limitation of the balancing current provides better dynamic drive characteristics. The system illustrated in Fig. 9 can also be adopted to mercury-arc exciter control systems for generators in reversing drives.

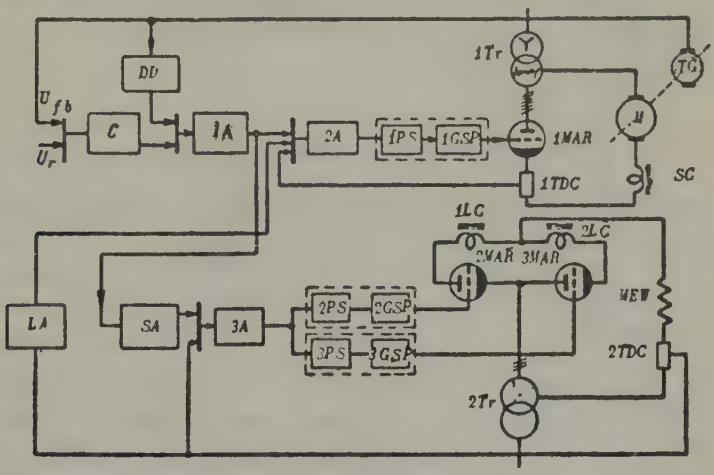

Fig. 10. Block-diagram of speed control system with two sets of rectifiers in the excitation circuit.

1 Tr, *2 Tr* – anode transformers; *1 MAR*, *3 MAR* – mercury-arc rectifiers; *1 LC*, *2 LC* – limiting chokes; *SC* – smoothing choke; *1 DCT*, *2 DCT* – d.c. transformers; *M* – motor; *MEW* – motor excitation winding; *TG* – tachometer generator; *C* – comparison circuit; *DD* – differentiating device; *1A* – adding amplifier; *2A* – amplifier of regulator for the armature circuit voltage; *3A* – amplifier of regulator for excitation current; *SA* – amplifier of excitation circuit switch; *LA* – amplifier for limiting of armature current; *1 PS* - *3 PS* – phase shifting systems; *1 GSP* - *3 GSP* – grid supply panels.

Figure 10 illustrates a possible drive system in which the speed is controlled by a mercury-arc rectifier in the excitation circuit of the motor. The armature circuit is supplied from the mercury-arc rectifier *1 MAR* which maintains the polarity of the rectified current constant. The excitation winding is supplied from the converter *2 MAR* which ensures reversal of polarity of the rectified current.

Unlike the system illustrated in Fig. 8, that in Fig. 10 provides for limited acceleration by virtue of the differentiating device *DD* whose input is connected to the tachometer generator. Reversal of the excitation current takes place on reversal of polarity at the output of the adding amplifier *1A*. On reversal of the field the output voltage of amplifier *1A* is limited by the limiting amplifier *LA* and the armature current decreases to zero. While the excitation current is steadying itself, it is necessary for the voltage at the output of *1A* to be limited so much that the rectifier in the armature circuit is "off". After the end of the process of field reversal, the system of acceleration limiting again comes into operation and protects the system from momentary excessive acceleration.

The reliability of MAR drives

The reliability of an MAR drive mainly depends on the reliability of the rectifier. In recent years a number of papers have been published in the U.S.S.R. and abroad [7,8,9, *et al.*] in which the probability of arcbacks has been determined and methods of reducing their probability have been suggested.

Actually the probability of arcbacks is only the main criterion of reliability for mercury-arc rectifiers operating as rectifiers (with pool cathode bulbs). In industrial plant where the mercury-arc rectifiers operate with large overloads, use has begun to be made in the U.S.S.R. of mercury-arc rectifiers with series-connected bulbs in order to reduce the probability of arcbacks.

It has been shown [9,10] that with series-connected bulbs the probability of arcbacks is equal to the product of the probabilities of arcbacks of the individual bulbs, and it can therefore be assumed that no arcbacks will occur at a voltage of 1000 V.

Figure 11*a* shows the simplified power circuit of a rectifier for the irreversible MAR drive of a rolling mill with a ratio of the load current amplitude to its mean value of 4 (at a mean current of the order of 3000 A). Arcbacks are very rare in this gear.

In the general case the reliability of an MAR drive depends on other factors besides the probability of arcbacks (which result in short circuits in the anode circuit): (*a*) the probability of extinction of the excitation arc in excitrons and the probability of failure to fire in ignitrons; (*b*) the probability of "break-through" of the grid; (*c*) the probability of faulty grid control.

Extinction of the excitation arc and the failure to fire of

ignitrons results in a short circuit in the load circuit when the rectifier is operating as an inverter. It is easy to show that there is twice the probability of short circuits in mercury-arc rectifiers with

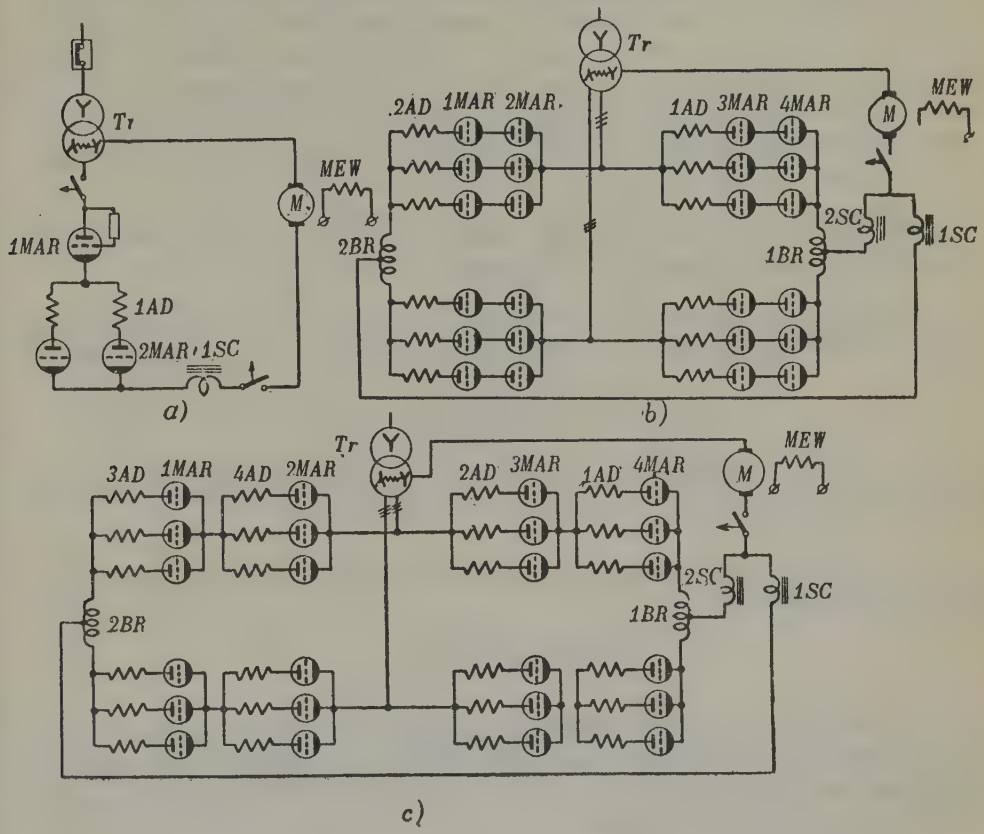

Fig. 11. Simplified circuit diagram of mercury-arc rectifier with series-connected bulbs.

a – circuit of converter for non-reversing drive; *b* – circuit of converter for reversing drive (with one set of anode dividers); *c* – circuit of divider for reversing drive with two sets of anode dividers; *Tr* – anode transformer; *1 MAR* - *4 MAR* – mercury-arc rectifiers; *1 AD* - *4 AD* – anode dividers; *1 SC* - *4 SC* – smoothing chokes; *1 Br*, *2 BR* – balancing reactors; *M* – motor; *MEW* – motor excitation winding.

series-connected bulbs (in this case the probabilities are added). An improvement in the reliability of MAR drives requires a great deal of theoretical and experimental research in order to obtain statistics of fault probability in particular bulbs and the rectifier as a whole.

The lack of statistical data results in a disproportionate increase in prime cost and running expenses for a small increase in reliability.

For example, Fig. 11*b* shows the circuit of a mercury-arc rectifier for a reversing rolling mill where series-connected bulbs are used. If both the bulbs in the series "chain" are controlled, the control system is greatly complicated, which can result in reduced reliability. If, however, the power circuit illustrated in Fig. 11*c* is used, there is nine times greater probability of arcbacks compared with that in Fig. 11*b*, but the control system itself is much simpler (in Fig. 11*c*).

The following calculation will show that a nine-fold increase in the probability of arcbacks is not very important in practice.

Suppose that one arcback occurs daily in each of the 18 bulbs of the three parallel circuits of a rectifier, i.e. the arcback probability is

$$P_1 = \frac{n}{Tf} = \frac{1}{24 \cdot 3\,600 \cdot 50} = 23 \cdot 10^{-8},$$

where n is the number of arcbacks, T the duration of arcback, and f the network frequency.

The probability of arcback with series-connected bulbs in each parallel circuit is

$$P_2 = P_1^2 = 5.3 \cdot 10^{-14},$$

i.e. an arcback will occur once in approximately 10^4 years. Naturally, if this figure is increased nine times there is in practice no significant increase in reliability, whereas operating costs are considerably reduced by the simpler system.

This example shows that the design of mercury-arc rectifiers has to be approached from all possible angles and that reliable gear can be designed which is cheaper to run. The scientific approach to the design of "reliable" MAR drives thus requires further investigation of currently produced rectifiers with a view to determining their reliability criteria.

Translated by O.M. Blunn

REFERENCES

1. J. Förster and H. Steinmüller; *AEG Mitt.*, No. 11/12 (1958).

2. D. Ströle and H. Vogl; *Regelungstechnik*, 6 (1960).

3. Ya. Yu. Solodukho; *The control apparatus of electric drives for continuous hot rolling mills (Avtomatika elektroprivodov nepreryvnykh stanov goryachei prokatki)*. Metallurgizdat (1960).

4. E.L. Ettinger, B.M. Gutkin and P.M. Borodavchenko; *Elektrichestvo*, No. 9 (1956); No. 1 (1957).

5. V.P. Shipillo; *MAR grid control systems for automatic electric drives (Sistemy setochnogo upravleniya rtutnymi vypryamitelyami dlya avtomaticheskikh elektroprivodov)*. Gosenergoizdat (1961).

6. J. Förster; *AEG Mitt.*, No. 11/12 (1958).

7. Th. Wasserab; *BB Mitt.*, No. 4/5 (1955); No. 3/4 (1956); No. 11 (1956).

8. M. Danders; *AEG Mitt.*, No. 11/12 (1958).

9. L.S. Fleishman; *Elektrichestvo*, No. 9 (1959).

10. J. Slepian and W.E. Pakala; *El. Eng.*, No. 6 (1941).

INVERTER SUBSTATIONS FOR OUTLYING REGIONS WITHOUT LOCAL POWER STATION COUNTER-E.M.F.'s*

N. M. MEL'GUNOV

(Leningrad)

(Received 2 December 1959)

The economical supply of electricity to outlying regions far from power systems and large power stations is an important aspect of the programme for general electrification in the U.S.S.R.

A d.c. transmission line costs much less than a comparable three-phase a.c. line. Centralized supply is therefore economic over much greater distances. Many new local power stations need not be built and some existing ones may be closed down.

The economy of d.c. transmission is not however determined by power and distance in absolute terms, but by the relationship between them. A small output can only be transmitted economically over a correspondingly shorter distance [1,2].

The essential problem is to develop simple and reliable terminal inverter substations. This is particularly so as regards inverter substations at the receiving end which have to operate with or without local power stations in the system (i.e. with or without counter-e.m.f.'s). This is a necessary condition for the exploitation of d.c. transmission on the largest possible scale.

In this paper it is proposed to consider and compare the principal inverter substation systems for operation into receiving systems without the counter-e.m.f.'s of local power stations. Such substations may differ from each other in design, performance, cost and reliability.

---

* *Elektrichestvo*, No. 11, 42-47, 1961.

1. Inverter substations with synchronous condensers

In this type of inverter substation the counter-e.m.f. required in the inverter for current commutation and the reactive power required for its operation and supplying the loads of the system are produced by a synchronous machine (see Fig. 1*a*) of a power 130 to 150 per cent of the rated active power of the substation inverter.

In order to improve the operating stability of the inverter in the presence of sudden load variations and provide an approximately sinusoidal voltage across its bus-bars, special measures must be taken to reduce the reactance of the machine. The operating stability of the inverter is favourably affected by lower values of the system power factor for an appropriately higher machine reactive power and excitation current; larger inertia constants of the machine also have a favourable effect.

Such a machine (synchronous condenser, generator) can be started at speeds and frequencies up to and including rated values by various methods from a small local power station or, if this is not available, from a special starting motor at the substation (e.g. a diesel engine). A synchronous condenser can be started direct by this type of prime mover or by an intermediate motor-driven generator. After running up the condenser and supplying the counter-e.m.f. to the inverter, the latter can be brought into operation in the usual way by control pulses to the valve (inverter) grids from the condenser bus and the supply of voltage along the line from the inverter. The power required subsequently for the operation of the condenser (and increasing its speed to the rated value if it has been below that figure) can be supplied from the d.c. line.

It is important to stress that in this type of inverter substation where the counter-e.m.f. is produced by a synchronous condenser, the control pulses must be supplied to the valves of the inverter for its stable operation from the bus of the synchronous condenser in the appropriate phase and not from an extraneous source of arbitrary phase.

In steady-state conditions the control system of this type of d.c. transmission must (*a*) maintain the quenching angle δ constant within given limits, (*b*) maintain rated voltage E_b across the inverter bus bars and (*c*) maintain the frequency f constant.

As regards the first requirement, this is necessary on the one hand because an excessive increase in δ results in an increased consumption of reactive power by the inverter and abrupt variation of the voltage across the inverter bulbs (a deterioration in operating conditions), whilst on the other hand a reduction in δ below 15 to 18° is dangerous

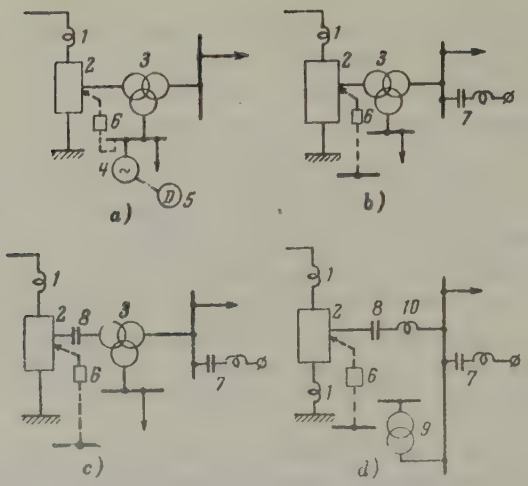

Fig. 1. Types of inverter substation for operation into a receiving system without the counter-e.m.f.'s local power stations.

a – system 1, with synchronous condenser; *b* – system 2, with parallel capacitor filter banks; *c* – system 3, with series-parallel capacitor phase compensation; *d* – system 4, with capacitive connexion of bridge converters; *1* – line reactor; 2 – bridge; *3* – transformer; *4* – synchronous condenser; *5* – motor; *6* – grid control; *7* – capacitor filter-banks; *8* – series capacitor banks; *9* – auxiliary and local supply transformer; *10* – phase reactors.

from the point of view of inverter reversal. The angle δ must therefore be held roughly constant during load variation or changes in inverter conditions.

The curves shown in Fig. 2 for the variation of the rectifier control angle α_r and the reactive power Q_c of the synchronous condenser as a function of the inverter load P_c have been calculated for an actual transmission system. Here the angle δ was held at appropriate constant values and conditions were also created to maintain f and E_b constant. The broken lines in the same diagram illustrate the upward shift of the α_r characteristic for δ = const when the rectifier voltage is increased by 5 per cent (e.g. by a tapping adjustment).

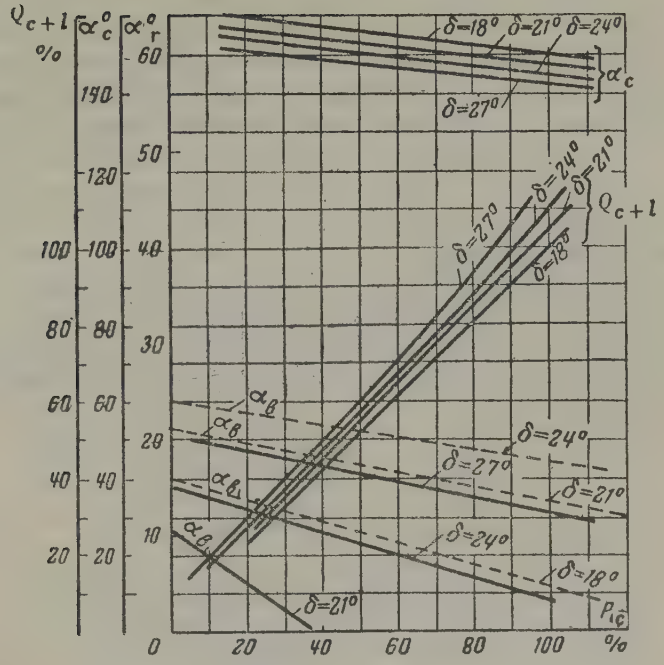

Fig. 2.

Various control systems can be employed in the design of an inverter with a synchronous condenser. The most efficient is as follows:

a) the angle δ is held constant across each inverter bulb by the supply of control pulses of appropriate phase α_c which is determined automatically for subsequent ignitions;

b) the voltage is automatically held constant on the inverter busbars by controlling the excitation system of the synchronous condenser;

c) the frequency of the receiving system is held constant by a frequency regulator which acts on the control angle α_r of the rectifier.

It is presupposed that the rectifier is provided with a maximum current regulator, so that the angle α_r can be adjusted by changing the setting, and that the inverter is provided with a minimum current regulator.

2. Inverter substations with parallel capacitor banks

Tests and calculations have established that synchronous condensers can be dispensed with, in which case, in order to ensure current commutation in the inverter and cover the reactive loads of the inverter in the network, use may be made of parallel capacitor banks (see Fig. 1*b*) in the form of several banks of filters for the higher current harmonics. For a six-phase inverter it is recommended that filters be used tuned to harmonics 5, 7, 11 and 13 with the bank power of the individual filters diminishing according to the increase in the harmonic number, and the overall bank power roughly equal to the reactive power consumption of the inverter and network at the rated inverter load. The presence of a set of such filters (or the first three of them) ensures that the appropriate current harmonics are short-circuited and the bus-bar voltage of the inverter is therefore approximately sinusoidal (see Fig. 3).

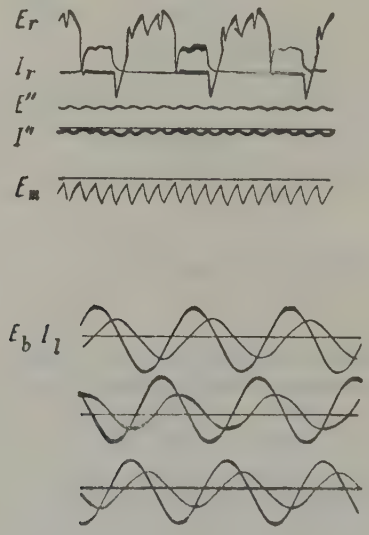

Fig. 3. Oscillograms of normal inverter conditions with a sinusoidal voltage ensured in the system by a set of parallel filter-banks.

The grid control of such an inverter must be effected from a separate independent control pulse source. The pulses are fed to the inverter bulbs at a fixed frequency (f = 50 c/s).

Figure 4*a* shows a vector diagram for the fundamental harmonic of the

current of an inverter with parallel static phase compensation under normal conditions. Figure 5 shows typical characteristics of the main operating indices when the inverter is regulated for varying active load. Changes in the angle δ are held within prescribed limits by automatic connexion and disconnexion of the individual filter banks. With decreasing active inverter load, the overall power of the connected capacitors is gradually reduced by disconnecting the individual filter

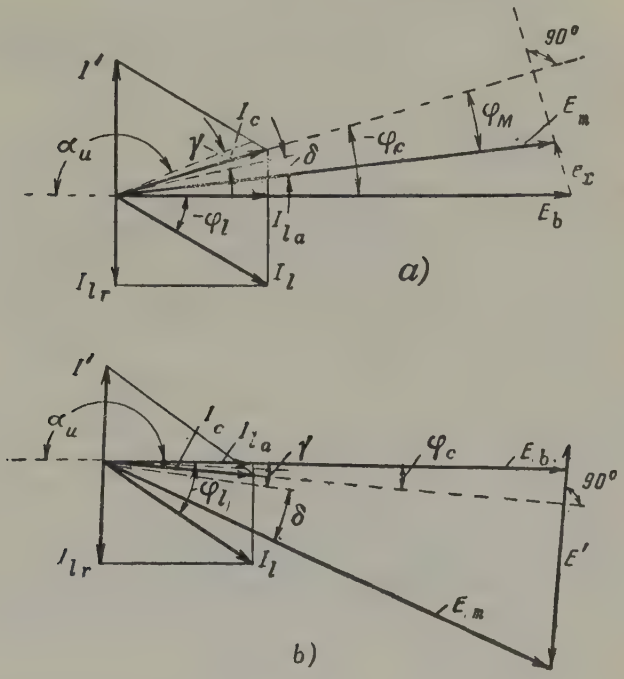

Fig. 4. Inverter vector diagrams.

a — for system with parallel static phase compensation; *b* — for systems with series-parallel static phase compensation.

banks (see Fig. 5) one (or a few) at a time in a definite sequence with increasing angle δ. The individual filter banks are disconnected in such a way that δ is not reduced below a given level (18 to 20°) when a bank is disconnected. In this way the operating stability of the inverter is maintained; as far as possible provision is also made for keeping the complete set of filters of all harmonics in the zone of normal load variations according to the daily graph (e.g. 50 to 100 per cent) in order to ensure an approximately sinusoidal voltage on the inverter bus-bars; only if great load reductions occur is the disconnexion of filters *en bloc* permitted (e.g. the 7th and 11th).

The voltage on the a.c. bus-bars of the inverter (of the receiving system) is held constant as required by gradual changes in the control angle α_r of the rectifier. These are made automatically according to deviations of the voltage from its rated value.

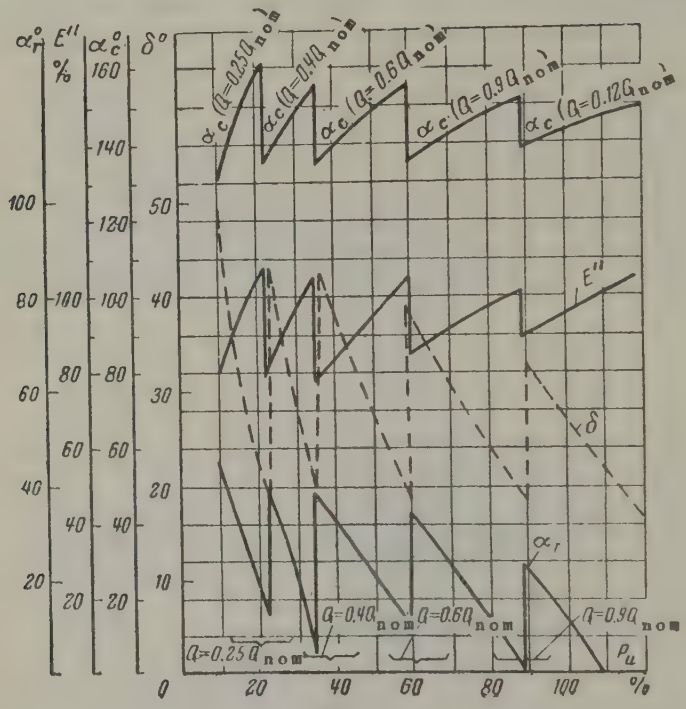

Fig. 5.

The rectifier voltage can be controlled in this way by altering the setting of the maximum current regulator.

It is obvious that the use of control pulses at a fixed repetition rate from an extraneous source removes the problem of maintaining the frequency of the inverter system constant by special control methods (a considerable simplification), and the control angle α_c of the inverter and the angle δ become functions of the inverter mode or state and cannot be varied or regulated arbitrarily (as in the case of a synchronous condenser).

An inverter with parallel capacitors is started simply by the supply of voltage from the rectifier to the inverter; if this method is used, the filter banks (or some of them) must first be connected to the bus-

bars of the inverter, and the setting of the maximum current regulator of the rectifier must so limit the current that no significant increase in voltage is produced on starting by the flow of inverter current through the capacitance connected to the bus-bars.

3. Inverter substations with series-parallel capacitor phase compensation

This type of system is illustrated in Fig. 1*c* [3]. The control pulses are again supplied to the inverter bulbs from an independent source at a set frequency (f = 50 c/s). The capacitor banks are connected in series with a transformer in the connecting phase of the bridge "converter". Each of these banks is in turn composed of smaller individual sets which are connected in series and parallel; the series phase bank passes alternating current during the operation of the converter and its half-waves are approximately rectangular in shape. As a result, a trapezoidal voltage is produced on the bank capacitance which can be replaced quite accurately by a corresponding fundamental sine curve.

Part of the capacitance is connected to the a.c. bus-bars of the inverter (the system bus-bars) in the form of an assembly of parallel filter banks which take part in the commutation of the inverter current, in covering the reactive load and in ensuring a sinusoidal voltage.

Figure 4*b* shows a rough vector diagram of such an inverter under normal operating conditions. The fundamental harmonic of the trapezoidal voltage is represented by the vector E'. The optimum value of E' must be 60 to 80 per cent of the bridge phase voltage E_m.

It will also be seen from this diagram that the series capacitance retards the voltage E_m (by the addition of the voltage vector E'), whilst the parallel capacitance advances the inverter current vector I_c (as a result of the addition of the bank current vector I'), ensuring the lead of the inverter current vector I_c over the voltage vector E_m and the presence of a quenching angle δ, which is necessary for successful current commutation and a stable inverter performance.

The power and capacitance of the series and parallel capacitors is selected by analysis of the plant criteria and the system power factor. From test results and calculations, about 50 to 70 per cent of the total capacitor power is connected in series and about 30 to 45 per cent is in parallel. The total power of the capacitors in this system is approximately the same as that of the foregoing system with parallel static phase compensation.

Figure 6 illustrates the characteristics of an inverter with series-

parallel static phase compensation. In this case it is advisable to connect two thirds of the overall capacitor power in series and about one third in parallel.

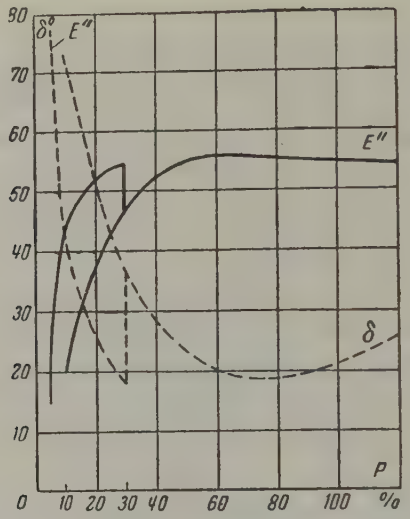

Fig. 6.

It will be seen from Fig. 6 that the angle δ and rectified voltage E'' are practically constant even if the inverter load is subject to wide variations for unchanged series- and parallel-connected capacitances.

This is the advantage of this particular system over the last system (see Section 2), since wide load variations require no connexion and disconnexion of the banks or "deep" voltage regulation on the rectifier side unless an unusually large load reduction occurs (below about 30 per cent). In this event the rectified voltage can be held constant by disconnecting part of the power of the parallel capacitors (see Fig.6). (Approximately 35 per cent of the power of the parallel capacitors is disconnected for a reduction in load to 30 per cent.)

It is therefore clear that in this system the bus-bar voltage of the inverter can be controlled either by the angle α_r of the rectifier, or, in the main range of load variation, merely by regulating the transformers on load, since the limits of such regulation are usually small.

The starting of the inverter in this system is similar to that described in Section 2.

4. Inverter substations with capacitive connexion of bridge converters

A simpler and cheaper system is sometimes possible. Here the converter bridges are connected across series capacitors without main transformers, but with a set of parallel filter banks at the inverter bus-bars (see Fig. 1*d*) [6]. The auxiliaries and local load of the substation are supplied from a small separate step-down transformer.

The series capacitors of the bank in the phases are different in this system, in that a voltage of constant sign is produced as well as the trapezoidal alternating voltage. This constant "support" voltage is equal in magnitude to half the rectified bridge voltage if it is the one "on pole"; and equal to one-and-a-half times that value if the second bridge is "on pole".

The capacitors of the series phase banks must be chosen with both voltage components in mind [6,7].

Calculations have shown that if a total gradient of 37 to 40 kV/mm is acceptable for the insulation of the series capacitor banks (for a usual maximum gradient of the alternating component of the voltage of 17.6 kV/mm), then no increase in capacitor power is required for one bridge in an arm in connexion when a constant voltage component is present, if use is made of conventional *KPM*-type series-capacitor compensation.

The neutral point of the system can in this case be "dead"-earthed, or else earthed via a resistance (usually an inductive resistance) or via a compensating coil; in the "dead"-earth method, or if earthing via a small resistance is employed, it is necessary to have a reactor in the pole of the bridge (see Fig. 1*d*); no such reactor is required if a large earthing resistance is used; the use of high-voltage filters in star entails the use of a large inductance for neutral earthing (at a small operating current).

In order to exclude the third harmonic of current from the network, one of the transformer windings is usually connected in delta for the local load.

Low-inductance reactors (5 to 6 per cent) are usually connected in series with the capacitor banks in order to retard the commutation of current in the bulbs in the phases of connexion of the bridge.

The vector diagram and analysis of normal conditions is similar to that in Section 3.

Reliability

A hybrid system has also been proposed in which a low-power (e.g. one third of the required total power) synchronous machine and a bank of static capacitors (e.g. two thirds of the required power) are used simultaneously for purposes of phase compensation at an inverter substation. It was hoped to reduce losses by maintaining smooth continuous control of the voltage on the system bus-bars.

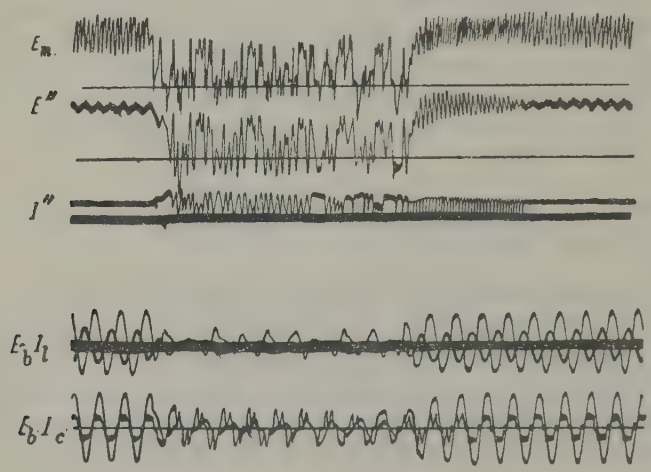

Fig. 7. Oscillograms of transient behaviour in an inverter with series-parallel static phase compensation in the presence of a momentary three-pole short circuit in the inverter system.

But investigations (and especially tests) have not confirmed that this is an expedient solution owing to its inadequate reliability in operation. If momentary disturbances occur in the operation of the inverters (e.g. failure to fire or breakdown of a bulb), or if short circuits occur, etc, reversal of the inverter usually takes place, and the process of pulling it back into operation is more difficult inasmuch as the power of the synchronous machine is lower, the corresponding inertia constant is less and the reactance in absolute terms is larger; in other words, a reduction in machine power (owing to the use of static capacitors) has a marked adverse effect on the operating stability of the machine and the inverter substation as a whole.

Even in the system with a synchronous condenser (version 1) a reduction in its excitation and loading with the voltage maintained constant (but the active load of the inverter reduced) has an unfavourable effect

on the operating stability of the synchronous machine and inverter, especially in the event of momentary disturbances to the normal operation of the inverters and system. If a disturbance occurs in the normal operation of the inverter in a system without a counter-e.m.f. and a stoppage of the synchronous machine takes place, this results in a lengthy shut-down of the system, since it takes time to re-start the machine and resume operation.

Tests on models have shown that with static systems (Sections 2,3,4) normal operation can quickly be resumed automatically after a momentary disturbance or short-circuit in the system. Automatic reclosure on the rectifier side is sometimes required in the parallel static compensation system. Systems 3 and 4 with series-parallel static compensation are the most stable. Here operation is resumed without external interference, provided an automatic device for shunting the reactor valves is used on the line reactors of the inverter [4].

Moreover, systems 3 and 4 can disconnect and connect the inverter by taking away the supply of control pulses of the inverter itself. No provision is made for this in system 2.

From test results, the stability of inverters with series-parallel static phase compensation is very high. This may be illustrated by the following example of a model. An operating loaded inverter with a normal quenching angle (δ = 18 to 20°) experienced a sudden large increase in load which reduced the angle δ and "reversed" the inverter. After a subsequent reduction in load, or on connexion of an additional parallel capacitance on the inverter bus-bars, the system resumed normal operation without any interference.

After the clearance of a short-circuit in the receiving network, different in polarity and distance (right up to the inverter bus-bars), the inverter resumed normal operation automatically. The oscillograms in Fig. 7 illustrate the case of a three-pole short-circuit in an inverter system using series-parallel static compensation.

Conclusions

1. To solve the problem of economical d.c. transmission of medium and low power, attention should be concentrated on producing simple and reliable inverter substations which are able to operate into receiving systems without the counter-e.m.f.'s of local power stations.

2. The most economical and reliable inverter substations for such outlying regions are those based on static phase compensation with series and parallel capacitor banks (the systems described in Sections 3 and 4).

3. Prototype inverter plants ought to be constructed in order to verify these conclusions under operating conditions and they should then be put into mass production.

Appendix I. Simplification of electrical calculations for operating conditions and converter characteristics

The commutating e.m.f. of an inverter at the end of a transmission line may be taken as the alternating voltage on the bus-bars; in this case a sinusoidal voltage shape must be ensured by connecting a set of filters tuned to higher harmonics of the converter current to the a.c. bus-bars.

This initial proposition is obviously correct and tests have confirmed that it is so. It considerably simplifies the analysis of normal inverter conditions, since it allows the criteria of the a.c. system at the inverter bus-bars to be ignored without loss of accuracy.

Appendix II. Correspondence with the rated voltage

In view of the possibility of designing inverter substations without main transformers, it is important to establish correspondence between the rated voltage of the system (a.c. side), the rectified voltage (d.c. transmission), and the probable number of bridges.

The relationships are given in the following table:

Rated alternating voltage, kV	Number of bridges per pole	Rectified transmission voltage, kV	Approximate power of circuit, MW
35	1	100	10 - 30
35	2	200	50 - 150
110	1	300	200 - 400
110	2	600	-
220	1	600	500 - 1000

Translated by O.M. Blunn

REFERENCES

1. Ya.M. Chervonenkis; *Long-distance d.c. transmission of low and medium power (Peredacha nebol'shikh i srednikh moshchnostei postoyannym tokom na dal'nye rasstoyaniya)*. Izd. MKKh., RSFSR, Moscow (1957).

2. N.N. Krachkovskii; *Elektrichestvo*, No. 12 (1959).

3. N.N. Mel'gunov and V.N. Vyatkin; Auth. Cert. No. 119598, 1958.

4. N.M. Mel'gunov and V.N. Vyatkin; Auth. Cert. No. 121177, 1958.

5. V.M. Kvyatkovskii; *Elect. stants.*, No. 11 (1958).

6. N.M. Mel'gunov; *The main features of circuits with capacitive connexion of bridge converters in d.c. transmission (Osnovnye osobennosti skhemy s kondensatornym prisoedineniem mostovykh preobrazovatelei v elektroperedachakh postoyannogo toka)*. Direct-current Research Institute, No. 3 (1958).

7. A.K. Gertsik; The ionization characteristics of paper-oil capacitor insulation under the influence of pulsating voltage (Ionizatsionnye kharakteristiki bumazhno-maslyanoi kondensatornoi izolyatsii pri vozdeistvii pul'siruyushchego napryazheniya). Direct-current Research Institute, No. 2 (1957).

THE THEORY OF TRANSFORMER OPERATION WITH A MAGNETIZED SHUNT*

V.I. SHAROV

(Moscow)

(Received 28 June 1961)

Use is now being made of devices which utilize the magnetization of transformers, auto-transformers and reactors (chokes) for the voltage control of all kinds of electrical gear. Such devices are very promising in view of their many advantages: reliability, durability, continuous high-speed control, high efficiency, etc.

Magnetized shunt transformers and auto-transformers occupy a special position. Elements of a theory of operation, a method of design and the means of using them in automatic control systems have already been worked out in the Gorkii Polytechnical Institute under the direction of A.M. Bamdas [1]. However, certain fundamental aspects of the theory of these devices still require further study from the design point of view.

It is possible to apply the general theory of magnetic amplifiers, since the devices in question can be represented as magnetic amplifiers operating as transformers.

The performance of a magnetized shunt transformer (see Fig. 1) will now be analysed under the same conditions as are adopted in studying the performance of an ideal magnetic amplifier, i.e. it will be assumed that the magnetization curve of the core material is rectangular in shape and that neither loss or leakage occurs. The total m.m.f. of a closed circuit consisting of non-saturated sections of a magnetic circuit will then be zero. Suppose that the bars *I* and *II* and the shunt *III* are equal in section and that the supply voltage U_1 is such that

---

* *Elektrichestvo*, 11, 64-66, 1961.

saturation of bar *I* does not take place. Consequently there will be no saturation of bar *II* or the shunt if the latter is not magnetized.

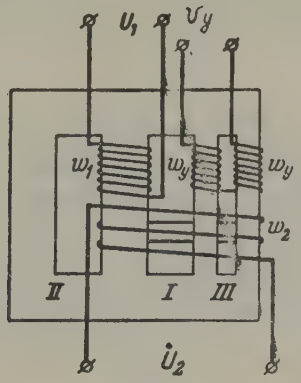

Fig. 1. Transformer magnetic amplifier with shunt magnetization.

Consider first the operation of the transformer on no load. If magnetization is absent, the secondary voltage U_2 is given by the transformation ratio and the distribution of the flux between bar *II* and the shunt owing to the primary winding. The flux distribution in the first instance depends on the relationship between the sections of the bar and shunt and that between the lengths of the adjoining portions of the yoke. To find the distribution of the magnetic flux it is also necessary to consider the air gaps in the core construction and the actual shape of the magnetization curve of the core material. With increasing magnetization of the shunt, the voltage U_2 rapidly builds up and reaches maximum even while the control m.m.f.'s are still quite negligible and the whole flux of the primary winding w_1 is closed across bar *II*

$$U_{2\,max} = U_1 \frac{w_2}{w_1}.$$

A magnetized shunt transformer can thus control the voltage even on no load, which is an advantage over conventional magnetic amplifiers.

Now consider a load resistance on the L.T. side. In the absence of magnetization the whole flux of the primary winding is closed across the shunt and the secondary voltage and current in the secondary winding are zero. But since it is assumed that the magnetization curve of the core material is ideal, it follows that the m.m.f. in a closed circuit consisting of bar *I* and the shunt must likewise be zero in the

absence of magnetization. Furthermore, since the only m.m.f. in this circuit is that produced by the primary winding, the primary winding current is zero too. The current in the secondary winding is also zero.

On magnetization of the shunt the m.m.f.'s are equal as for a simple magnetic amplifier:

$$F_1 = F_2 = F_y,$$

where F_1 is the m.m.f. of the primary winding, F_2 that of the secondary winding, and F_y that on each bar of the shunt.

It will be seen by considering the closed circuit of bars *I* and *II* (i.e. that of the non-saturated portions of the magnetic circuit) that F_1 is equal to F_2 for any degree of magnetization and any load:

$$F_1 = F_2.$$

Moreover, in order that part of the flux of the primary winding may be closed across the shunt, a.c. and d.c. m.m.f.'s must be equal, as in a conventional magnetic amplifier, i.e.

$$F_1 = F_y.$$

Like a conventional magnetic amplifier, conditions of over-excitation and saturation can occur during the operation of a magnetized shunt transformer, and the a.c. and d.c. m.m.f.'s are then no longer equal. Over-excitation sets in when the shunt cross section is such that the induction in the shunt periodically attains the value of saturation induction during operation of the transformer on load in the absence of magnetization. In this case the magnitude of the current in the secondary and primary windings will be greater for the same load, the smaller the section of the shunt, since from the instant of saturation the flux begins to close across bar *II* and the device operates as a conventional transformer until the instant the shunt is de-saturated. The condition of saturation sets in when the current in the secondary winding attains its maximum value

$$I_{2\,max} = \frac{U_{2\,max}}{r},$$

where r is the load resistance.

A further increase in magnetization results in no further increase in load current.

Thus, the main characteristic of a magnetized shunt transformer which relates the load current to the control current or the a.c.

m.m.f. to the control m.m.f. (see Fig. 2) is exactly the same in shape as that of a simple magnetic amplifier. A device with this characteristic can easily be converted into a current stabilizer since it is only necessary to maintain the control m.m.f. constant.

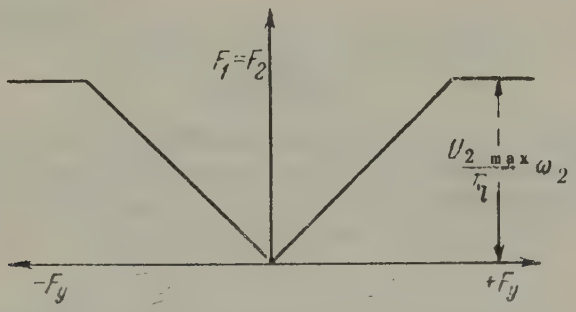

Fig. 2. The fundamental characteristic of an ideal transformer amplifier with shunt magnetization.

The shape of the curve for the variation of the load current and control-circuit current varies with the degree of suppression of even harmonics in the control circuit and transient phenomena in the windings, and is similar in shape to that of the curve for a conventional magnetic amplifier.

It should, however, be pointed out that the core magnetization curve is substantially non-rectangular in practice and especially so for large magnetized shunt transformers, large magnetic amplifiers and saturable reactors in view of the use of normal electrical steel and the presence of air gaps. Actual test curves for real magnetized shunt transformers will differ considerably from the foregoing ideal characteristic, and a detailed analysis of such devices must be based on an approximation of the core magnetization curve by some mathematical function. The characteristics of magnetized shunt transformers are also greatly affected by the increased leakage inductance of the windings due to the rather unusual arrangement (for transformers) of the power windings and the position of the magnetization windings in relation to the a.c. windings.

It will be seen from Fig. 1 that a magnetized shunt transformer possesses the property of reversibility, i.e. if the winding w_2 is connected to the alternating voltage, the voltage from the winding w_1 can be regulated by varying the magnetization of the shunt. The foregoing analysis remains valid for this case also.

There is such great similarity between magnetized shunt transformers and conventional magnetic amplifiers that magnetic-amplifier theory can be used to determine the efficiency of such transformers in various applications and for preliminary design analysis.

Translated by O.M. Blunn

REFERENCES

1. A.M. Bamdas, V.A. Somov and A.O. Shmidt; *Magnetized shunt transformers and stabilizers (Transformatory i stabilizatory, reguliruemye podmagnichivaniem shuntov)*. Gosenergoizdat (1959).

TEMPERATURE COMPENSATION OF TRANSISTORIZED RELAY STAGES*

S.V. KULIKOV

(Moscow)

(Received 9 November 1959)

Transistorized relay systems are now widely used for the control of electromagnetic devices and electrical motors. The explanation is that transistors acting as switches are capable of switching a considerably greater power than the leakage power on the collector. Their capacity is only restricted by the maximum current and voltage. For example, a PD-4-type transistor is capable of switching 200 W and a P207 transistor about 1 kW.

Industrial control systems often require relay circuits with a low and highly stable threshold of operation. In the design of transistorized relay circuits which are sensitive to changes in temperature it is therefore important to determine the effect of temperature on the "threshold quantities" (see below) and find methods of reducing this effect.

Factors determining threshold stability

The transistorized relay circuit is usually a non-linear amplifier with total positive feedback. Since the feedback circuit is in the majority of cases composed of passive stable elements, it follows that the amplifier is the main cause of instability of the threshold quantities, i.e. the instability of the regions of cut-off, saturation and the active region. It is expedient and convenient to express these regions in terms of the forward transfer characteristic of the transistor

---

* *Elektrichestvo*, 11, 66-70, 1961.

$$I_k = Y_{21e}(U_{e.b}) \qquad \text{a}$$

or

$$I_k = Y_{21e}(I_b) \qquad \text{b}$$

where I_k is the transistor collector current, $U_{e.b}$ the voltage between the emitter and base, and I_b the base current.

An analysis of the forward transfer characteristics of the most common Soviet transistors (types P13 - P15 and P4) has shown that a change in temperature form - 50° C to + 60° C both shifts and alters the slope of the characteristic.

The cut-off region is defined by the following equations:

$$U_{e.k} \approx E_k \qquad (1)$$

$$I_b = I_{b0} = I_{k0} + I_{e0} \qquad (2)$$

$$I_{k0} = I_{sk} + I_{rk} \qquad (2')$$

$$I_{e0} = I_{se} + I_{re} \qquad (2'')$$

where $U_{e.k}$ is the voltage between the emitter and collector, E_k the supply source voltage of the collector circuit, I_{b0} the base current in the cut-off state, I_{k0} the reverse current of the collector junction, I_{sk}, I_{rk} the saturation current and leakage current of the collector junction, I_{e0} the reverse current of the emitter junction, and I_{se}, I_{re} the saturation current and leakage current of the emitter junction.

For practical purposes it can be assumed that for transistors of the types under consideration at cut-off voltages much less than the supply source voltage of the collector circuit and for the boundary point corresponding to the commencement of the active section [1]

$$I_b = I_{b0} = I_{k0} \qquad (2''')$$

An earlier equation [2] holds good for a boundary point between the region of cut-off and the active regions:

$$U_{e.b} = U_{e.b0} \qquad (3)$$

where $U_{e.b0}$ is the threshold voltage between the base and emitter corresponding to the commencement of the active section on the forward transfer characteristic $I_k = Y_{21e}(U_{e.b})$ if $U_{e.k} \approx E_k$.

Strictly speaking, expressions (2‴) and (3) are contradictory, since the voltage $U_{e.b}$ is in the cut-off region if $I_{b0} = I_{k0}$ (i.e. if $I_e = 0$).

In practice, however, there is a basis for the consistency of these equations in a very slight increase in the emitter current I_e at a voltage $U_{e.b}$ approximately equal to its value at the boundary with the active region.

Both I_{k0} and $U_{e.b0}$ depend on the temperature and determine the stability of the "initial" operating threshold of the relay circuit. The region of saturation is defined by the following equations:

$$U_{e.k} \approx 0; \tag{4}$$

$$I_k = \frac{E_k}{r_k \quad r_e} = I_{k.sat} \tag{5}$$

$$I_b > \frac{I_{k.sat}}{\beta} - I_{k0} \tag{6}$$

where r_k, r_e are the respective resistances in the collector and emitter circuits, $I_{k.sat}$ the saturation current of the transistor, and $\beta = H_{21e}$ the transfer constant of the base current.

The equal sign in expression (6) corresponds to a boundary point on the characteristic between the region of saturation and the active region. However, the following equation also holds for this point:

$$U_{e.b} = U_{e.b.k} = \frac{I_{k.sat}}{S_k} + U_{e.b0} \tag{7}$$

where $S_k = Y_{21e}$ is the total slope of the forward transfer characteristic $I_k = Y_{21e} = Y_{21e}(U_{e.b})$ on the active section.

It will be seen from equations (6) and (7) that a change in β and S_k with a change in temperature alters the slope of the forward transfer characteristic. But if β and S_k only change slightly in the given temperature range, the forward transfer characteristics are only displaced, as follows from formulae (2), (3), (6) and (7). Equations (6) and (7) define the stability of the "final" threshold of release (relay opening time) in a transistorized relay circuit.

Classification of temperature compensation methods

In a transistorized relay circuit use may either be made of stage-by-stage thermal compensation with the temperature changes of adjacent

stages included, or else thermal compensation of the amplifier as a whole. In this case the temperature changes of the transistor criteria (I_{k0}, $U_{e.b0}$, β, S_k) are compensated and the forward transfer characteristics of the stages (the amplifier) are stabilized, thereby stabilizing the threshold quantities of the relay. If not a single one of the stages of the relay circuit is in equilibrium in the active region, then unfortunately the temperature compensation methods of linear amplifiers in which constant negative feedback is introduced are no longer acceptable, because the latter assumes the presence of amplification [3].

Special methods are required for relay stages (amplifiers). These can be divided into three groups.

Use of fixing diodes and bias voltages. This method of temperature compensation produces an "artificial" forward transfer characteristic with fixed boundary points between the cut-off, active and saturated regions [3].

Thermal resistors (thermistors) may be used to compensate shifts and changes in slope of the transistor forward transfer characteristic. With a low-impedance input signal source between the emitter and base of the transistor in the first stage, it is expedient to connect the thermistor in series in the emitter-base circuit. For a high-impedance source, it should be connected in parallel in that circuit.

Two control circuits for the next stage are indicated in Fig. 1 for high-impedance and low-impedance signal sources. Figure 1*a* shows a typical control circuit if the switch K is open (the first stage performs the role of this switch), and the next stage is correspondingly "non-conducting". Figure 1*b* refers to the case when the switch K is closed and the next stage is non-conducting. In the first case (Fig. 1*a*) temperature compensation is effected by connecting the thermistors in parallel across a "bias battery". The bias battery can be connected in series in the base or emitter circuit. The bias battery can in some cases be replaced by a voltage drop such as that across the resistance r_4 (indicated by a broken line) due to the load current of another stage. In the second case (Fig. 1*b*), temperature compensation is effected by series connexion of resistance r_4 across which the voltage drop is determined by the value of the thermistor r_t. But if the emitter-base circuit in the state indicated in Fig. 1 is connected to a resistance which is commensurate with the input resistance, then both methods of compensation are equally applicable.

It is, however, necessary to point out that these methods of temperature compensation only allow compensation of *shifts* in the forward transfer characteristic. Two methods may be used to compensate changes in the slope of this characteristic: the connexion of the thermistors

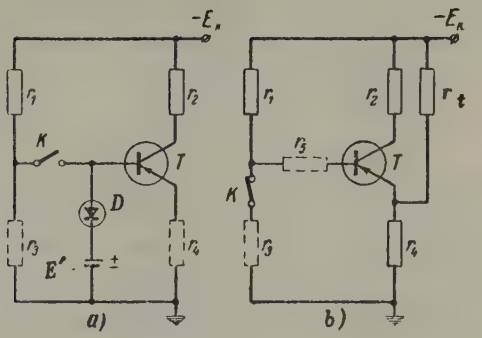

Fig. 1.

in parallel with the input to the stage [2], or in series with the d.c. negative feedback circuit [4].

The use of temperature changes of the characteristic of a subsequent stage to compensate the temperature changes of a preceding stage in order to obtain a constant resultant characteristic for both stages. This method of temperature compensation can be realized without the use of thermistors according to the design of the relay circuit.

A method of designing two such systems of compensation will now be considered.

Design method

The forward transfer characteristics of the majority of Soviet P13 - P15 and P4 - type transistors are not altered in shape at positive temperatures, but only shifted to right or left (see Figs. 2 and 3*a*). Only such shifts need therefore be compensated. With a small resistance in the emitter-base circuit it is necessary to design the temperature compensation circuit so as to compensate changes in the threshold voltage $U_{e.b0}$, but if a large resistance is involved (Fig. 1*a*), it is the collector current I_{k0} which has to be compensated. In the general case, changes in both $U_{e.b0}$ and I_{k0} are considered.

Suppose it is required to specify temperature compensation for the transistorized relay circuit shown in Fig. 4. A silicon transistor T_1 (P102-type) is used in the first stage and P4D-type transistor T_2 is used in the output stage. Both stages are provided with positive feedback across the resistance r_4. The input signal can be supplied between

points a and b, a and c, or b and c; the output signal is taken from the resistance r_2. Temperature compensation of the first stage is effected by means of an MMT-1 thermistor, and that of the output stage

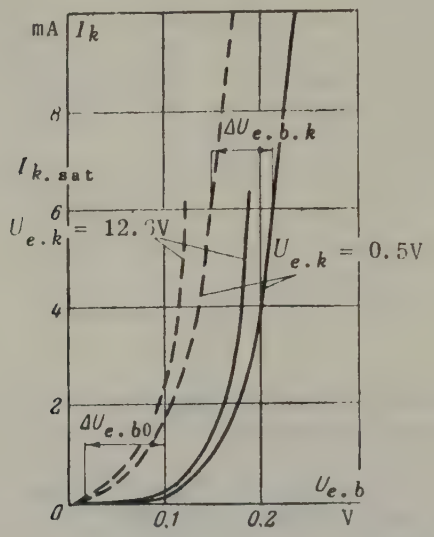

Fig. 2. Forward transfer characteristic $I_k = Y_{21e}(U_{e.b})$ of a transistor in a common emitter circuit: ——— $t = +20°C$; — — — — $t = +60°C$.

by a P3V transistor T_3 "in diode connexion". The collector current of the silicon transistor T_1 is negligibly small in the cut-off state and so the temperature compensation of the output stage can be considered separately (Fig. 1a).

By way of comparison Fig. 3b shows the characteristics of an output stage in which bias across the constant resistance $r_b = 5.1\ k\Omega$ is used (in place of T_3 in Fig. 4). The forward transfer characteristic was taken for two temperatures: $+20°C$ and $+60°C$ at $E_k = -20$ V, $r_2 = 100\Omega$, and various bias voltages E'. It will be seen from the curves in Fig. 3b that the displacement of the boundary points of cut-off and saturation is about 1 mA after a change in temperature. The displacement of these boundary points is much less if the transistor T_3 is used.

The required bias voltage E' is calculated graphically. Figure 3c shows the voltampere characteristics of P4D- and P3V-type transistors "in diode connexion" with open emitters. Marking off the supply voltage E_k of the collector circuit at point a on the base, a perpendicular is

then erected from this point to the curve T at point a'. A straight horizontal line is now drawn across to the point b' on curve D. The required bias voltage R' is then obtained at point b by dropping a perpendicular line to the base. It was assumed in finding E' that $U_{e.b0}$ and $\Delta U_{e.b0}$ were zero, which is quite permissible for the method of compensation in question.

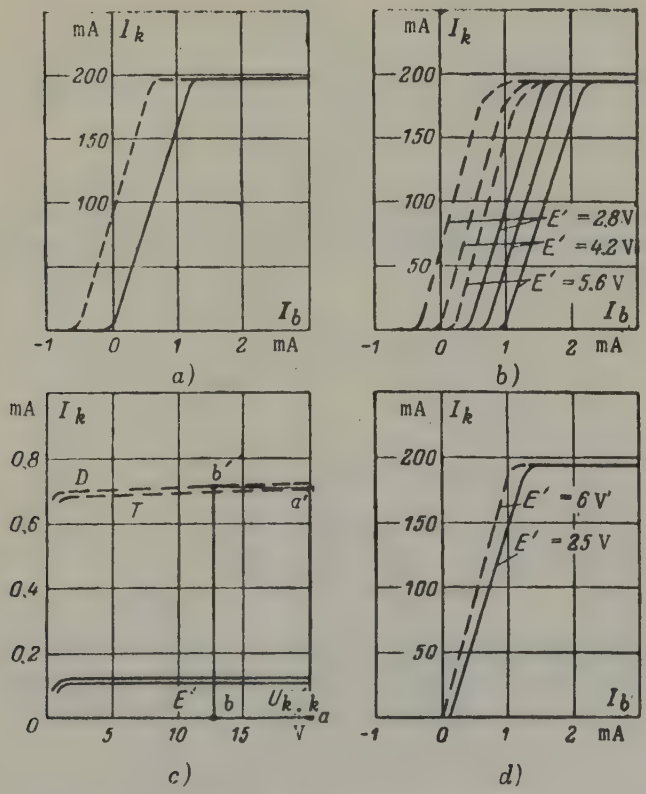

Fig. 3. Forward transfer characteristics $I_k = H_{21e}(I_b)$ and a graphical method of determining the compensation:

——— $t = +20°C$; — — — — $t = +60°C$.

E' - bias voltage

Figure 3*d* shows the characteristics of a stage where the above method of temperature compensation is used. It will be seen from these curves that the boundary points of cut-off and saturation are hardly moved at all by a change in temperature (0.05 mA for the cut-off point and 0.15 mA for the saturation point).

It is a corollary of the non-linearity of the voltampere

characteristic D (Fig. 3c) that the temperature compensation circuit is insensitive to changes in the bias voltage E'. Owing to this non-linearity the load in question can be included direct in the emitter circuit of the triode without any appreciable shunting of the input (the resistance r_4 in Fig. 1a).

The temperature compensation circuit of the first stage is given by the equation

$$(\Delta I_t - \Delta I_{\text{K0(1)}})\left(r_3 + \frac{r_5 r_7}{r_5 + r_7}\right) = \Delta U_{e.b0(1)}, \qquad (8)$$

where Δt_t is the change in the current through the thermistor:

$$I_t \approx \frac{E_K r_5}{(r_5 + r_7) r_t}.$$

The thermal resistance r_t must operate on the linear section of its voltampere characteristic without any notable heating from the current flowing through it.

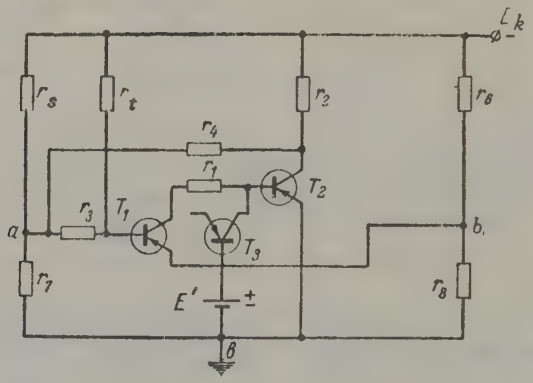

Fig. 4.

From test results of relays using the circuit in Fig. 4 and with $r_1 = 1.2\,\text{k}\Omega$, $r_2 = 100\,\Omega$, $r_3 = 0$, $r_4 = 18\,\text{k}\Omega$, $r_5 = 1145\,\Omega$, $r_6 = 250\,\Omega$, $r_7 = 855\,\Omega$, $r_8 = 250\,\Omega$, $r_t = 112\,\text{k}\Omega$, $E_k = -12$ V and $E' = 12$ V:

On supply of the input signal between points a and b, the operating current was $\pm 50\,\mu$A at temperatures between $+20\,^\circ$C and $+60\,^\circ$C. The output (collector) current of the transistor T_2 did not exceed 1 mA in the cut-off state at $+60\,^\circ$C.

Temperature compensation by the third of the foregoing methods was adopted in a relay with the circuit shown in Fig. 5. Here the output stage (the transistor T_2) is controlled by the first stage (the

transistor T_1) by the type of circuit shown in Fig. 1*b*. Serial positive feedback was provided across the resistance r_5. As a result of compensation of changes in the forward transfer characteristic of the first stage corresponding to changes in that of the second stage, the instability of the relay threshold quantities was eliminated.

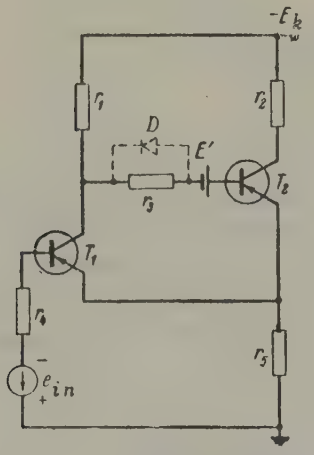

Fig. 5.

The conditions of stable threshold values are obtained by forming and solving Kirchoff equations for the two extreme temperatures of the operating range of the first and second stages.

The stability condition of the "initial" threshold of release (opening time) is given by the formula

$$\frac{\beta_{i1}(\Delta U_{e.b0(1)} + r_4 \Delta I_{K0(1)}) r_1}{(r_1 + r_3)(r_4 + r_{11i(1)} + \beta_{i1} r_5)} = \Delta I_{K0(2)} + \frac{\Delta U_{e.bf(2)}}{r_1 + r_3}, \qquad (9)$$

where $r_{11i(1)}$ is the input resistance of the transistor T_1 in a circuit with a common emitter on the *initial* section of the forward transfer characteristic at the maximum temperature; $\Delta U_{e.b0(1)}$, $\Delta U_{e.bf(2)}$ are quantities obtained from the graph in Fig. 2 (the subscript f refers to the *final* section and i to the initial section of the forward transfer characteristic; the subscripts 1 and 2 refer to transistors T_1 and T_2 respectively).

The stability condition of the "final" operating threshold is

$$\frac{\beta_{f1}(\Delta U_{e.bf(1)} + r_4 \Delta I_{K0(1)}) r_1}{(r_1 + r_3)(r_4 + r_{11\,f(1)} + \beta_{f1} r_5)} = \Delta I_{K0(2)} + \frac{\Delta U_{e.b0(2)}}{(r_1 + r_3)}. \tag{10}$$

The condition of saturation of transistor T_2 has still to be added to equations (9) and (10):

$$\frac{\beta_2 (E_K - E')}{r_1 + r_3} \geq \frac{E_K}{r_2} \tag{11}$$

and also its condition of cut-off

$$E' \geq I_{K0(2)} r_3. \tag{12}$$

Since in all there are seven independent criteria (r_1, r_2, r_3, r_4, r_5, E_k and E') and four equations (9), (10), (11) and (12), a more definite solution of the problem can be obtained if the desired amount of bias and the hysteresis loop are considered [5,6]. It should be noted that equations (9) and (10) can be replaced by one expression if $\Delta U_{e.b01} = \Delta U_{e.b\,f(1)}$, $\Delta U_{e.b\,0(2)} = \Delta U_{e.b\,f(2)}$, $\beta_{i1} = \beta_{f1}$, $r_{11\,f(2)} \ll r_1 + r_3$, $r_{11\,i(1)} \ll r_4$, and $r_{11\,f(1)} \ll r_4$, which is sometimes the case in practice.

From test results of a relay which had the circuit shown in Fig. 5 and $r_1 = 1$ kΩ, $r_2 = 40$ Ω, $r_3 = 1.1$ kΩ, $r_4 = 1.1$ kΩ, $r_5 = 3$ Ω, $E_k = 12.6$ V and $E' = 3.75$ V, the relay threshold values remained constant and equal to $e_{in(1)} = 0.6$ V and $e_{in(2)} = 1.1$ V at temperatures between +20°C and +60°C. The output current of the transistor T_2 did not exceed 1 mA in the cut-off state at +60°C. If the criteria had been selected without using relationships (9) and (10), a change in temperature would have caused a substantial shift (0.3 to 0.5 V) in both the threshold values of the relay [5].

Translated by O.M. Blunn

REFERENCES

1. B.N. Kononov; Trigger and relaxation circuits with junction triodes (Spuskovye i relaksatsionnye skhemy na ploskostnykh triodov). In collection of articles: *Semiconductor electronics (Poluprovodnikovaya elektronika)*. Gosenergoizdat (1959).

2. S.V. Kulikov; *Priborostroyenie*, No. 9 (1959).

3. Lo, Endres *et al.*, *Fundamentals of semiconductor electronics.* Sov. Radio (1958).

4. Ya.K. Trokhimenko; *Radiotekhnika,* No. 9 (1956).

5. F.L. Varpakhovskii and R.A. Lipman; *Avtomat. i telemekh.,* No. 11 (1958).

6. S.V. Kulikov; *Radiotekhnika,* No. 4 (1960).

ABSTRACTS FROM PAPERS PUBLISHED IN ELEKTRICHESTVO No. 11, 1961

Leading article

The material and technical basis of Communism and the development of power engineering in the U.S.S.R. (pp. 1-6).

Prime importance is attached to the development of electricity supply in the new long-term plans of the U.S.S.R. government. Special attention is to be paid to larger coal-burning power stations and generating plant. Low-cost gas-turbine plant is also being developed. The work on the single national grid is to continue. Research is being carried out on alternative sources of energy (thermo-nuclear reaction, the wind, sun, and the interior heat of the earth) and its conversion into electrical energy.

Computer engineering

Transient phenomena in a circuit with an inductance of capacitance and a ferro-magnetic substance with a rectangular hysteresis loop. V.E. Bogolyubov *et al.*, (pp. 60-64).

To fill a gap in the published literature, a method is proposed for analysing transient phenomena in circuits having coils with ferromagnetic cores with rectangular hysteresis loops operating into reactive loads.

Control engineering

An automatic regulator for the bit feed in drilling boreholes. M.G. E'skin *et al.*, (pp. 55-59).

A d.c. machine with a wide range of speed control has been developed for semi-automatic control of the bit feed in borehole drilling. The desired axial load or feed speed is maintained constant, as well as the equivalent sum. The proposed system is suitable for many other applications. The regulator consists of a reduction gear, executive

motor and amplifier and measuring parts. A position pickup is used to measure the main control item, the weight. A full description of the device is given.

Domestic meters

The class of accuracy of single-phase domestic electricity meters. B.N. Dol'nitskii *et al.*, (pp. 70-73).

Suitable domestic electricity meters are considered. Great individual accuracy is not considered essential.

Power systems

The effect of additional torque components on the dynamic stability of a transmission system with hydro-electric generators. V.V. Yezhkov, (pp. 35-41).

Previous investigations have apparently shown that considerable error can occur in the analysis of dynamic stability of a power system when a short circuit occurs near the generator bus, unless the aperiodic component of the stator current and the corresponding periodic component of the rotor current is included. A method is proposed which includes these components and also takes into account the power loss in the stator and rotor circuits and the restraint of the generator motor associated with the conversion of its kinetic energy into magnetic energy.

Insulation

Various regularities in the breakdown of polyethylene insulation. G.P. Delektorskii, (pp. 73-77).

An account is given of tests on high-voltage polyethylene cable insulation at 50 c/s and higher frequencies. A mathematical method of determining the permissible sustained alternating voltage in polyethylene cables is proposed. The same formula is claimed to be of great value in determining the reliability of components and in tests on electrical machines and capacitors.

The electrical characteristics of multi-layer impregnated capacitor paper. D.S. Varshavskii, (pp. 78-82).

A mathematical method is proposed for determining certain electrical properties of multi-layer impregnated paper for power capacitors. The

method is based on simple equivalent circuit analysis. Good agreement with test results has been found.

Rotating machines

The problem of motor reliability. N.A. Tishchenko, (pp. 7-14).

The principles of motor design are considered from the point of view of minimum constructional and operating costs. The concept of motor reliability is formulated mathematically. An analysis is made of capital repairs on 237,000 motors at 122 industrial undertakings. Opinions are expressed regarding optimum design.

Special features of the choice of armature windings for certain d.c. machines. I.Z. Ageev, (pp. 48-55).

The author considers the effect of the type of winding and its design on the commutation of 24 kW 30 V d.c. machines with a comparatively large range of speed control. Recommendations are made concerning the choice of winding and the commutation properties of armature windings.

Transformers

The technical limits of transformer loads at a.c. traction substations in multi-purpose power-supply systems. P.K. Denisov, (pp. 23-28).

On grounds of economy, a.c. traction systems and local consumers are supplied from common three-phase three-winding transformers. A mathematical method of selecting their power is proposed on the basis of daily consumption.

Special features of series-connected transformers and performance analysis. R.N. Urmanov *et al.*, (pp. 29-35).

The non-linearity of series-connected transformer units is considered with a view to improving the method of analysis and estimating its effect on performance. An example is given.

THE TECHNICAL AND PRICE ADVANTAGES OF SYNCHRONOUS MOTORS*

I.A. SYROMYATNIKOV

Moscow

(Received 4 August 1961)

The resolutions of the XXII congress of the C.P.S.U. pay considerable attention to electrification, mechanization and automation.

Much success has already been achieved in the development of automated drives in the U.S.S.R.

From power considerations, the best machines for large electrical group drives are synchronous motors. They improve not only the power factor, but the stability of the load units and electrical system as well.

Synchronous motors are now replacing asynchronous motors with flywheels and reduction gears in many branches of industry wherever sustained outputs are required (centrifugal pumps, fans, ball mills, crushers, regeneration plant, rolling mills and so on), as well as for shock loads.

Medium and large synchronous motors may be used in conjunction with hydraulic and electromagnetic clutches and couplings in speed-controlled drives.

Synchronous motors can alter the magnitude and "sign" of reactive power by varying the excitation current. The mode of operation with a "lagging" cos ϕ can in some cases be used for voltage regulation on reduced loads.

The scope for the use of synchronous motors has been greatly widened by the compounding system without machine exciters.

---

* *Elektrichestvo*, 12, 20-27, 1961.

Contactless synchronous motors are very promising. They have no brushes on the rotor and their construction is simplified accordingly, especially for special purposes (proof against arcing or freedom from arcing, etc).

The salient-pole ("claw-shaped") rotor with the excitation winding on the stator must be regarded as the best construction for relatively small contactless synchronous motors.

The system with a "dynamic transformer" can be used for synchronous motors of conventional construction with the excitation winding on the rotor. A "dynamic transformer" is an a.c. machine with the winding on the rotor. A slip-ring induction motor can be used as such a machine. This machine is on the same shaft as the synchronous machine. Semiconductor rectifiers on the same shaft as the synchronous machines are connected to the excitation winding on the rotor of the exciter and supply the excitation winding of the synchronous machine. Excitation is controlled on the stator side. Compounding ensures the necessary excitation forcing in all motor operating conditions including reductions in the mains supply voltage. This system of excitation is used by several foreign firms for large turbo generators as well as for synchronous motors [1].

It is advisable to regulate the excitation of synchronous motors from considerations of a constant voltage on the substation bus-bars with maximum and minimum current limiting and momentary excitation forcing in the event of voltage reductions. It is a necessary condition for the use of other types of excitation that forcing should be applied at reduced voltages.

For synchronous motors with suddenly applied loads, the use of excitation forcing considerably improves the overload capability of the motor so that its rated power can be reduced and its operating stability improved [2].

When considering the choice between synchronous motors and static capacitors as reactive power sources, it must be kept in mind that a synchronous motor designed and installed for this purpose is always in a position to provide it, and that static capacitors have a much shorter service life. Synchronous motors allow control of the voltage and permit momentary increases in the supply of reactive power to the network in the event of fault voltage reductions.

Sometimes it is necessary to increase the power of motors to cope with starting conditions. Clutches and magnetic particle couplings are very effective here. The motors can be started before the load is connected. The coupling is not energized until the motor has attained rated speed, and engagement takes place only then. The use of such

couplings allows the use of smaller synchronous motors at much less cost since their starting winding is lightened. Friction clutches can also be used.

Despite the advantages of synchronous motors, some experts still stick to the old opinion that their use is inadvisable. Apparently the early difficulties with starting and protection have not been forgotten. In these advanced times the starting and protection of synchronous motors is in most cases simple and very little different from that of asynchronous motors.

New models and the 100 kW series in particular have been held back because their advantages were under-estimated. Only recently has the Armelektro works' branch of the All-Union Electrical Power Research Institute started work on the development of a series of synchronous motors with semiconductor rectifier excitation. Technical specifications have so far been approved for four series of machines: 55 kW 1000 rev/min, 55 kW 1500 rev/min, 75 kW 1500 rev/min and 100 kW 1500 rev/min.

But the value of such machines also depends upon their cost. A comparative cost analysis must consider the fixed capital outlay, working capital requirements and power losses. The value of a particular series depends on its purchase price and running cost. Its utility cannot be judged from production cost, operating cost or capital outlay separately.

In comparative cost analysis, it is necessary to consider the time taken to recover the investment and relate the extra capital outlay or purchase price to future savings in production or operating cost [3].

The recovery time T is definable as the difference in purchase price divided by the annual savings from the acquisition. It is given by the formula:

$$T = \frac{K_2 - K_1}{C_1 - C_2}, \qquad (1)$$

where K_1 and C_1 are respectively the fixed capital outlay and *annual* working capital requirements (production costs or running costs) for the one alternative; and K_2, C_2 the same for one other alternative.

This recovery time T is then compared with the standard recovery time T' for the industry in question (e.g. 8 y).

To compare more than two alternatives, the estimated annual expenditure E on each alternative is obtained by adding a standard proportion of the purchase price (or capital outlay) to the annual running costs (or production costs) by the formula

$$E = C + \frac{K}{T'} = C + p'K. \qquad (2)$$

where E is the estimated annual expenditure; and p' a standard coefficient of efficiency (the reciprocal of the standard recovery time T).

The version with the lowest value of E is considered to be the best proposition.

The efficiency coefficient p' is taken as 0.125, which corresponds to a standard recovery time $T' = 8$ y.

To decide whether to use synchronous or asynchronous motors, it is necessary to compare:

1. A synchronous motor operating at $\cos \phi = 1$ with an asynchronous motor and static capacitors whose power is selected so that $\cos \phi = 1$;

2. A synchronous motor at $\cos \phi = 1$ with an asynchronous motor without static capacitors for the case when the reactive power can be obtained from other sources at very little expense;

3. A synchronous motor and static capacitors at $\cos \phi = 1$ and a synchronous motor at $\cos \phi < 1$. In this case the power of the static capacitors is made such that $\cos \phi$ is the same in both cases. To compare synchronous motors having $\cos \phi < 1$ which are now in production, the decrease in cost for operation at $\cos \phi = 1$ is not to be included.

It is a different matter when adopting $\cos \phi = 1$ for a new synchronous motor. The variation in the price of a motor with the reactive power it produces has to be included then. The specific cost of 1 kVAR of reactive power is always much less than the specific cost of 1 kVA of total power in a synchronous generator or motor. The explanation is that for the same active power the total power varies in inverse proportion to $\cos \phi$ whilst the reactive power is proportional to $\tan \phi$. Thus, the total power of a synchronous machine with (the standard) $\cos \phi' = 0.9$ is as much as 11 per cent greater than that of a synchronous machine with $\cos \phi' = 1$. At the same time, the reactive power is 0.48 of the active power.

The specific cost of 1 kVAR for synchronous machines is

$$K = \frac{C' - C}{Q_{nom}} \text{ [roubles/kVAR]} \qquad (3)$$

where C' is the cost of a synchronous machine with the standard power factor less than 1; Q_{nom} the rated reactive power; and C the cost of a synchronous machine with the standard power factor $\cos \phi' = 1$ at the same rated active power.

Formula (3) can be written in the form

$$K = \frac{DS' - D_1 S'_1}{Q_{nom}}, \quad (4)$$

and hence for synchronous motors

$$K_m = \frac{D}{\sin \varphi'} \left(1 - \frac{\eta' D_1}{\eta'_1 D} \cos \varphi'\right), \quad (5)$$

and for synchronous generators

$$K_g = \frac{D}{\sin \varphi'} \left(1 - \frac{D_1}{D} \cos \varphi'\right). \quad (6)$$

where η_1' is the efficiency of the motor at the standard power factor of 1; D the specific cost of 1 kVA at the standard power factor $\cos \phi' < 1$; D_1 the same for $\cos \phi' = 1$.

The ratio D_1/D is always greater than 1. It varies between 1.02 and 1.09 for different types of motor at $\cos \phi' = 0.9$. This cost ratio can be replaced by the ratio of the gross or specific weights.

From (6), if $D_1/D = 1$, for $\cos \phi' = 0.9$:

$$K_g \approx K_m = D \frac{1 - 0.9}{0.436} = 0.23D, \quad (7)$$

and for $\cos \phi' = 0.8$:

$$K_g \approx K_m = D \frac{1 - 0.8}{0.6} = 0.33D. \quad (8)$$

Actually K_g and K_m are less, since the specific cost of a machine decreases with increasing rated power.

The value of K_m for various types of synchronous motor is shown in Table 1.

The cost of static capacitors is relatively high: (with erection cost included) 8.5 roubles/kVAR if U_{nom} = 380 V, and 6.5 roubles/kVAR if U_{nom} = 6 kV. The advantage therefore lies undisputedly with synchronous motors as sources of reactive power from the point of view of capital outlay.

To compare these alternatives it is necessary to determine the losses in the synchronous motor in operation with $\cos \phi = 1$. Under these conditions the stator and excitation currents are minimum. The variation in the iron loss can be ignored. The voltage at the stator terminals is equal to the rated voltage. If the losses in the stator windings ΔP_{sv} and rotor ΔP_{rv} are known in rated operating conditions,

TABLE 1.

Standard efficiency coefficient p', kW	75	250	1300	3000	1500	3500
Standard power factor ($\cos \phi'$)	0.9	0.9	0.9	0.9	0.8	0.9
Speed n, rev/min	1000	1000	1500	1500	3000	3000
Rated voltage, U_{nom}, kV	0.38	0.38	6	6	6	6
Specific cost of 1 kVAR (motor), roubles/kVAR	1.49	0.99	0.485	0.465	1.72	0.92

then in operation on rated active load and at $\cos \phi = 1$, the losses are found from the formula

$$\Sigma \Delta P = \Delta P_x + \Delta P_{s.v} \cos^2 \varphi' + \Delta P_{rv} k_1^2, \qquad (9)$$

where ΔP_x are the losses in the stator steel and mechanical losses; and $k_1 = I_{ex\ 1}/I_{ex.v}$ is the excitation current multiple at $\cos \phi = 1$.

Values of k_1 are given in Table 2 for $\cos \phi' = 0.9$ and 0.8 as a function of the short-circuit ratio k_{scr} on rated load.

TABLE 2.

Short-circuit ratio, k_{scr}	0.5	0.7	1	1.5	2
Standard power factor, $\cos \phi'$ 0.9	0.77	0.77	0.79	0.79	0.81
" " " , $\cos \phi'$ 0.8	0.68	0.68	0.69	0.72	0.73

At an active load other than rated load, the excitation-current multiple can safely be found from the formula

$$k_1 = \sqrt{\frac{1 + \beta^2 x_d^2 \cos^2 \varphi'}{1 + x_d^2 + 2 x_d \sin \varphi'}}, \qquad (10)$$

where

$$\beta = \frac{P_1}{P_{1nom}} = \frac{P_1 \eta'}{P_{nom}};$$

P_1 is the active power consumed from the network; and x_d the synchronous inductive reactance in relative units.

The stator current multiple is

$$\frac{I}{I_{nom}} = \beta \cos \varphi'. \qquad (11)$$

The loss component of a synchronous motor, which depends on the reactive power other than the rated power, can be found from the formula

$$\Delta P_Q = A \frac{Q^2}{Q_{nom}^2} + B \frac{Q}{Q_{nom}}. \qquad (12)$$

If

$$Q = Q_{nom}$$

$$\Delta P_{Q\,nom} = A + B$$

The total losses in a motor on operation with cos ϕ = 1 are

$$\Sigma \Delta P = \Sigma \Delta P_{nom} (A + B). \qquad (13)$$

The value of A and B for various types of synchronous machine is given in the appendix (see also *Elektrichestvo* No. 3, 1961 [4]).

Incidentally, on operation with cos ϕ = 1, there is a reduction in losses and heating of the rotor and stator windings in synchronous motors and consequently their working life is greater. The reduction in winding temperature gives an additional reduction in losses of about ten per cent.

In some cases it is also necessary to consider the additional saving due to the reduced active power loss in the supply sources and network with the reduction in reactive power owing to the installation of synchronous motors or static capacitors.

The losses in the resistances r of the network elements (overhead lines, cables, reactors, transformers) are found from the formula

$$\Delta P = \frac{rQ^2}{U^2} = \Delta P_c \frac{Q^2}{Q_{nom}^2}, \qquad (14)$$

where

$$\Delta P_c = \frac{rQ_{nom}^2}{U^2}. \qquad (15)$$

If the change ΔQ in reactive load affects the load of the synchronous machine or network appreciably, the loss variation is given by the formula

$$\Delta p = \Sigma \Delta P_1 - \Sigma \Delta P_2, \qquad (16)$$

where $\Sigma \Delta P_1$ represents the losses in the synchronous machine or in the

network at the reactive load Q; $\Sigma\Delta P_2$ the same, but at the reactive load $Q - \Delta Q$.

But if the reactive load of the synchronous machine or network were to change by a relatively small amount ΔQ, the loss variation would be

$$\Delta p = \Delta Q g, \tag{17}$$

where g is the "relative increment" (see below).

This relative increment is defined as the first derivative of the reactive power loss:

for synchronous machines

$$g = \frac{2AQ}{Q_{nom}^2} + \frac{B}{Q_{nom}}; \tag{18}$$

for the network

$$g = \frac{2rQ}{U^2} = \frac{2\Delta P_c Q}{Q_{nom}^2}; \tag{19}$$

for static capacitors

$$g = 0.003 \text{ to } 0.005 = \text{const.} \tag{20}$$

It will be seen from these formulae that the relative increments vary according to a linear law for the network and synchronous machines. A reduction in the requirements of reactive power reduces losses in a synchronous machine and the network relatively more for larger reactive loads.

The reactive load must be distributed between the reactive-power sources connected in the network (synchronous generators, condensers, motors and static capacitors) according to the criterion of equal relative increments. In the first instance, sources with the smallest relative increments should be loaded. The relative increments of synchronous machines have been published elsewhere [2].

A comparative cost analysis will now be made of an asynchronous motor with static capacitors and a synchronous motor operating at $\cos\phi = 1$.

The estimated expenditure on each system is

$$E_{am} = K_{am}(P_{nom} + P_{am}) + K_c(P_{nom} + P_{ac}) + rE_e\Delta P_{am} + TE_e\Delta P_c \tag{21}$$

$$E_{sm} = K_{sm}(P_{nom} + P_{sm}) + rE_e\Delta P_{sm} \tag{22}$$

where K_{am} and K_{sm} are the prime cost of the asynchronous motor and synchronous motor respectively; P_{am}, P_{sm} and P_{ac} depreciation coefficients for the asynchronous motor, synchronous motor and capacitors

respectively; r the duration of loss for motors at the rated shaft load, hr; E_e the estimated expenditure on electricity, roubles/kW. hr; K_c the cost of 1 kVAR of capacitors with the cost of erection and the gear for forcing them at reduced voltages included, roubles/kVAR; ΔP_c the specific active power loss of the capacitors, kW/kVAR; and T the number of hours that the capacitors are connected.

Whenever a synchronous motor costs more than an asynchronous motor with or without capacitors, the expediency of using a synchronous motor depends on the saving in electricity costs. The saving in electricity is proportional to the product of the number of loss hours times the cost of 1 kWh. It therefore follows that synchronous motors are advantageous in sustained operation.

Example 1. The specifications of the asynchronous motor are: 55 kW, 1000 rev/min, 380 V, $\eta' = 0.91$, $\cos \phi' = 0.87$, $Q_{nom} = 34$ kVAR, $\Sigma \Delta P = 5.5$ kW, price 242 roubles.

Those of an SM-type synchronous motor are:

56 kW, 80 kVA, 380 V, $\cos \phi' = 0.8$, $\eta' = 0.88$, $Q_{nom} = 48$ kVAR, $\Delta P_x = 1.71$ kW, $\Delta P_{sv} = 3.45$ kW, $\Delta P_{rv} = 2.43$ kW, $\Sigma \Delta P = 7.6$ kW, price 700 roubles.

The capacitor specifications are:

$U = 380$ V, $K_c = 8.5$ roubles kVAR, $\Delta P_c = 0.005$ kW/kVAR.

The purchase cost of the motor and capacitors is $242 + 8.5 \times 34 = 531$ roubles.

If the synchronous motor were planned to operate at $\cos \phi' = 1$, its price would then be about 560 roubles. Thus, in this case the synchronous motor would cost 29 roubles more than an asynchronous motor with capacitors.

Since capacitors have larger depreciation allowances, the estimated expenditure, which is proportional to capital investment, will be somewhat less for the synchronous motor.

In fact, for the synchronous motor

$$560 (0.125 + 0.06) = 104 \text{ roubles},$$

and for the asynchronous motor and capacitors

$$242 (0.125 + 0.06) + 8.5 \cdot 34 (0.125 + 0.1) = 110 \text{ roubles}.$$

Since the losses of a synchronous motor at $\cos \phi = 1$ are less than those of an asynchronous motor even if the capacitor losses are ignored, a synchronous motor designed for operation at $\cos \phi = 1$ is more

economical.

A 56 kW synchronous motor with cos ϕ' = 0.8 which can be operated at cos ϕ = 1 is only more economical than an asynchronous motor and capacitors at an electricity cost of 0.01 roubles/kWh if the number of loss hours is 4220. In this case the estimated expenditure is the same for both systems (ignoring capacitor losses). In this example an old-type synchronous motor with a machine exciter has been considered. New synchronous motors with cos ϕ' = 1 without machine exciters are cheaper than asynchronous motors with capacitors. For example, the ESM-91-6-type synchronous motor with semiconductor rectifier excitation at cos ϕ' = 0.9 has losses of 4.94 kW, η' = 91.75 per cent and its price is only 427 roubles. At cos ϕ = 1, the losses are 4.25 kW. This motor is cheaper than an asynchronous motor with capacitors and lower losses even in operation with cos ϕ = 0.9. Its use is therefore rational whether for sustained or shock loads. Cases occur in practice when there is no need to produce reactive power, e.g. when synchronous motors are connected to the generator voltage bus-bars. In such cases operation of synchronous motors with cos ϕ = 1 is advantageous. In practically every case the synchronous motors have a higher efficiency than asynchronous motors. In any particular case the advisability of using synchronous motors should be worked out without including the cost of the static capacitors for the asynchronous motors.

The conditions under which the greater purchase price of a synchronous motor can be recovered out of savings in electricity will now be considered.

It can be assumed that the depreciation coefficients are the same for synchronous and asynchronous motors. It is supposed that $P_{nom} + P_{am} = P$. The estimated expenditure for a synchronous motor is

$$E_{am} = K_{am}P + rE_e \Delta P_{am}; \tag{23}$$

that for the asynchronous motor is

$$E_{sm} = K_{sm}P + rE_e \Delta P_{sm} \tag{24}$$

Substituting in (23) and (24) respectively

$$\Delta P_{am} = P(1 - \eta_{am})/\eta_{am} \text{ and } \Delta P_{sm} = P(1 - \eta_{sm})/\eta_{sm} \tag{e}$$

the estimated expenditures are

$$E_{am} = K_{am}P + (rE_eP(1 - \eta_{am})/\eta_{am}) \tag{23a}$$

$$E_{sm} = K_{sm}P + (rE_eP(1 - \eta_{sm})/\eta_{sm}) \tag{24a}$$

Example 2. The specifications of the DS-13-52-8A-type synchronous motor are:

575 kW, $\cos \phi' = 0.9$, $\cos \phi = 1$, $\eta'_1 = 94\%$, $\Sigma \Delta P = 36.7$ kW, price 4410 roubles.

The specifications of a DAMSO-1512-8 asynchronous motor are:

570 kW, $\eta' = 92.5\%$, price 3580 roubles, $\Sigma \Delta P = 46.2$ kW.

The loss difference is 9.5 kW.

Assuming that $r = 4000$ hr, $E_e = 0.1$ roubles/kWh and that $P_{a\,nom} + P_{am} = 0.125 + 0.06 = 0.185$,

$$E_{am} = 3580 \cdot 0.185 + \frac{4000 \cdot 0.01 \cdot 570 (1 - 0{,}925)}{0.925} = 2512 \text{ roubles};$$

$$E'_{am} = 4410 \cdot 0.185 + \frac{4000 \cdot 0.01 \cdot 570 (1 - 0.94)}{0.94} = 2265 \text{ roubles}.$$

Thus the synchronous motor is the better economic proposition. Moreover, the decrease in reactive power is

$$Q = \frac{P_{nom} \tan \phi'}{\eta'} = \frac{570}{0.925} \cdot 0.62 = 382 \text{ kVAR}.$$

Now consider the extra saving when supply is from a T-2-25-2-type 25 MVA turbo-generator for which the relative increment (see the appendix) is

$$g = \frac{2 \cdot 57.2}{25\,000 \cdot 0.75} \frac{Q}{Q_{nom}} + \frac{38.7}{25\,000 \cdot 0.75} = 0.006 \frac{Q}{Q_{nom}} + 0.002.$$

If the generator is operating with approximately rated reactive load, the saving in power in the generator is

$$\Delta P = 382 \cdot 0.008 = 3.06 \text{ kW and } 4000 \cdot 0.01 \cdot 3.06 = 122 \text{ roubles, or } 5.4\%$$

which favours the synchronous motor system. The loss difference is 12.56 instead of 9.5 kW.

If the reactive power load of the generator were 0.25 of rated, the saving would be

$$\Delta P = 382 (0.006 \cdot 0.25 + 0.002) = 1.34 \text{ kW}.$$

Example 3. The specifications of an STM-1500-2-type synchronous motor are:

1500 kW, 1740 kVA, 6 kV, cos $\phi' = 0.9$, $\eta' = 95.65\%$, 760 kVAR, constant losses 36.3 kW, stator copper loss 11 kW, additional losses 11 kW, excitation loss 10 kW, $\Sigma\Delta P = 68.3$ kW, price 14,600 roubles.

It is connected to a 10 MVA works transformer with short-circuit losses of 92 kW.

Operation at cos $\phi = 1$ will be considered.

From the appropriate table in the appendix

$$A = 4.68 \text{ kW and } B = 3.5 \text{ kW}$$

The losses in a synchronous motor at cos $\phi = 1$ are

$$\Sigma\Delta P = 68.3 - 4.68 - 3.5 = 60.1 \text{ kW} \quad (\eta' = 96.15\%).$$

The total power is 1560 kVA.

The estimated expenditure at $\tau = 4000$ hr and $E_e = 0.01$ roubles/kWh is

$$E_{sm} = 14\,600 \cdot 0.185 + 4\,000 \cdot 0.01 \cdot 60.1 = 5\,140 \text{ roubles}$$

The specifications of an ATM-type asynchronous motor are:

1500 kW, 6 kV, cos $\phi' = 0.88$, $\eta' = 95\%$, 855 kVAR and the price 9810 roubles.

The losses in the asynchronous motor are

$$\Sigma\Delta P = \frac{1\,500}{0.95} \cdot (1 - 0.95) = 79 \text{ kW}.$$

The loss difference is 18.9 kW.

The estimated expenditure is

$$E_{am} = 9\,810 \cdot 0.185 + 4\,000 \cdot 0.01 \cdot 79 = 4\,970 \text{ roubles}$$

We also require to determine the decrease in losses in the transformer if the reactive power is reduced by 855 kVAR. The losses in the transformer due to the reactive power are

$$\Delta P_t = \Delta P_{sc} \frac{Q^2}{S^2_{nom.t}} = 0.92Q^2.$$

Assuming that the transformer load is 9 MVA in the period of maximum at cos $\phi = 0.8$, the losses in the transformer from the reactive power $Q_1 = 9 \times 0.6 = 5.4$ kVAR are

$$\Delta P_t = 0.92 \cdot 5.4^2 = 26.8 \text{ kW}.$$

The relative increment for the reactive load of 5.4 MVAR is

$$g = \frac{2 \cdot 26.8Q}{5\,400Q_1} = 0.01\frac{Q}{Q_1}.$$

If a synchronous motor at cos ϕ = 1 is used instead of the asynchronous motor, the reactive power of the load is reduced by 855 kVAR and the reactive power transmitted through the transformer will be 4.54 MVAR. The active losses in the transformer are reduced by

$$\Delta P_{t1} - \Delta P_{t} = 0.92 \cdot \frac{92}{10^2}(5.4^2 - 4.54^2) = 7.85 \text{ kW}.$$

The same result (7.85 kW) is produced by the formula

$$\Delta P_{t1} - \Delta P_{t2} = g_1 \frac{Q_{av}}{Q_1}\Delta Q,$$

where

$$Q_{av} = \frac{Q_1 + Q_2}{2} = 4.94 \text{ MVAR}.$$

The loss difference is 26.75 kW. The extra saving is 4000 × 0.01 × 7.85 = 315 roubles.

Thus, the estimated expenditure for a synchronous motor at cos ϕ = 1 is 5140 − 315 = 4825 roubles if the change in reactive power requirements is included, i.e. it is 145 roubles less than that for an asynchronous motor.

Now consider operation at cos ϕ = 0.9.

The decrease in reactive power is

$$Q = 760 + 855 = 1\,615 \text{ kVAR}.$$

The decrease in active losses in the transformer is

$$\Delta P_{t1} - \Delta P_{t2} = 0.92(5.4^2 - 3.785^2) = 13.7 \text{ kW}.$$

The estimated expenditure is

$$E_{av} = 14\,600 \cdot 0{,}185 + 4\,000 \times$$
$$\times 0.01(68.3 - 13.7) = 4\,890 \text{ roubles}$$

Thus, a synchronous motor with cos ϕ = 1 is the more advantageous, since the estimated annual expenditure is in this case less by 4890 − 4825 = 65 roubles.

Example 4. The specifications of an STM-3500-2 synchronous motor are:

3500 kW, 4050 kVA, 1770 kVAR, 6.3 kV, cos ϕ' = 0.9, η' = 96.1%, $\Sigma\Delta P$ = 142 kW, price 20,900 roubles.

Assuming that the distribution of the losses is the same as for a 1500 kW motor, the constant losses are 77 kW, the stator copper loss (including additional losses) is 45 kW and the excitation loss is 20 kW;

$$A = 0.19 \cdot 45 + 0.05 \cdot 20 = 9.5 \quad \text{kW};$$
$$B = 0.35 \cdot 20 = 7 \quad \text{kW}.$$

If $\cos \phi = 1$, then $\Sigma \Delta P = 142 - 9.5 - 7 = 125$ kW, and

$$S_{\text{nom.1}} = 3.625 \text{ kVA}, \quad \eta'_1 = 96.54\%$$

The specification of an ATM-3500-2 asynchronous motor are:

3500 kW, 6 kV, $\cos \phi' = 0.85$, $\eta' = 95.4\%$, price 19,000 roubles.

For an asynchronous motor

$$Q_{\text{nom}} = \frac{3\,500}{0.954} \cdot 0.621 = 2\,280 \quad \text{kVAR};$$

$$\Sigma \Delta P = \frac{3\,500}{0.954} (1 - 0{,}954) = 169 \quad \text{kW}.$$

The estimated expenditure for the two systems (the synchronous motor and the asynchronous motor without static capacitors), if $r = 4000$ hr and $E_e = 0.01$ roubles/kWh, is

$$E_{\text{sm}} = 20\,900 \cdot 0.185 + 125 \cdot 4\,000 \cdot 0{,}01 = 8\,870 \text{ roubles}$$
$$E_{\text{am}} = 19\,000 \cdot 0.185 + 169 \cdot 4\,000 \cdot 0.01 = 10\,270 \text{ roubles}$$

Thus the synchronous motor with $\cos \phi = 1$ is the better economic proposition. Moreover, the decrease in reactive power is 2280 kVAR.

In this particular case the synchronous motor with $\cos \phi = 0.9$ is more advantageous than the synchronous motor with $\cos \phi = 1$ and static capacitors. The estimated expenditure for this system is

$$E_{\text{sm}} = 20\,900 \cdot 0.185 + 6.5 \cdot 1\,770 \cdot 0.225 + \\ + 125 \cdot 4\,000 \cdot 0{,}01 + 8\,000 \cdot 0{,}005 \times \\ \times 1\,770 \cdot 0.01 = 11\,100 \text{ roubles}$$

That for the motor with $\cos \phi = 0.9$ is

$$E_{\text{sm}} = 20\,900 \cdot 0.185 + 142 \cdot 4\,000 \cdot 0.01 = 9\,570 \text{ roubles}$$

i.e. it is 1530 roubles less each year.

Example 5. For a shaft load of 3900 kW at 3000 rev/min, it is necessary to choose a synchronous motor. The reactive power can be provided by capacitors or by the synchronous motor. An STM-3500-2-type synchronous motor with $\cos \phi = 1$ and capacitors may in fact be used. Subtracting the losses (125) from the total power (4050 kVA), the shaft power is

$$P = 4\,050 - 125 = 3\,925 \text{ kW}$$

It is assumed that the efficiency remains the same even though it slightly increases due to a reduction in rotor current. The losses in this motor have already been determined (see example 4).

The alternative is an STM-6000-2-type motor:

4000 kW, $\cos \phi' = 0.7$, $\eta' = 0.952$, price 24,500 roubles.

The reactive power and losses are

$$Q = \frac{4\,000 \cdot 1.054}{0.952} = 4\,400 \text{ kVAR};$$

$$\Sigma \Delta P = \frac{4\,000}{0.952} \cdot (1 - 0.952) = 200 \text{ kW}.$$

To simplify the analysis, it is assumed that the motor losses and the reactive power are the same for a shaft load of 3900 kW as for 4000 kW.

Compare now the estimated expenditure for a shaft load of 3900 kW and a reactive power of 4400 kW. If r = 3500 hr, T = 7000 hr and E_e = 0.012 roubles/kWh, then

$$E_{3\,500} = 20\,900 \cdot 0.185 + 4\,400 \cdot 6.50 \cdot 0.225 + \\ + 142 \cdot 3\,500 \cdot 0.012 + 4\,400 \cdot 0.005 \times \\ \times 7\,000 \cdot 0.012 = 18\,100 \text{ roubles}$$

$$E_{6\,000} = 24\,500 \cdot 0.185 + 200 \cdot 3\,500 \cdot 0.012 = 12\,850 \text{ roubles}$$

In this case the synchronous motor with the larger rated power is the better proposition.

It has been seen that synchronous motors with $\cos \phi' = 1$ are to be preferred in practice to asynchronous motors and capacitors for small powers. It has also been shown that in a number of cases synchronous motors with $\cos \phi' < 1$, if operated with $\cos \phi = 1$, are a better proposition than asynchronous motors, owing to the savings in electricity.

After a certain point it is more economical to use synchronous motors as reactive power sources than capacitors. In this case it is necessary to compare a synchronous motor and static capacitors for which $\cos \phi = 1$ with a synchronous motor for which $\cos \phi < 1$.

From a certain rated power onwards, synchronous motors are cheaper and have better weight indices than asynchronous motors for a particular rotational speed. In such cases the capital and electricity costs of synchronous motors are lower. For example, the weight of a DSP 1300 kW synchronous motor with solid shoes and starting winding with $\cos \phi = 0.9$ and n = 1500 rev/min is very little different from that of a DAZ asynchronous motor of the same power.

Conclusions

Synchronous motors should be used extensively in place of asynchronous motors. For small synchronous motors it is necessary to dispense with machine exciters and use semiconductor rectifiers instead. This will considerably widen the field of application for synchronous motors. For example, a 55 kW synchronous motor with $\cos \phi' = 0.9$ costs less and is cheaper to run than an asynchronous motor with static capacitors.

There is however a wider field of application for relatively small synchronous motors (especially in operation with $\cos \phi = 1$) than for asynchronous motors with static capacitors.

After a certain rated power it is expedient to use synchronous motors with a "leading" power factor ($\cos \phi < 1$). The larger the number of loss hours, it becomes economically expedient to use them with a lower rated power. In certain conditions it is economically expedient to increase the rated power of synchronous motors in order to produce reactive power.

In a number of cases synchronous motors with $\cos \phi' < 1$, if operated with $\cos \phi = 1$, are a better proposition than asynchronous motors without static capacitors, owing to their higher efficiency.

Synchronous motors should be preferred in all cases for drives which are in continuous use for a relatively large number of hours, since their economic effect is then maximum.

Synchronous motors should be used for voltage regulation.

Synchronous motors must be provided with an excitation forcing device which comes into operation at reduced voltages. A similar device should be provided for motors with suddenly applied loads.

The reactive power should be distributed between parallel-operating sources from consideration of equal relative increments.

It is necessary to speed up the development and mass production of synchronous motors of all types and designs, including excitation systems through semiconductor rectifiers without the excitation winding on the salient-pole rotor, without contacts in the excitation circuit, but using a "dynamic transformer" and semiconductor rectifiers on the motor shaft.

Appendix

AIR-COOLED TURBO GENERATORS

Type	T-2-6-2	T-2-12-2	T-2-25-2	T-2-50-2
P_{nom}, MW	6	12	25	50.000
$\cos \phi'$	0.8	0.8	0.8	0.85
$A + B/Q_{nom}$, kW/kVAR	0.0047	0.0055	0.0051	0.0032
A, kW	11.9	30.6	57.2	62.1
B, kW	9.5	18.5	38.7	36.7
B/Q_{nom}, kW/kVAR	0.0021	0.002	0.002	0.0012

HYDROGEN-COOLED TURBO GENERATORS

Type	TV-2-30-2	TV-50-2	TV-60-2	TV-2-100-2	TV-2-150-2
P_{nom}, MW	30	50	60	100	100
$\cos \phi'$	0.85	0.85	0.85	0.85	0.9
$A + B/Q_{nom}$, kW/kVAR	0.0056	0.0041	0.0046	0.0031	0.0025
A, kW	63.4	75.1	107	116	86.5
B, kW	41	51	64	76	98
B/Q_{nom}, kW/kVAR	0.0022	0.0016	0.0017	0.0012	0.0013

DS-TYPE SYNCHRONOUS MOTORS, 380 V, $\cos \phi' = 0.9$

Rated Power	Rated speed rev/min	1500	1000	750	600	500
P_{nom} = 55 kW	$A + B/Q_{nom}$, kW/kVAR		-	0.044	0.052	0.050
	A, kW	-	-	0.54	0.66	0.62
	B, kW	-	-	0.75	0.91	0.90
	B/Q_{nom}, kW/kVAR	-	-	0.025	0.03	0.03

Rated Power	Rated speed rev/min	1500	1000	750	600	500
P_{nom} = 75 kW	$A + B/Q_{nom}$, kW/kVAR	-	1.042	0.043	0.048	0.043
	A, kW	-	0.80	0.75	0.80	0.76
	B, kW	-	0.89	0.94	1.13	0.98
	B/Q_{nom}, kW/kVAR	-	0.022	0.023	0.027	0.024
P_{nom} = 100 kW	$A + B/Q_{nom}$, kW/kVAR	0.034	0.038	0.037	0.043	0.042
	A, kW	0.82	0.90	0.78	0.87	0.91
	B, kW	0.95	1.13	1.15	1.40	1.34
	B/Q_{nom}, kW/kVAR	0.018	0.021	0.022	0.026	0.025
P_{nom} = 125 kW	$A + B/Q_{nom}$, kW/kVAR	0.030	0.035	0.034	0.037	-
	A, kW	0.92	1.06	0.95	0.95	-
	B, kW	1.04	1.26	1.28	1.50	-
	B/Q_{nom}, kW/kVAR	0.016	0.019	0.020	0.023	-
P_{nom} = 160 kW	$A + B/Q_{nom}$, kW/kVAR	0.027	0.031	0.030	-	-
	A, kW	1.04	1.19	1.12	-	-
	B, kW	1.17	1.43	1.38	-	-
	B/Q_{nom}, kW/kVAR	0.014	0.017	0.016	-	-
P_{nom} = 200 kW	$A + B/Q_{nom}$, kW/kVAR	0.023	0.024	-	-	-
	A, kW	1.12	1.24	-	-	-
	B, kW	1.29	1.29	-	-	-
	B/Q_{nom}, kW/kVAR	0.012	0.012	-	-	-

Rated Power	Rated speed rev/min	1500	1000	750	600	500
P_{nom} = 250 kW	$A + B/Q_{nom}$, kW/kVAR	0.022	0.022	-	-	-
	A, kW	1.50	1.47	-	-	-
	B, kW	1.37	1.48	-	-	-
	B/Q_{nom}, kW/kVAR	0.010	-	-	-	-
P_{nom} = 320 kW	$A + B/Q_{nom}$, kW/kVAR	0.02	-	-	-	-
	A, kW	1.7	-	-	-	-
	B, kW	1.62	-	-	-	-
	B/Q_{nom}, kW/kVAR	0.01	0.011	-	-	-

ESM-TYPE SYNCHRONOUS MOTORS WITH SEMICONDUCTOR RECTIFIER EXCITATION, $\cos \phi' = 0.9$

Rated power, kW	55	55	75	100
n_{nom}, rev/min	1500	1000	1500	1500
$A + B/Q_{nom}$, kW/kVAR	0.0215	0.0235	0.0184	0.0155
A, kW	0.45	0.45	0.5	0.534
B, kW	0.19	0.245	0.235	0.285
B/Q_{nom}, kW/kVAR	0.0064	0.00827	0.00588	0.0054

DS-TYPE SYNCHRONOUS MOTORS 6 kV, 1500 rev/min, $\cos \phi' = 0.9$

Rated power, kW	400	500	630	800	1000
$A + B/Q_{nom}$, kW/kVAR	0.0191	0.0181	0.0158	0.0137	0.0134
A, kW	2.40	2.90	3.10	3.03	3.81
B, kW	1.45	1.78	2.06	2.62	3.05
B/Q_{nom}, kW/kVAR	0.00695	0.0069	0.00635	0.00635	0.0060

STM-TYPE SYNCHRONOUS MOTORS 6 kV, 3000 rev/min, $\cos \phi' = 0.9$

Rated power, kW	750	1500	1500 (sic)	4000	6000	12,000
A, kW	2.58	4.17	5.03	7.30	9.70	14.8
B, kW	2.80	3.44	4.40	7.30	7.00	13.4
$A + B/Q_{nom}$, kW/kVAR	0.014	0.010	0.0074	0.0073	0.0055	0.0021
B/Q_{nom}, kW/kVAR	0.0072	0.0054	0.0035	0.0036	0.0023	0.0010

Translated by O.M. Blunn

REFERENCES

1. Rosenberry; Brushless d.c. excited rotating field synchronous motor. *Applications and Industry*, July (1960).

2. V.I. Pleskov and G.G. Magazinnik; *Elektrichestvo*, No. 10 (1960).

3. The fundamentals of costing in power engineering (Osnovnye metodicheskiye polazheniya tekhniko-ekonomicheskikh raschetov v energetike). *Elektrichestvo*, No. 10 (1959).

4. I.A. Syromyatnikov; *Elektrichestvo*, No. 3 (1961). (Translated in *Electric Technology U.S.S.R.*, Vol. 1, 1961).

THE THEORY AND DESIGN OF ELECTROMAGNETIC VIBRATION EQUIPMENT*

A. E. CHESNOKOV

Odessa

(Received 9 July 1960)

Electromagnetic vibrators are simple devices and are widely used in industry, but their operation has not been adequately studied. The existing methods of analysis fail to take into account several factors which determine their output capability as electrical machines. Moskvitin's simplified approach [1] does not provide an adequately rigorous analysis of their operating conditions.

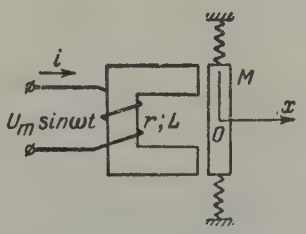

Fig. 1. The circuit of an electromagnetic vibrator.

As in the case of a more complicated problem [2], this paper considers the non-linear variation of the inductance in the operation of electromagnetic vibrators. If it is assumed that the inductance L is only a function of the displacement x of the armature, i.e. that the magnetic system is non-saturated and that hysteresis phenomena are absent, a vibrator with the vibrating mass M can be described by the following differential equations:

---

* *Elektrichestvo*, 12, 37-40, 1961.

$$\frac{d}{dt}(Li)+ir=U_m\sin\omega t; \tag{1}$$

$$M\frac{d^2x}{dt^2}+\mu\frac{dx}{dt}+fx=\frac{1}{2}i^2\frac{dL}{dx}. \tag{2}$$

The following approximating function can be used for $L(x)$:

$$L=L_0\exp(-\gamma x+\rho^2x^2). \tag{3}$$

Here γ and ρ are independent of x. If these coefficients are selected appropriately, function (3) quite accurately characterizes $L(x)$ quantitatively and qualitatively.

Suppose as a first approximation that the oscillation of the armature is governed by the following harmonic law:

$$x=A\cos(2\omega t-\psi), \tag{4}$$

the inductance is expressible by the time function

$$L=L_0\exp[-m\cos(2\omega t-\psi)+ +2m_\rho\cos^2(2\omega t-\psi)],$$

where

$$m=\gamma A=\frac{1}{2}\ln\frac{L_{max}}{L_{min}}; \qquad m_\rho=\frac{\rho^2A^2}{2}=\frac{1}{4}\ln\frac{L_{max}L_{min}}{L_0^2}. \tag{5}$$

The coefficient m defines the relative variation of inductance; the coefficient m_ρ defines the shape of the curve $L(x)$ (its concavity). Inasmuch as the shape of the curve $L(x)$ depends on the relation between the magnetic conductances for the operating flux and the leakage flux for the various positions of the armature (i.e. it depends on the configuration of the magnetic circuit), the most efficient shape can be specified for the magnetic circuits of vibrators by introducing the coefficient m_ρ and studying its effect on the characteristics of the vibrator.

Since m is always less than 1 and m_ρ is much less than m, equation (1) reduces to Mathieu's equation

$$\ddot{v}+[a-2q\sin(2\omega t-\psi)]v=\frac{\omega}{Lu}\cos\omega t. \tag{6}$$

Here

$$i = vu; \quad u = \exp[m\cos(2\omega t - \psi) - m_\rho \cos(4\omega t - 2\psi)];$$

$$a = -\delta^2; \quad q = 2\omega\delta m; \quad \delta = \frac{r}{2L_0} e^{-m_\rho}.$$

For an electromagnetic vibrator $|a|$ is always much less than $|2q|$. An approximate solution of Mathieu's equation therefore is [3]

$$i = I_0 \sin(\omega t - \varphi) \exp[m\cos(2\omega t - \psi) - 2m_\rho \cos^2(2\omega t - \psi)], \tag{7}$$

where

$$I_0 = \frac{U_m}{L_0\sqrt{4\delta^2 + \omega^2 - 8\omega\delta m}};$$

$$\varphi = \arctan\frac{\omega - 4\delta m}{2\delta}.$$

Hence the current in the vibrator circuit can be regarded as a sinusoidal current which varies in amplitude with time. The expressions for I_0 and ϕ reflect the variation of these quantities with the non-linear variation of the vibrator's inductance defined by the quantities m and m_ρ. In particular, if $m = 0$ and $m_\rho = 0$, these expressions provide formulae which hold good for circuits with a constant resistance and inductance.

Oscillation amplitude and phase

Equation (7), when considered with (3) and (4), allows the right-hand side of equation (2) to be represented as the function $P(x, t)$. Equation (2) can then be transformed into the following non-linear equation by expanding the quantity $\exp(\gamma x - \rho^2 x^2)$ as a power series:

$$\ddot{w} + b\dot{w} + a^2 w = -\frac{\gamma^2}{m^2 M} \cdot \frac{L_0 I_0^2}{2}\left[\left(\frac{m}{2} + \alpha_0 w + \beta_0 w^2 + \gamma_0 w^3 + \ldots\right) - \left(\frac{m}{2} + \alpha_0 w + \beta_0 w^2 + \gamma_0 w^3 + \ldots\right)\cos(2\omega t - 2\varphi)\right], \tag{8}$$

where $w = x/A = (\gamma/m)x$ is the relative displacement; α_0, β_0, γ_0, ... are coefficients depending on the shape of the curve $L(x)$ and the relative variation of the inductance m; and $b = \mu/M$ and $a^2 = f/M$.

A new time scale is selected:

$$n\tau = 2\omega t - 2\varphi \quad (n = 1, 2, 3, \ldots)$$

and w is added to the left- and right-hand sides of (8). This equation then becomes

$$\begin{aligned} w + w = {} & \xi w - n\vartheta w - \\ & - n^2\lambda_0\left(\frac{m}{2} + \alpha_0 w + \beta_0 w^2 + \gamma_0 w^3 + \ldots\right) + \\ & + n^2\lambda_0\left(\frac{m}{2} + \alpha_0 w + \beta_0 w^2 + \gamma_0 w^3 + \ldots\right)\cos n\tau. \end{aligned} \tag{9}$$

The following notation is used for the sake of simplicity:

$$\vartheta = \frac{b}{2\omega}; \quad \xi = \frac{4\omega^2 - n^2\alpha^2}{4\omega^2};$$

$$\lambda_0 = \frac{\gamma^2}{4\omega^2 m^2 M} \cdot \frac{L_0 I_0^2}{2}.$$

All the coefficients on the left-hand side of (9) are less than one; the solution of equation (9) in w can be found by Mandel'shtam and Papaleksi's method [4] for any whole-number value of n. Solutions for $n > 1$ permit a thorough examination of the possibility of multiple oscillations occurring and existing in electromagnetic vibrators; the terms on the right-hand side of (9) which determine their non-linearity are most important.

For normal oscillations (i.e. if $n = 1$), an approximate solution of (9) can be obtained by considering only terms to the first power of w:

$$w = \frac{m\lambda_0}{2\sqrt{\xi_d^2 + \vartheta^2}} \sin(2\omega t - 2\varphi - \theta), \tag{10}$$

where

$$\theta = \arctan\frac{\xi_d}{\vartheta};$$

$$\xi_d = \xi - \alpha_0\lambda_0.$$

Using the same notation, the following expression can be written for the armature displacement according to (10):

$$\begin{aligned} x = {} & \frac{P_m}{\sqrt{(4\omega^2 - \alpha^2 - \alpha_e^2)^2 + 4\omega^2 b^2}} \times \\ & \times \sin\left(2\omega t - 2\varphi - \arctan\frac{4\omega^2 - \alpha^2 - \alpha_e^2}{2\omega b}\right), \end{aligned} \tag{11}$$

where $P_m = \gamma/2M \times L_0 I_0^2/2$ is the maximum value of the force per unit of vibrating mass M; and

$$\alpha_e^2 = \alpha_0 \frac{\gamma^2}{m^2 M} \cdot \frac{L_0 I_0^2}{2}.$$

Formula (11) defines the nature of the oscillations of an electromagnetic vibrator which is supplied from a sinusoidal voltage source.

The motion of a mechanical vibrator due to a force $F = F_m \cos(2\omega t - 2\phi)$ which varies periodically with time is described by a linear differential equation

$$\ddot{x} + b\dot{x} + a^2 x = P_m \cos(2\omega t - 2\varphi).$$

The forced oscillations can be found by the formula

$$x = \frac{P_m}{\sqrt{(4\omega^2 - a^2)^2 + 4\omega^2 b^2}} \times \sin\left(2\omega t - 2\varphi - \arctan\frac{4\omega^2 - a^2}{2b\omega}\right). \quad (12)$$

Comparison of formulae (11) and (12) permits a comparison of the displacement which obtains when the periodic variation of the inductance is included to be made with that which occurs due to a periodically varying force. The presence in (11) of a term with α_e^2, which depends on the electrical criteria of the vibrator, indicates that the resonance conditions of an electromagnetic vibrator are somewhat different from those of a mechanical vibrator. Calculations have shown that this difference is sometimes considerable; even though the quantity α_e^2 may be no more than four to five per cent of $4\omega^2$ if $\omega = 314$, the oscillation amplitude may be under-estimated by 17 to 20 per cent if it is ignored.

Oscillation power

From (5) and (7), the flux coupling of the vibrator winding is

$$\Psi = Li = L_0 I_0 \sin(\omega t - \varphi). \quad (13)$$

Relationships $\Psi(i)$ and $i(t)$ are plotted from equations (7) and (13) in Fig. 2. The area bounded by the curve $\Psi(i)$ is proportional to the mechanical work of the vibrator.

The power of the vibrator is

$$P = \frac{1}{T}\int_0^T i \, d\Psi. \quad (14)$$

Expanding the amplitude factor in (7) as a power series and substituting the value obtained for the current in the integral (14)

$$P = \omega \frac{L_0 I_0^2}{2} M_1 \cos\theta, \tag{15}$$

where

$$M_1 = \frac{1}{2}\left[m\left(1 - \frac{3}{2}m_\rho\right) + \frac{m}{8}(m^2 + 10m_\rho) - \dots\right];$$

$$\theta = \text{arc tan}\ \frac{4\omega^2 - \alpha^2 - \alpha_e^2}{2\omega b}.$$

From (15), the power of the vibrator increases with increasing relative variation of the inductance and depends on the concavity of the curve $L(x)$.

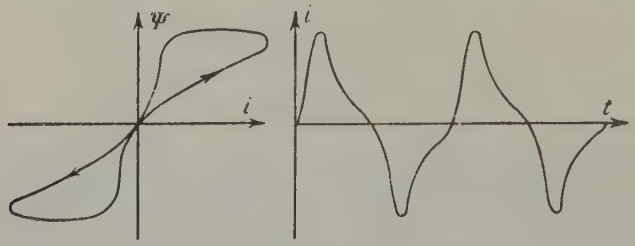

Fig. 2. The relationship $\Psi(i)$ and the current curve of a vibrator for $\theta = 0$.

The coefficient M_1 defines the efficiency of energy conversion. Its relationship with the electrical criteria of the vibrator on the one hand and the required maximum force upon the armature on the other can be found in the following way. Suppose $x = A \sin(2\omega t - 2\phi - \theta)$ is the displacement and $F = F_m \cos(2\omega t) - 2\phi)$ the force on the armature. The mechanical power of the vibrator is then

$$P = \frac{1}{T}\int_0^T F dx = \omega A F_m \cos\theta, \tag{16}$$

Equating the right-hand sides of equations (15) and (16):

$$F_m = \frac{M_1}{A} \cdot \frac{L_0 I_0^2}{2}. \tag{17}$$

Example

Suppose it is required to design a vibrator for which the mechanical power P is 500 W, the fibrating mass M = 20 kg, the oscillation amplitude A = 3 mm, the angular frequency of vibration 2ω = 628 1/sec, and

the rated voltage U = 380 V.

Given average values of the coefficients m and m_ρ, a start is made by calculating the current, the number of turns in the winding, the cross-section of the magnetic circuit and its shape and dimensions.

In practice, the "modulation coefficient" of L is between 0.6 and 0.9. Suppose it is m = 0.75. Initially it can be assumed that $m_\rho \approx m/4$. M_1 is 0.317 for these two values of m and m_ρ.

The maximum linear speed of the armature is

$$v_m = 2\omega A = 2 \cdot 314 \cdot 0.003 = 1.884 \text{ m/sec}$$

The force acting on the armature is found from (16). At resonance (θ = 0)

$$F_m = \frac{P}{\omega A} = \frac{500}{314 \cdot 0.003} = 530 \text{ n}.$$

Expression (17) provides the energy of the magnetic field corresponding to maximum flux coupling:

$$W_0 = \frac{L_0 I_0^2}{2} = \frac{A F_m}{M_1} = \frac{0{,}003 \cdot 530}{0.317} = 5 \text{ J}$$

The inductance for the central position of the armature can be estimated from the following considerations. Assuming that the air-gap δ is small

$$I_0 \approx \frac{U_m}{\omega L_0}.$$

By definition

$$W_0 = \frac{U_m^2}{2\omega^2 L_0},$$

and hence

$$L_0 = \frac{U_m^2}{2\omega^2 W_0} = \frac{(380\sqrt{2})^2}{2 \cdot 314^2 \cdot 5} = 0.292 \text{ H}$$

The preliminary estimate of the current is

$$I_0 = \sqrt{\frac{2W_0}{L_0}} = \sqrt{\frac{2 \cdot 5}{0.292}} = 5.87 \text{ A},$$

The number of turns in the winding and the cross-section of the magnetic circuit can be selected by assuming that the magnetic reluctance of the armature is equal to that of the air-gap δ_0. Then

$$L_0 = \frac{w^2}{R_0} = \mu_0 \frac{S}{2\delta_0} w^2.$$

Putting δ_0 = 3.9 mm and specifying a cross-section S of 25 cm^2, the

number of turns w is 840.

The maximum flux is

$$\Phi_m = \frac{L_0 I_0}{w} = \frac{0{,}292 \cdot 5.87}{840} = 2.04 \cdot 10^{-3} \text{ V.sec}$$

The effective flux density

$$B = \frac{\Phi_m}{S\sqrt{2}} = \frac{2.04 \cdot 10^{-3}}{25 \cdot 10^{-4}\sqrt{2}} = 0.578 \text{ V/m}^2$$

The specific m.m.f. corresponding to this density is H = 133 A/m.

The magnetic permeance of steel is

$$\mu = \frac{B}{H} = \frac{0.578}{103} = 5.6 \cdot 10^{-3} \text{ H/m}.$$

Given the shape and dimensions of the magnetic circuit (see Fig. 3), its magnetic reluctance is

$$R = \frac{l}{\mu S} = \frac{44 \cdot 10^{-2}}{5{,}6 \cdot 10^{-3} \cdot 25 \cdot 10^{-4}} = 3.14 \cdot 10^4 \text{ 1/H}.$$

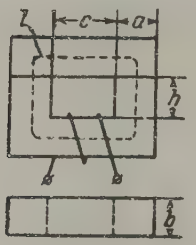

Fig. 3. The magnetic circuit of a vibrator.

Bearing in mind that

$$\psi = 2\varphi + \theta + \frac{\pi}{2},$$

and expanding the exponential factor in equation (7) as a power series (apart from the third term)

$$I = \sqrt{\frac{1}{T}\int_0^T i^2 dt} = \frac{I_0}{\sqrt{2}}\left[\left(\frac{11}{8} + m^2 - 2m_\rho\right) + m\sqrt{2}\left(1 - \frac{m_\rho}{4}\right)\sin\theta\right].$$

If the vibrator is turned to resonance, the effective current is

$$I = \frac{5.87}{\sqrt{2}}\left(\frac{11}{8} + 0.75^2 - 2\cdot\frac{0.75}{4}\right) = 6.9\ \text{A}.$$

Finally, the values L_{max}, L_0 and L_{min} for the selected magnetic circuit are found by the formula

$$L = \frac{w^2}{R + \frac{1}{G_s + G'}},$$

where R is the magnetic reluctance of the magnetic circuit; G_S the conductance for the leakage flux; G' the conductance of the air-gap.

Sotskov's formula [5] can be used to calculate G_S for the particular shape of magnetic circuit:

$$G_s = h\left(\frac{b}{c} + \frac{2a}{c + a\frac{\pi}{2}}\right)\mu_0 =$$

$$= 5\left(\frac{5}{8} + \frac{2\cdot 5}{8 + 5\cdot 1.57}\right)4\pi\cdot 10^{-9} = 0.786\cdot 10^{-7}\ \text{H}.$$

For a gap $\delta_{min} = 0.9$ mm, the corresponding values are

$$G'_{max} = \mu_0\frac{S}{2\delta_{min}} = 4\pi\cdot 10^{-9}\cdot\frac{25}{2\cdot 0.09} = 17.5\cdot 10^{-7}\ \text{H}$$

and

$$L_{max} = \frac{840^2}{3.14\cdot 10^4\cdot\frac{1}{0.786\cdot 10^{-7} + 17.5\cdot 10^{-7}}} = 1.22\ \text{H}.$$

Likewise for $\delta_0 = 3.9$ mm:

$$G_0 = 4.62 \times 10^7\ \text{H and } L_0 = 0.334\ \text{H}$$

for $\delta_{max} = 6.9$ mm:

$$G_{min} = 2.38 \times 10^7\ \text{H and } L_{min} = 0.22\ \text{H}$$

The actual value of the coefficient m is

$$m = \frac{1}{2}\ln\frac{L_{max}}{L_{min}} = 0.855.$$

The actual value of the coefficient m_ρ is

$$m_\rho = \frac{1}{4}\ln\frac{L_{max}L_{min}}{L_0^2} = 0.22.$$

The actual value of the efficiency of energy conversion is $M_1 = 0.3$.

The damping of the coil circuit for $r = 2.6\ \Omega$ is

$$\delta = \frac{r}{2L_0} e^{-m_\rho} = \frac{2.6}{2 \cdot 0.334} 0.8 = 3.1 \text{ 1/sec}$$

The true current value is

$$I_0 = \frac{U_m}{L_0 \sqrt{4\delta^2 + \omega^2 - 8\omega\delta m}} = \frac{380\sqrt{2}}{0.334 \cdot 310} = 5.18 \text{ A}.$$

The maximum mechanical power of the vibrator is

$$P = \omega \frac{L_0 I_0^2}{2} = 314 \cdot \frac{0.334 \cdot 5.18^2}{2} 0.3 = 420 \text{ W}$$

This power is 16 per cent below that specified. The desired power can be obtained by repeating the calculations and bearing in mind that the power can be increased by increasing M_1. This can be done by reducing m_ρ with a smaller conductance for the leakage flux and by increasing, for example, the width of the "window" of the magnetic circuit and reducing its height if possible. The following table shows recalculated values for larger window widths 9 and 10 cm. It will be seen that relatively small alterations in the shape of the magnetic circuit produce considerable changes in the work capability of a vibrator.

c cm	h cm	L_{max} H	L_0 H	L_{min} H	m	m_ρ	I_0 A	M_1	P W
8	5	1.22	0.334	0.22	0.855	0.22	5.18	0.3	420
9	5	1.215	0.33	0.216	0.867	0.221	5.23	0.355	502
10	5	1.205	0.322	0.206	0.883	0.218	5.37	0.364	527

Translated by O.M. Blunn

REFERENCES

1. A.I. Moskvitin; *Electrical reciprocating machines (Elektricheskiye mashiny vozvratno-postupatel'nogo dvizheniya)*. Izd. Akad. Nauk SSSR (1950).

2. A.E. Chesnokov; A study of the oscillation of an electromagnetic vibrator with a series-connected capacitor included in its circuit (Issledovanie kolebanii elektromagnitnogo vibratora pri malichii v ego tsepi posledovatel'no vklyuchennogo kondensatora). *Odessa Polytechnical Institute*, Vol. 16 (1959).

3. N.V. Maclachlan; *The theory and application of Mathieu functions.* Foreign Literature Publishing House (1953).

4. L.I. Mandel'shtam and N.D. Papaleksi; Resonance phenomena of order *n* (O yavleniyakh rezonansa *n*-go roda); *Collected works of L.I. Mandel'shtam,* Vol. 2. Izd. Akad. Nauk SSSR (1947).

5. B.S. Sotskov; *Fundamentals of the design and development of elements for automatic and telemechanical devices (Osnovy rascheta i proyektirovaniya elementov avtomaticheskikh i telemekhanicheskikh ustroistv).* Gosenergoizdat (1953).

AN ANALOGUE COMPUTER STUDY OF CURRENT TRANSFORMER TRANSIENTS*

YA. S. GEL' FAND

(All-Union Electrical Power Research Institute)

(Received 21 July 1961)

It takes a great deal of time to analyse the transient behaviour of current transformers with steel cores even when the load is linear.

The difficulties are multiplied for non-linear loads.

Analogue computers are of great assistance in this respect in that formerly intractable problems can be solved.

The All-Union Electrical Power Research Institute (A.E.P.R.I.) used mathematical simulation on analogue computers in the development of the new current transformer ferro-resonant supply units [1].

The method was based on the transformer equivalent circuit shown in Fig. 1*a*. The simulation circuit for current transformers with linear *RL* loads in Fig. 1*b* can be formed without difficulty from the equations

$$\left.\begin{aligned} \psi(i_\mu) &= Li_2 + r\int i_2\,dt + \psi_0; \\ i_1 &= i_\mu + i_2, \end{aligned}\right\} \qquad (1)$$

where $\psi(i_\mu)$ is the flux coupling of the secondary winding of the current transformer; ψ_0 the residual flux coupling; $L = L_t + L_l$ the total inductance of the secondary circuit (t = transformer, l = load); $r = r_t + r_l$ the total resistance of the secondary circuit; and i_μ the magnetization current of the current transformer**.

---

* *Elektrichestvo*, 12, 40-44, 1961.

** All the quantities refer to the secondary winding of the current transformer.

Most interest centres on the simulation of the non-linear magnetization branch of this circuit. Atabekov [1] and Sirota [2] have already shown that neglect of magnetic polarity reversal in the analysis of transient behaviour results in errors which are particularly marked at relatively small currents when the load impedance is small. The simulation of hysteresis curves with special cycles requires a rather complicated computing system with directly selected parameters [4]. To simplify the computing system and ensure its stable operation at large amplification factors of the resolving amplifiers, use has been made of a simple method of delaying the flux variation relative to the magnetization current. The main magnetization branch is simulated by means of a resolving amplifier with diode limiting cells in the feedback (see Fig. 2). The phase shift between the magnetization current and the flux is produced by a capacitor included in the feedback of this amplifier. The extent of this shift depends on the magnetic polarity reversal loss and eddy currents. The delay in flux variation relative to the magnetization current produces loops with special cycles which are analogous to hysteresis loops. It is too much to expect complete agreement between actual and simulated magnetization characteristics, but tests have shown that transient behaviour is reproduced with a fully acceptable degree of accuracy.

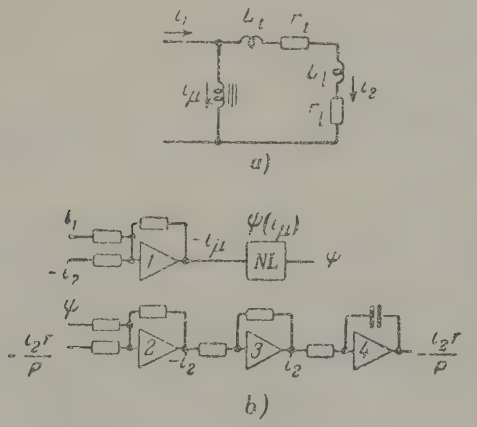

Fig. 1. *a* – equivalent circuit; *b* – simulation circuit for a current transformer with a linear *RL* load.

To determine the phase shift, a loss impedance is introduced which is calculated by the formula for the power loss in steel

$$P_{st} = k_c \left(\frac{B}{10\,000}\right)^2 \left(\frac{f}{50}\right)^{1.3} G,$$

where k_c is the specific loss W/g (State Standard 802-54), and G the weight of the core g.

For sinusoidally varying induction at a frequency of 50 c/s, this formula becomes

$$P_{st} = \frac{k_c l d \cdot 10^4}{4.95 s w^2} U^2.$$

Hence the conditional value of r_0 is

$$r_0 = \frac{4.95 s w^2 \cdot 10^{-4}}{k_c l d}, \qquad (2)$$

where d is the specific gravity of steel (7.65 for grade E3 electrical steel and 7.55 for grade E4 electrical steel); l, s the length of the middle line of force and the cross-section of the transformer core and w the number of turns in the secondary winding.

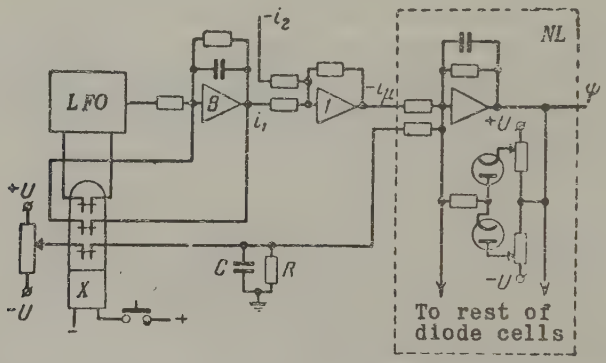

Fig. 2. The input circuit and system of establishing the residual magnetization in the non-linear unit:

LFO – low-frequency oscillator; if no works oscillator is available, the required sinusoidal oscillations can be produced by three amplifiers with the structural scheme corresponding to the equation

$$p^2 x + \omega^2 x = 0.$$

Considering that the method is only an approximation, the value of r_0 from (2) can also be used for actual non-sinusoidal variation of induction.

Figure 3 shows a test hysteresis loop simulated by the proposed method. The diagram clearly shows the limits of the piecewise linear approximation of the magnetization curve.

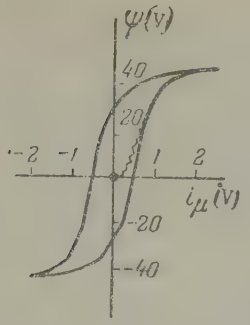

Fig. 3. Hysteresis loop recorded on the screen of an MN-7 machine's electronic indicator.

The proposed approximate method of simulating the magnetization characteristic cannot reproduce the residual magnetization in the current transformer core after large short-circuit currents. But this quantity can be found from test curves relating the residual induction to the maximum induction during the flow of short-circuit current [2].

The transient behaviour of a current transformer can be simulated in the presence of residual core induction by artificially shifting the initial magnetization curve. This can be done by supplying a direct voltage of appropriate sign to an additional input of the non-linear unit (NL) (see Fig. 2). The displacement must gradually decrease since the hysteresis loop of the current transformer is symmetrical at the end of transient behaviour. This reduction is brought about by an RC circuit with a time constant approximately equal to that of the aperiodic component of the short-circuit current.

The accuracy with which the transient behaviour of a current transformer could be simulated has been checked by comparing calculations by Sirota's method [3.6] with oscillograms taken during simulation on an MN-7 electronic machine. The test transformer was a TV-35-type 200/5 current transformer with a load $r = 0.3\ \Omega$ and $x = 0.1\ \Omega$ (including the winding resistance), a primary current of 450 A, and a time constant for the aperiodic component of current of 0.1 sec.

Figure 4 shows the core magnetization curve (grade E41 electrical steel) [5] and its piecewise linear approximation.

The following scales were used:

frequency – 0.7 c/s, $m_f = 0.014$;

current 1 V – 2 A, $m_i = 0.5$ V/A;

flux coupling 100 V – 0.4 V.sec, m_ψ = 250 V/V sec.

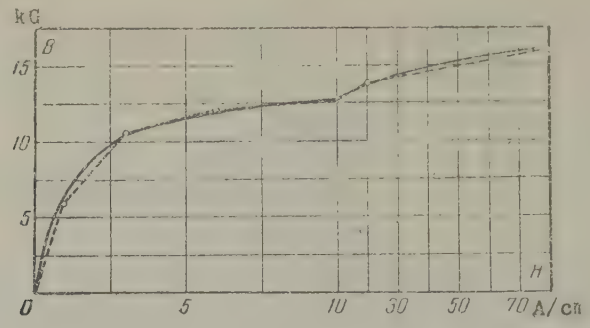

Fig. 4. ——— – original magnetization curve for grade E41 electrical steel; ––○––– its piecewise linear approximation on the MN-7 machine.

The oscillograms are given in Fig. 5.

The calculated magnetization currents were as follows:

without residual magnetization

6.3 A for t = 40 msec,

7.3 A for t = 50 msec;

with residual magnetization

6.0 A for t = 20 msec,

10.5 A for t = 30 msec.

The oscillograms show that good agreement is obtained.

This system of simulation permits the analysis of transient behaviour in any current transformer for different load resistances provided the core is made of the same steel. A change to other criteria is made by altering the amplification factors of the resolving amplifiers: the scale of the magnetization curve along the axis i_μ is changed by altering the feedback resistance of amplifier *1*; the scale of the magnetization curve in the ψ-direction is changed by altering the input resistance of the appropriate input of amplifier 2; r is changed by altering the input resistance of integrator *4*; L is changed by altering the feedback resistance of amplifier 2 (see Fig. 1*b*). The time constant of the aperiodic component of the short-circuit current can be changed by the feedback resistance of the amplifier *B* in the input (perturbation) circuit (see Fig. 2). The new A.E.P.R.I. ferro-resonant supply

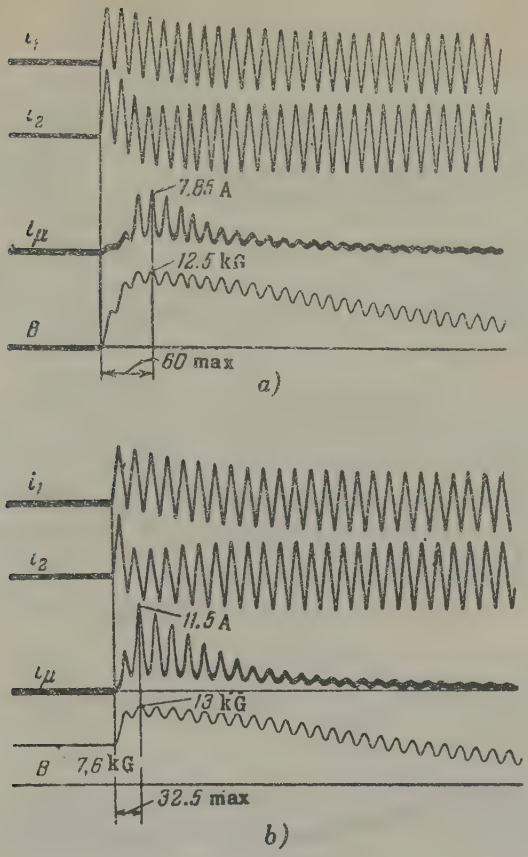

Fig. 5. Oscillograms of the transient behaviour of a TV-35 200/5 current transformer as obtained on the MN-7 machine. Value of the current i_μ referred to the secondary winding.

units were simulated like transformers with a parallel RC load. The initial system of equations differs from (1) by the expression for the flux coupling

$$\psi = Li_2 + \frac{i_2 r}{p} + \frac{i_c}{p^2 C}, \qquad (3)$$

where i_c is the current through the capacitance C of the ferro-resonant circuit.

Since the load resistance is connected in parallel with the capacitor, therefore

$$\frac{i_c}{p^2C} = \frac{i_l r_l}{p},$$

where i_l is current in the load resistance r_l.

Figure 6 shows the simulation circuit for a ferro-resonant supply unit connected to a current transformer.

The A.E.P.R.I. used the results of this type of investigation in the development of supply units for a.c. relay protection systems. A fully acceptable degree of accuracy was obtained between test results and computations [7].

The proposed system features simplicity and stability, and only a few resolving amplifiers are required. The same method can also be applied to devices which are transformer loads. In particular, it is fairly simple to simulate current circuits in differential protection with rapidly saturated single and three-phase transformers. Abrupt variations in the magnetization current of power transformers can also be analysed.

Conclusions

1. The transient behaviour of current transformers can be studied quite simply on analogue computers.

2. A simple, stable and accurate system of simulation has been described which dispenses with tedious analytical methods.

Appendix

The criteria of the resolving amplifiers for the simulation of current transformers.

1. Loss in the transformer core. Putting k for the shape of the initial section of the simulated curve $\psi(i_\mu)$ and R' for the appropriate feedback resistance of the amplifier in the non-linear unit, the corresponding feedback capacitance is

$$C' = km_i/m_\psi m_f R' r_0 \qquad \text{(A.1)}$$

2. Constructional criteria. If the non-linearity of $\psi(i_\mu)$ is simulated in the non-linear unit in such a way that the flux coupling ψ_0 corresponds to the arbitrary flux density B_0 and the current $i_{\mu 0}$ to the field intensity H_0, the items w, s and l may vary as follows:

$$R_{fb1} = R_{fb10} \frac{i_{\mu 0}}{H_0} \cdot \frac{w}{l}, \qquad (A.2)$$

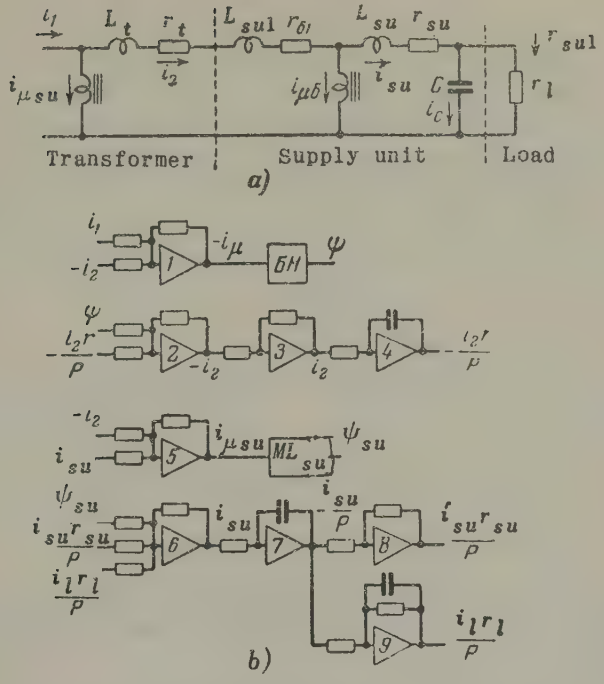

Fig. 6. *a* – equivalent circuit of current transformer with a ferro-resonant supply unit connected to it; *b* – its structural simulation circuit. (*su* – supply unit)

where R_{fb1} and R_{fb10} are the feedback resistances of the amplifier *1* (see Fig. 1*b*);

$$R_{in\ 2} = \frac{\psi_0 R_{in\ 20}}{B_0\ 10^{-2}} \cdot \frac{1}{ws}, \qquad (A.3)$$

where $R_{in\ 2}$ and $R_{in\ 20}$ are the input resistances of amplifier 2 (see Fig. 1*b*).

3. *Inductance.* If the input resistance $R_{in\ 20}$ of amplifier 2 is constant

$$R_{fb2} = \frac{m_i R_{in\ 20}}{m_\psi} \cdot \frac{1}{L}. \qquad (A.4)$$

4. *Resistance.* If the capacitance C_{fb4} of the feedback capacitor of amplifier 4 is constant

$$R_{in4} = \frac{m_l}{m_\psi m_f C_{fb4}} \cdot \frac{1}{r} \qquad (A.5)$$

5. r_{su} (Fig. 6)

$$R_{in8} \quad (R_{fb8} m_i / R_{in7} C_{fb7} m_f m_\psi) \times 1/r_{su} \qquad (A.6)$$

6. c_l *and* C_l. The relationship between the resistance and capacitance of the feedback capacitor of amplifier 9 is selected from considerations of equality between the angle of feedback impedance in the scale m_f and the angle of impedance of the parallel-connected r_l and C_l:

$$m_f C_{fb9} R_{fb9} = C_l r_l \qquad (A.7)$$

The input resistance of amplifier 9 is found from one of the following expressions:

$$\begin{aligned} R_{in9} &= (R_{fb9} m_i / R_{in7} C_{fb7} m_f m_\psi) \times 1/r_l \\ R_{in9} &= (m_i / R_{in7} C_{fb7} C_{fb9} m_f m_\psi) \times 1/C_l \end{aligned} \qquad (A.8)$$

7. *The time constant* τ *of the short-circuit current.* The time constant is adjusted by changing the feedback resistance of the amplifier B (see Fig. 2):

$$R_{fbB} = \tau / m_f C_{fbB} \qquad (A.9)$$

Translated by O.M. Blunn

REFERENCES

1. Ya.S. Gel'fand and M.I. Tsarev; Operative a.c. relay protection and control apparatus (Releinaya zashchita i elektroavtomatika na peremennom operativnom toke). *Inf. mat. All-Union Electrical Power Research Institute*, No. 41. Gosenergoizdat (1959).

2. G.I. Atabekov; *Relay protection of high-voltage networks (Releinaya zashchita vysokovol'tnykh setei)*. Gosenergoizdat (1949).

3. I.M. Sirota; *Elektrichestvo*, No. 2 (1959).

4. V.G. Vasil'ev and V.A. Zverev; *Izv. vys. ucheb. zaved., Elektronika*, No. 9 (1959).

5. A.S. Zaimovskii and L.A. Chudnovskaya; *Magnetic materials (Magnitnye materialy)*. Gosenergoizdat (1957).

6. I.M. Sirota; *Izv. vys. ucheb. zaved., Energetika*, No. 7 (1960).

7. Ya.S. Gel'fand; Forced steady-state oscillations in parallel ferroresonant circuits connected to the current source, (Vynuzhdennye kolebaniya v parallel'nykh ferrorezonansnykh konturakh, vklyuchennykh na istochnik toka). *Trud. All-Union Electrical Power Research Institute*, No. 11. Gosenergoizdat (1961).

DESIGN OF DEEP GROUNDING RODS FOR TRANSMISSION LINE TOWERS*

A.B. OSLON

(Perm')

(Received 6 June 1961)

The increasing use of mechanization in the construction of transmission lines has attracted attention to the design of the grounding rods which are placed in pits beneath the foundations or footings of the towers (deep grounding rods). In this paper a method of determining their grounding resistance is proposed on the assumption that the rods are in homogeneous ground.

The design of deep grounding rods was considered in a recent paper published in the Soviet journal *Elektricheskie stantsii* [1]. A method was proposed which involved utilization coefficients. Its drawback is the possibility of subjective estimates since the choice of coefficients is based on analogy and depends on the experience of the person performing the calculations. The method proposed in this paper is free of this shortcoming.

Deep grounding rods beneath the foundations of pylons are of comparatively small dimensions, their dimensions being approximately the same in the horizontal and vertical direction.

It has been shown elsewhere [2] that when the line density of the current flowing from each element making up the grounding system can be assumed to be the same, the resistance of a grounding rod is

$$R = \frac{\alpha_{11} + \sum_{k=2}^{n} \frac{l_k}{l_1} \alpha_{1k}}{1 + \sum_{k=2}^{n} \frac{l_k}{l_1}}, \qquad (1)$$

* *Elektrichestvo*, 12, 59-63, 1961.

where n is the number of elements in the grounding system; a_{11} the natural resistance of each element 1; a_{1k} the mutual resistances between element 1 and all the other elements; and l_k the lengths of the respective elements.

Consider, for example, the grounding system illustrated in Fig. 1. It consists of four horizontal conductors 5 m in length, which form a square at the bottom of the pit, and four vertical conductors 2.5 m in height set up at the corners of the square. Together with their specular images, these conductors form a cube with edges 5 m long (l = 5 m).

If the individual conductors of circular section are 1 cm in diameter (d = 1 cm), and the specific resistance of the ground is ρ (in ohm-metres), then the natural resistance of a conductor is

$$a_{11} = \frac{\rho}{2\pi l} \ln \frac{2l}{d} = \rho.0.220. \tag{2}$$

The mutual resistance between conductor *1* and the conductors parallel to it (*3*, *9*, *11*) can be found by the formula

$$a_{1k} = \frac{\rho}{2\pi l}\left(\operatorname{ar\,sinh} \frac{l}{a} + \frac{a}{l} - \sqrt{\left(\frac{a}{l}\right)^2 + 1}\right), \tag{3}$$

where a is the distance between conductors *1* and k, $a = l$ for conductors *3* and *9* and $a = \sqrt{2}l$ for conductor *11*.

From formula (3)

$$a_{13} = \rho.0.0150; \tag{3a}$$

$$a_{1-11} = \rho.0.0109. \tag{3b}$$

For the mutually perpendicular conductors *1* and *2* (and also *4*, *5* and *8*), the mutual resistance is found from the formula

$$a_{12} = \frac{\rho}{4\pi l_1 l_2}\left(l_1 \operatorname{ar\,sinh} \frac{l_2}{l_1} + l_2 \operatorname{ar\,sinh} \frac{l_1}{l_2}\right). \tag{4}$$

If $l_1 = l_2$, then

$$a_{12} = \frac{\rho}{2\pi l} \operatorname{ar\,sinh} 1 = \frac{\rho}{2\pi l} \ln(\sqrt{2} + 1) = \rho.0.0280. \tag{4a}$$

Using the mean potential method [2], for the conductors *1* and *6*, *7*, *10*, *12* in different planes

$$a_{16} = \frac{\rho}{4\pi l}\left(\ln \frac{\sqrt{2l^2 + a^2} + l}{\sqrt{2l^2 + a^2} - l} - \frac{a}{l} \operatorname{arc\,tan} \frac{l^2}{a\sqrt{2l^2 + a^2}}\right), \tag{5}$$

where a is the distance between the planes in which the conductors lie

In the case in question, $a = l$. Therefore

$$\alpha_{16} = \frac{\rho}{4\pi l}\left(\ln\frac{\sqrt{3}+1}{\sqrt{3}-1} - \operatorname{arc\,tan}\frac{1}{\sqrt{3}}\right) = \frac{\rho}{4\pi l}\cdot 0.793 = \rho\cdot 0.0126. \tag{5a}$$

Thus, in a homogeneous conducting medium, the leakage resistance of a cube made up of conductors 5 m long and 1 cm in diameter is

$$R = \frac{\alpha_{11}+2\alpha_{13}+4\alpha_{12}+4\alpha_{16}+\alpha_{1-11}}{12} = \rho\cdot 0.0353.$$

The resistance R' of the grounding system under consideration is twice as much, i.e.

$$R' = \rho\cdot 0.0706.$$

Formulae (3)-(5) are too cumbersome to calculate the mutual resistances. A satisfactory alternative is the formula for the potential of a point in a radially spherical field

$$\alpha_{1k} = \frac{\rho}{4\pi r_{1k}}, \tag{6}$$

where r_{1k} is the distance between the mid-points of the respective conductors.

In fact, using formula (6)

$$\alpha_{12} = \rho\cdot 0.0225;\ \alpha_{16} = \rho\cdot 0.013;$$

$$\alpha_{13} = \rho\cdot 0.016;\ \alpha_{1-11} = \rho\cdot 0.011.$$

Hence

$$R = \rho\cdot 0.034;$$

$$R' = \rho\cdot 0.068.$$

As a second example, consider a ring 7 m in diameter (D = 7 m) laid at a depth t = 2.5 m and provided with four vertical rods which are arranged uniformly on its circumference (Fig. 2). These rods are about 5 m apart. They too are made from circular rod of diameter d = 1 cm.

Using the above notation, the natural resistance of the ring according to Margolin's formula is

$$\alpha_{11} = \frac{\rho}{2\pi^2 D}\ln\frac{8D}{d} = \rho\cdot 0.0628. \tag{7}$$

The mutual resistance between the ring and its vertical image is found by integrating the potentials formed by the currents flowing from all points of the ring at some point of its specular image. Owing to the symmetry of the system, it is unnecessary to integrate the potential formed at all points of the specular image. After

transformations

$$\alpha_{12} = \frac{\rho}{2\pi^2 \sqrt{D^2 + 4t^2}} \int_0^{\frac{\pi}{2}} \frac{d\beta}{\sqrt{1 - K^2 \sin^2\beta}}, \tag{8}$$

where

$$K^2 = \frac{D^2}{D^2 + 4t^2}.$$

The integral in formula (8) is a total elliptic integral of the first kind. In the case in question $K^2 = 0.663$ and the integral is 2.024. Consequently, $\alpha_{12} = 0.0119$.

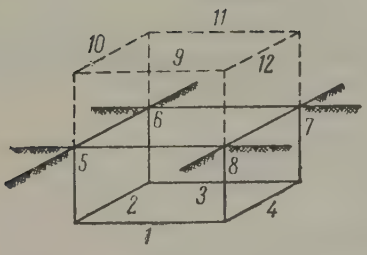

Fig. 1.

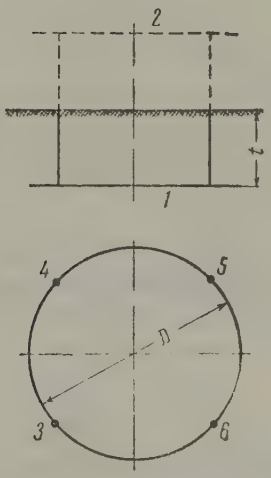

Fig. 2.

Elliptic integrals are usually difficult to use. Formula (8) is therefore best replaced by an approximate expression

$$\alpha_{12} = \frac{\rho}{2\pi^2 D} \ln \frac{2D}{t} \tag{8a}$$

(t is half the distance between the ring and its specular image), provided the ratio t/D is small, and when it can be assumed that the elliptic integral of the first kind is equal to

$$\ln \frac{2\sqrt{D^2 + 4t^2}}{t},$$

and the quantity $4t^2$ can be ignored since it is small in comparison with D^2. Expression (8a) provides a close approximation if $t/D \leqslant 1/2$. In the particular case in hand

$$\frac{t}{D} = 0.357.$$

Consequently

$$\alpha_{12} = \rho \cdot 0.0125.$$

Five per cent error is quite permissible.

Expression (8a) provides a simple formula for the mutual resistance between the ring and the vertical conductors. Here it is necessary to integrate (8a) over the length of the conductor and divide the result by the length of the conductor. As a result

$$\alpha_{13} = \frac{\rho}{2\pi^2 D}\left(\ln\frac{4D}{l} + 1\right) = \rho \cdot 0.0197, \tag{9}$$

where $l = 2t$, since α_{13} refers to the vertical conductor and its specular image.

If the length of the vertical conductor is greater than the diameter of the ring, formula (9) leads to errors because (8a) provides only a rough approximation.

Applying formula (1), the leakage resistance of a system consisting of a ring and four vertical conductors with their specular images is

$$R = \frac{\alpha_{11} + \alpha_{12} + \frac{2t}{\pi D} 4\alpha_{13}}{1 + 1 + \frac{2t}{\pi D} 4} = \rho \cdot 0.032.$$

The grounding resistance is twice as much:

$$R' = \rho \cdot 0.064.$$

In this analysis it has been assumed that the density of the current flowing from the ring and vertical rods was the same. This assumption can be dropped if the grounding system is regarded as consisting of two parts, one of which incorporates the horizontal elements (i.e. the ring and its specular image), whilst the other includes the vertical conductors and their specular images.

Suppose that α_{I} and α_{II} represent the natural resistances of these parts and $\alpha_{\mathrm{I\,II}}$ their mutual resistance. The earthing resistance R' of the grounding system as a whole is then given by Schwarz' formula

$$R' = \frac{\alpha_{\mathrm{I}}\alpha_{\mathrm{II}} - \alpha_{\mathrm{I\,II}}^2}{\alpha_{\mathrm{I}} + \alpha_{\mathrm{II}} - 2\alpha_{\mathrm{I\,II}}}. \tag{10}$$

According to formula (1):

for the natural resistance of the horizontal conductors

$$\alpha_h = \frac{\alpha_{11} + \alpha_{12}}{2} = \rho \cdot 0.0377;$$

for that of the vertical conductors

$$\alpha_v = \frac{\alpha_{33} + 2\alpha_{34} + \alpha_{35}}{4} = \rho \cdot 0.0614$$

(the values $\alpha_{34} = \rho \times 0.0150$ and $\alpha_{35} = \rho \times 0.0109$ have been calculated for the grounding system of Fig. 1).

Their mutual resistance is

$$\alpha_{hv} = \alpha_{13} = \rho \cdot 0.0197.$$

Substituting these quantities in formula (10)

$$R = \rho \cdot 0.0324.$$

The result is very close to that obtained previously. This shows that it is permissible to assume a uniform distribution of the current along the conductors when calculating the grounding resistance [2,5].

Now consider a typical grounding system in the form of a small ring with one conductor (Fig. 3). Formulae (8a) and (9) are not applicable to this case because $t \gg D$. The mutual resistance between the ring and its specular image is calculated by the approximate formula (6):

$$\alpha_{12} = \frac{\rho}{4\pi 2t} = \rho \cdot 0.0159.$$

Fig. 3.

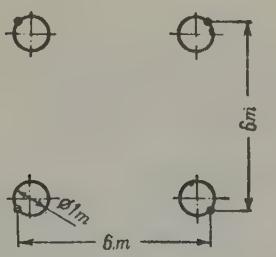

Fig. 4.

The natural resistance of the ring is found from formula (7):

$$\alpha_{11} = \rho \cdot 0.337.$$

The resistance of the horizontal elements is

$$\alpha_h = \rho \frac{0.337 + 0.0159}{2} = \rho \cdot 0.1765.$$

The natural resistance of the vertical element is calculated by formula (2):

$$\alpha_v = \rho \cdot 0.220.$$

To calculate the mutual resistance α_{hv}, it is necessary to integrate expression (8) over the length of the vertical element. This operation can only be performed by numerical integration. The quantity α_{hv} is therefore found approximately.

It is obvious that the total resistance of the grounding system hardly varies if the top of the vertical element is moved to the centre of the ring. This implies that the quantity α_{hv} hardly varies either, and it can be calculated like the potential created by a unit of current flowing from the vertical grounding rod at any point of the ring, i.e. the following formula can be used [2]:

$$\alpha_{hv} = \frac{\rho}{4\pi l} \ln \frac{2a + l}{2a - l}, \qquad (11)$$

where $2a$ is the sum of the distances from the point to the ends of a rectilinear conductor, and $l = 2t$ is the length of this conductor.

From formula (11), the mutual resistance is

$$\alpha_{hv} = \rho \cdot 0.0478.$$

In accordance with formula (10)

$$R = \rho \frac{0.1765 \cdot 0.220 - 0.0478^2}{0.1765 + 0.220 - 2 \cdot 0.0478} = \rho \cdot 0.122,$$

$$R' = \rho \cdot 0.244.$$

Now suppose that grounding systems similar to that shown in Fig. 3 are laid under the four footings of a tower at the vertices of a square with sides 6 m long (see Fig. 4).

The mutual resistance between the individual grounding systems can be found quite accurately by formula (6) because the distance between them is greater than their own size (here the grounding systems are again considered together with their specular images, and the distance between their mid-points is taken as r_{1k}). As a result

$$\alpha_{12} = \alpha_{14} = \rho \times 0.0133 \text{ and } \alpha_{13} = \rho \times 0.0095.$$

In accordance with formula (1)

$$R = \rho \frac{0.122 + 2 \cdot 0.0133 + 0.0095}{4} = \rho \cdot 0.0395.$$

The resistance of an actual grounding system is

$$R' = \rho \cdot 0.079.$$

It is typical of the grounding systems shown in Figs. 1, 2 and 4 that their grounding resistances are approximately the same. The explanation is that they occupy approximately the same volume of earth. The volume of the cube in Fig. 1 is 125 m^3. A sphere of the same volume has a radius of 3.1 m. The resistance of a hemisphere grounding system of the same radius is

$$R' = \frac{\rho}{2\pi r} = \rho \cdot 0.0515.$$

This quantity can be used for estimating the lower limit of grounding resistance for deep grounding systems occupying a corresponding volume of earth. The better the surface of the volume is used to arrange the grounding conductors, the closer is the grounding resistance of an actual system to that stated above. This explains the relatively high grounding resistance of the system shown in Fig. 4 in which there are no "cross-pieces" in the earth between its four individual parts.

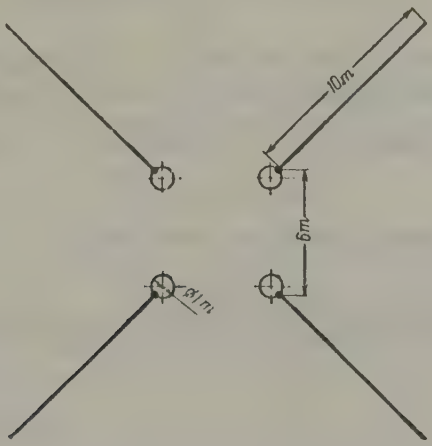

Fig. 5.

Thus, there are two ways of reducing the grounding resistance of deep grounding systems. Either a larger volume of earth can be occupied, or else its surface can be utilized better in the arrangement of the grounding conductors.

Finally, consider a grounding system consisting of a deep part and

Finally, consider a grounding system consisting of a deep part and four arms (Fig. 5). Formula (10) is applied. The grounding resistance of the deep part is denoted by a_1.. It has already been defined in the last example:

$$a_1 = \rho \cdot 0.079.$$

The grounding resistance of arms which form a "four-arm star", according to Oslon [2], is

$$a_2 = \frac{\rho}{2\pi L} \ln \frac{8.45L^2}{dt} = \rho \cdot 0.058,$$

where L is the total length of the arms; t the depth at which they are laid (assumed to be 0.5 m); and d the diameter of the rod of circular section (1 cm).

The mutual resistance is found as follows. The field of the sunk grounding system is nearly radial-spherical. Using the method of mean potentials to calculate a_{12} and bearing in mind the proximity of the earth surface (i.e. assuming for the radial-spherical field that $a = \rho/2\pi r$ and not $\rho/4\pi r$):

$$a_{12} = \frac{1}{2\pi l} \int_0^l \frac{dl}{r} = \frac{1}{2\pi l} \int_{r_1}^{r_2} \frac{dr}{r} = \frac{1}{2\pi l} \ln \frac{r_2}{r_1}, \qquad (12)$$

where l is the length of an arm; and r_1, r_2 the distances between the centre of the grounding system and the ends of a rod.

In the case in question (r_1 = 4.25 m and r_2 = 14.25 m):

$$a_{12} = \rho \cdot 0.019,$$

and hence for the total grounding resistance

$$R' = \rho \frac{0.079 \cdot 0.058 - 0.019^2}{0.079 + 0.058 - 2 \cdot 0.019} = \rho \cdot 0.0425.$$

Translated by O.M. Blunn

REFERENCES

1. Yu.I. Lyskov and A.N. Sherentsis; *Elek. stants.*, No. 10 (1957).

2. A.B. Oslon; *Elektrichestvo*, No. 4 (1958).

3. N.F. Margolin; *Ground currents* (*Toki v zemle*). Gosenergoizdat (1947).

4. S.J. Schwarz; *Trans. Amer. Inst Elect. Engnrs.*, Pt. III-B, Vol.73 (1954).

5. A.B. Oslon; *Elektrichestvo*, No. 7 (1959).

GRAPHICAL ANALYSIS OF THE THERMAL BREAKDOWN VOLTAGE OF HIGH-FREQUENCY INSULATORS*

N.P. BOGORODITSKII, Yu.M. VOLOKOBINSKII
and I.D. FRIDBERG

(Lenin Electrical Engineering Institute)

(Received 11 August 1961)

Introduction

To calculate the thermal breakdown voltage of insulators and capacitors analytically, it is necessary to solve the differential equation

$$div(K \text{ deg } T) = -Q, \tag{1}$$

where K is the coefficient of thermal conductivity of the dielectric; T the temperature; and Q the specific heat dissipation in the dielectric.

For h.f. thermal breakdown

$$Q = (\epsilon \tan \delta / 1.8 \times 10^6) f E^2 [\text{ W/cm}^3], \tag{2}$$

where ϵ is the dielectric permeability; $\tan \delta$ the tangent of the dielectric loss angle; f the frequency of the alternating electrical field, c/s; and E the intensity of the electrical field, kV/cm.

The analytic solution of equation (1) is confronted with great difficulties which can only be overcome by simplifications. To integrate equation (1) it is necessary to represent K, ϵ, $\tan \delta$ and E as comparatively simple functions of co-ordinates and temperature. In particular, the relationship between $\tan \delta$ and temperature is written in the form

$$\tan \delta = Ae^{aT}, \tag{3}$$

---

* *Elektrichestvo*, 12, 63-69, 1961.

where A and α are constants.

But if this relationship is written thus, α is no longer a constant quantity for ceramic materials. It in fact increases by a factor of 1.5 to 5 for a temperature rise from 0 to 200°C [1]. The existing theory cannot therefore be used to calculate the thermal breakdown voltage of ceramic insulators.

Moreover, the existing theory was evolved for specimens of comparatively simple shape which can be regarded as flat infinite plates or circular tubes and bars [2-4]. The relationship between E and the co-ordinates is then comparatively simple and equation (1) may be solved.

Insulators with uniform fields have the relatively greatest operating voltages for minimum dimensions [5] (see Fig. 1). The electrical fields of these insulators are illustrated in Fig. 2 from the results of an electrolytic tank study of models of porous material. A study of these fields shows that the relationship $U = El$ exists between the voltage U applied to the insulator and the intensity E of the electrical field in the insulator, where l is the shortest distance between the electrodes in the body of the insulator.

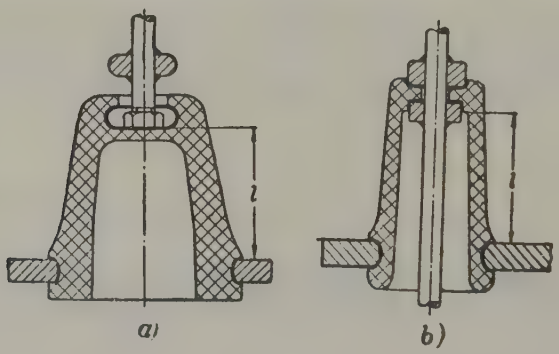

Fig. 1. Sectional view of typical insulators with a "uniform field": a – "support" insulator; b – "transfer" insulator.

If the intensity E_b of the field at which breakdown occurs in the insulator is known, the thermal breakdown voltage U_b can be found by multiplying E_b by l. The first step in the determination of U_b is the calculation of E_b. If the heat transfer on to electrodes can be ignored for the insulators shown in Fig. 1, the quantity E_b is independent of l and decreases with increasing wall thickness.

If the diameter of the insulator is much greater than the thickness of the wall D, the wall of the insulator can be regarded as approximately flat. The problem therefore reduces to that of a plane-parallel plate in which heat transfer takes place in X direction perpendicular to its surface, and the electrical field vector is directed along the surface of the plate (see Fig. 3). The mathematical solution is the same for a finite plate in which surface heat transfer is ignored as for an infinite plate in a uniform field.

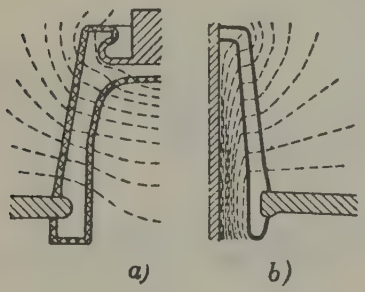

Fig. 2. Electrical fields of insulators in Fig. 1: a – "support"; b – "transfer".

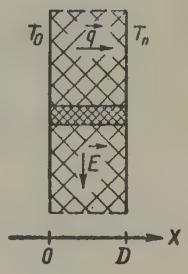

Fig. 3. A contribution to the calculation of E_b.

The thermal breakdown voltage of ceramic insulators and capacitors can be determined by the following graphical method whenever the variation of tan δ with temperature is not to be regarded as exponential.

Fundamentals of the method

To illustrate the method, it is proposed to consider a dielectric plate in a uniform high-frequency electrical field with its intensity vector parallel to the surface of the plate. Suppose that the thermal insulation of one surface of the plate is ideal at $X = 0$ and that the other is cooled by air at $X = D$ (see Fig. 3). Heat transfer takes place in the X direction which is perpendicular to the electrical field vector E. The direction of this vector E at the instant t and that of the vector of heat flow density q are shown in Fig. 3. It is assumed that the variation of K, ϵ and tan δ with temperature is known. The following notation is used:

$$\eta = \epsilon \tan \delta f/1.8 \times 10^6 \, [\mathrm{W/cm \times kV^2}], \qquad (4)$$

where η differs by a constant factor from the specific a.c. conductance in $\Omega^{-1} \times \mathrm{cm}^{-1}$. This quantity η is plotted as a function of temperature (see Fig. 4). It follows from (2) that the specific heat dissipation is

$$Q = \eta E^2. \tag{5}$$

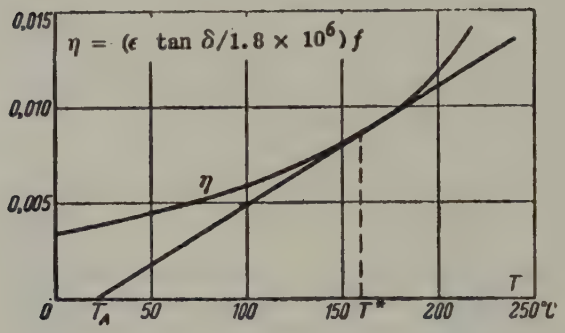

Fig. 4. The relationship between η and temperature.

A power P_{dis} is dissipated in a column of unit section which is equal in height to the thickness D of the plate. If the temperature T_n of the cooled surface is greater than the ambient temperature T_A, the power P_{off} from a unit area of the plate's surface is determined by convection and radiation and depends on the position of the plate in air [6-8]. In the general case the power P_{off} from a unit of surface area is a non-linear function of the difference $(T_n - T_A)$ and depends on the shape and dimensions of the component and the state and chemical composition of its exposed surface. It is to be supposed that

$$P_{off} = \lambda (T_n - T_A), \tag{6}$$

where the coefficient λ of external heat transfer is independent of temperature and where the variation of K with temperature can be ignored.

In thermal equilibrium

$$P_{dis} = P_{off} = -K \frac{dT}{dX}\Big|_{X=D} = \lambda (T_n - T_A) \tag{7}$$

or

$$-\frac{dT}{dX}\Big|_{X=D} = -\frac{\lambda}{K}(T_n - T_A), \tag{8}$$

where $dT/dX|_{X-D}$ is the temperature gradient of the dielectric on the surface $X = D$. It follows from (7) that the amount of heat dissipated in the plate at the temperature T_n in question is given. If the temperature distribution in the dielectric and T_n are known, it is therefore

possible to calculate the intensity E of the field in the dielectric which heats the plate such that the temperature of the cooled surface is T_n. Suppose the condition of thermal equilibrium is written in the form

$$E^2 \int_0^D \eta(T)\, dX = \lambda (T_n - T_A), \tag{9}$$

Then

$$E^2 = \frac{\lambda (T_n - T_A)}{\int_0^D \eta(T)\, dX}. \tag{10}$$

Using the notation

$$\bar{\eta} = \frac{1}{D} \int_0^D \eta(T)\, dX, \tag{11}$$

expression (10) simplifies to

$$E^2 = \frac{\lambda (T_n - T_A)}{\bar{\eta} \cdot D}. \tag{12}$$

The field intensity which causes the temperature of the cooled surface to rise to T_n can therefore be determined by finding the distribution of the temperature in the plate and calculating its mean value.

The surface temperature $T_{n.b}$ at which the intensity of the field is maximum E_b can be found by plotting E as a function of T_n if the condition of thermal equilibrium is fulfilled (see Fig. 5). The maximum field intensity E_b can be found by substituting in 12 $T_{n.b}$ for T_n and η_b for the value η if thermal equilibrium is unstable.

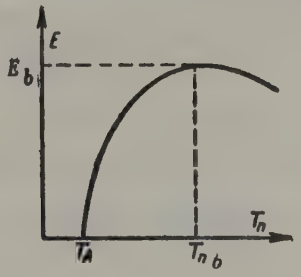

Fig. 5. The relationship between E and T_n in thermal equilibrium.

To determine the thermal breakdown voltage it is sufficient in

practice to know those values of T_n', T_n'', E' and E'' for which

$$T_n' < T_{n\,b} < T_n'' \tag{13}$$

and

$$E' < E_b < E''. \tag{14}$$

For unstable thermal equilibrium

$$T_{n\,b} < T^* < T_{0\,b}, \tag{15}$$

where $T_{0.\,b}$ is the maximum temperature in the plate at breakdown, and T^* is defined as the temperature at the point where a straight line from T_A on the base is tangential to the curve representing the variation of η with temperature (see Fig. 4).

The temperature T_n' is obtained on the assumption that the temperature distribution in the plate is linear at the maximum temperature T^*. The other temperature T_n^{**} is found by assuming that the temperature distribution is parabolic and that the mean temperature is T^*. The intensity E' is obtained by putting in (12) the increased value of η and T_n' instead of T_n. The intensity E'' is found by putting in (12) the reduced value of η and T_n'' instead of T_n. Formulae may then be obtained for the thermal breakdown voltage and maximum temperatures of insulators and capacitors.

The coefficient of external heat transfer λ decreases with decreasing component size and increases with increasing temperature. For surface areas greater than 200 cm^2, λ can be taken as 0.001 $W/cm^2 \times deg$ [9]. Its value may be several times greater for small insulators and capacitors.

The proposed graphical method is accurate enough for practical purposes. For example, if it is assumed that ϵ is independent of temperature and that the variation of tan δ with temperature is in the form (3), for a plate 100 mm thick by the graphical method

$$E_{av} = \frac{1}{2}(E' + E''), \tag{16}$$

which is within 0.5 per cent of the calculated value of E_b. The error

$$\Pi = \frac{E'' - E'}{E'' + E'} \tag{17}$$

is less than 5 per cent. The error can be calculated by formula (17) in those cases when the variation of tan δ with temperature is not to be regarded as exponential.

According to Fridberg, the thermal breakdown voltage of rutile ceramic capacitors (see Fig. 6) is between 7 and 13 kV at ambient air

temperatures of 25 to 30° C and a frequency of 1.7 Mc/s. The figure produced by the graphical method for the same capacitors was 10 kV with a coefficient of external heat transfer λ equal to 0.006 W/cm^2 × deg.

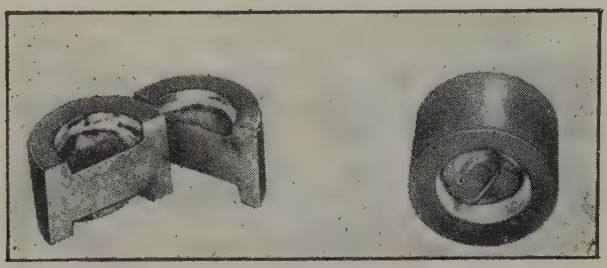

Fig. 6. KVKB-13 rutile ceramic capacitors.

Application of the method

The proposed method can be used for the design of all ceramic insulators which can be regarded as plates in a homogeneous field, e.g. insulators with a uniform field.

Suppose it is required to find E_b and the plate temperature at the frequency f = 1 Mc/s. The plate is in a uniform field. Heat transfer parallel to the surface of the plate is negligible.

Given.

1. The variation of ϵ and tan δ with temperature at the operating frequency F = 1 Mc/s.

2. Air cooling on one side of the plate; plate thickness D = 5 cm.

3. The coefficient of thermal conductivity K is independent of temperature and equal to 0.01 W/cm × deg.

4. The coefficient of external heat transfer λ = 0.001 W/cm^2 × deg.

5. Ambient temperature T_A = 20°C.

The method and formulae are as follows.

The relationship η

$$\eta = \epsilon \tan \delta f / 1.8 \times 10^{+6} [\text{ W/cm} \times \text{kV}^2] \qquad (18)$$

is plotted as a function of temperature on a linear scale. The variation of ϵ tan δ with temperature can be plotted instead, in which case arbitrary scale units can be used on both co-ordinate axes. The

variation of η with temperature for this example is plotted in Fig. 4.

A tangent is drawn from point T_A on the base to the curve for the temperature relationship of η and the temperature T^* at the point of tangency is determined (see Fig. 4). In the case in question $T^* = 160°C$.

The following difference is then calculated:

$$\psi = T^* - T_A \text{ [deg]}. \tag{19}$$

For the plate in question, $\psi = 140°C$.

The following quantity is then determined:

$$\theta = \frac{\lambda}{K} D. \tag{20}$$

Here $\theta = 0.5$.

The following temperature is calculated:

$$T^{**} = T^* + \frac{\theta}{4+\theta}\psi, \tag{21}$$

which in this case is 175°C.

The temperature of the hottest zone $T_{0.b}$ when thermal equilibrium is disturbed is defined by the inequality

$$T^* < T_{0b} < T^{**} \tag{22}$$

or the expression

$$T_{0b} = \left(T^* + \frac{\theta\psi}{2(4+\theta)}\right) + \frac{\theta\psi}{2(4+\theta)} \text{ [deg]}. \tag{23}$$

For the plate in question: $160° < T_{0.b} < 175°$ C, or $T_{0.b} = 168 \pm 8°C$.

The lowest temperature T_n' of the cooled surface is then calculated for which thermal equilibrium is not disturbed:

$$T_n' = T_A + \frac{1}{1+\theta}\psi \text{ [deg]}; \tag{24}$$

For the plate in question $T_n' = 113°C$.

The temperature of the cooled surface at which thermal equilibrium is disturbed is

$$T_n'' = T_A + \frac{4}{4+\theta}\psi \text{ [deg]}. \tag{25}$$

i.e. $T_n'' = 144°C$.

The temperature of the cooled surface satisfies the following condition at the instant when thermal equilibrium is disturbed:

$$T_n' < T_{nb} < T_n'' \tag{26}$$

and is equal to

$$T_{n.b} = T_A + \frac{8+5\theta}{2(1+\theta)(4+\theta)}\psi \pm \frac{3\theta}{2(1+\theta)(4+\theta)}\psi. \quad (27)$$

In this example, 113°C < $T_{n.b}$ < 144°C, or $T_{n.b}$ = 129 ± 16°C.

The temperature drop ΔT in the dielectric between the hottest and coldest regions is determined and, if $\theta < 2$, it satisfies the condition

$$T^{**} - T_n'' = \frac{2\theta}{4+\theta}\psi < \Delta T < \frac{\theta}{1+\theta}\psi = T^* - T_n'. \quad (28)$$

If $\theta > 2$, then

$$T^* - T_n' = \frac{\theta}{1+\theta}\psi < \Delta T < \frac{2\theta}{4+\theta}\psi = T^{**} - T_n''. \quad (29)$$

In this example 31°C < ΔT < 47°C.

The maximum temperature gradient $dT/dX\,|_{X=D}$ on the cooled surface is calculated. If $\theta < 2$, it is defined by the inequality

$$\frac{0\psi}{(1+\theta)D} < \left.\frac{dT}{dX}\right|_{X=D} < \frac{4\theta\psi}{(4+\theta)D} \quad [\text{deg/cm}]. \quad (30)$$

If $\theta < 2$, the signs in (30) are the other way round. In this example 9.4°C/cm < $dT/dX\,|_{X=D}$ < 12.4°C/cm.

The values of η at the temperatures T^* and T_n' are then found. It will be seen from Fig. 4 that in this example

$\eta(T^*)$ = 0.0085 W/cm × kV^2

$\eta(T_n')$ = 0.0063 W/cm × kV^2

The dissipated power per unit of surface area at approximately breakdown field intensity is

$$P' = \lambda(T_n' - T_A) = \frac{\lambda\psi}{1+\theta} \quad [\text{W/cm}^2]. \quad (31)$$

In this example P' is 0.093 W/cm^2.

The dissipated power per unit of surface area at a greater field intensity than the breakdown intensity is

$$P'' = \lambda(T_n'' - T_A) = \frac{4\lambda\psi}{4+\theta} \quad [\text{W/cm}^2]. \quad (32)$$

In this example, P'' = 0.124 W/cm^2.

The dissipated power P per unit of surface area at breakdown satisfies the condition:

$$P' < P < P''. \quad (33)$$

The intensity of the electrical field near breakdown intensity is

$$E' = \sqrt{\frac{2P'}{[\eta(T^*) + \eta(T_n')]\,D}} \ [\text{kV/cm}]. \tag{34}$$

In this example $E' = 1.58$ kV/cm.

That at a greater intensity than the breakdown intensity is

$$E'' = \sqrt{\frac{P''}{\eta(T^*)D}} \ [\text{kV/cm}]. \tag{35}$$

In this example $E'' = 1.70$ kV/cm.

The electrical field intensity E_b which leads to breakdown satisfies the condition

$$E' < E_b < E'' \tag{36}$$

and is found from the expression

$$E_b = \frac{1}{2}[(E' + E'') \pm (E'' - E')]. \tag{37}$$

In this case, $E_b = 1.6 \pm 0.1$ kV/cm.

The proposed method is clearly accurate enough for solving practical problems.

Formulae (18) to (37) can also be used for the analysis of plates which are air-cooled on both sides if D is regarded as the "half-thickness" of the plate.

The method is also applicable to tubular h.f. ceramic insulators with a uniform field if the radius of the tube is large compared with the thickness of the wall. For example, the critical field intensity E_b of the insulators shown in Fig. 1 is found by formulae (34)-(37) and the corresponding thermal breakdown voltage is

$$U_b = E_b l \ [\text{kV}], \tag{38}$$

where l is shortest distance between the insulator electrodes [5].

Sometimes the method can be used for complex problems. For example, Mantrov has applied the thermal analysis of a two-layer plate to the determination of the thermal breakdown voltage of paper-oil capacitors [10].

The temperature drop in the dielectric can be ignored for thin plates and the critical field intensity is then found by the formula

$$E_b = \sqrt{\frac{\lambda (T^* - T_A)}{\eta (T^*) D}} . \tag{39}$$

The formula for the thermal breakdown voltage of small ceramic insulators with a uniform field and a negligible temperature drop is

$$U_b = l \sqrt{\frac{\lambda (T^* - T_A)}{\eta (T^*)} \cdot \frac{S}{V}} , \tag{40}$$

where S is the area of insulator's cooled surface; V the volume of the ceramic part of the insulator; and l the shortest distance between the insulator electrodes.

The thermal breakdown voltage of small capacitors has already been considered elsewhere [11].

Conclusions

1. Given the frequency f, the ambient temperature T_A, a constant coefficient of external heat transfer λ, and a constant coefficient of dielectric thermal conductivity K:

a) the temperature T^* in the plate at breakdown is independent of plate thickness D, the coefficients λ and K and the electrical field intensity at breakdown E_b;

b) the value of T^* is determined solely by the variation of the loss coefficient $\epsilon \tan \delta$ with temperature at the frequency for which breakdown occurs;

c) the maximum temperature $T_{0.b}$ in the plate at breakdown only increases with increasing plate thickness D if D is small. For thick plates, $T_{0.b}$ is practically independent of D and remains less than $2T^* - T_A$ (T_A is the ambient temperature);

d) the temperature $T_{n.b}$ of the cooled surface at breakdown decreases with increasing plate thickness and tends to T_A;

e) the temperature drop between the hottest and coldest regions of a plate increases in proportion to D for thin plates, but for thick plates it is practically independent of D and remains less than $2(T^* - T_A)$;

f) the maximum temperature gradient declines with increasing D and tends to zero;

g) the electrical field intensity E_b at which breakdown occurs

decreases with increasing thickness. For thin plates E_b diminishes roughly in proportion to $1/\sqrt{D}$, but for thick plates $1/D$. It can therefore be assumed that the product of $E_b^2 D$ is constant for thin plates. For thick plates $E_b D$ is a constant;

h) the thermal breakdown voltage U_b of a plate capacitor with cooling via the electrodes increases approximately in proportion to $\sqrt{l}$ if the distance l between the electrodes is short, but if l is large it is independent of the thickness of the dielectric and is a constant, in which case

$$U_b < 4\sqrt{\frac{K(T^* - T_A)}{\eta(T^*)}}; \qquad (41)$$

i) the thermal breakdown voltage U_b of a capacitor with ideally cooled electrodes is independent of l and is the same as that of a very thick air-cooled plate. The value of U_b for an ideally cooled capacitor is such that inequality (41) is fulfilled.

Thus, the thermal breakdown voltage of a plate capacitor has a certain maximum.

2. For a given plate thickness and frequency:

a) the critical intensity E_b increases with increasing value of λ and K and decreases with increasing ϵ and $\tan\delta$;

b) the maximum temperature in the dielectric at breakdown increases with increasing λ and tends to the limit;

c) the temperature of the cooled surface decreases with increasing λ and tends to T_A.

3. A rise in ambient air temperature leads to:

a) an increase in T^*;

b) a reduction in E_b;

c) a lower temperature drop between the hottest and coldest regions of the dielectric; and

d) a reduction in the maximum temperature gradient in the plate.

4. The relationship between the loss coefficient $\epsilon \tan\delta$ and temperature changes with increasing frequency. Therefore:

a) T^* increases with increasing frequency;

b) E_b decreases with increasing frequency, but it can only be assumed as a first approximation that this decrease is in inverse

proportion to the square root of frequency; if it is assumed that E_b does vary in inverse proportion to $1/\sqrt{f}$ at thermal breakdown, it is necessary to acknowledge other mechanisms of breakdown when the breakdown is thermal and the variation of E_b with frequency is not governed by the law $E_b \approx 1/\sqrt{f}$.

5. The theory of thermal breakdown on direct current, in which it is assumed that the conductance γ increases exponentially with the temperature T, leads to the conclusion that the thermal breakdown voltage U_b varies exponentially with ambient temperature T_A, a linear relationship having being predicted between log U_b and T_A in the case when $\gamma = \gamma_0 e^{\alpha T}$ (where α and γ_0 are constants).

For $\gamma = \gamma_1 e^{-b/T}$, the conclusion is reached that log U_b varies roughly in inverse proportion to the ambient temperature. The linear relationship between log U_b and T_A (or $1/T_A$) may not always obtain in thermal breakdown at high frequencies owing to the complex relationship between the loss coefficient and temperature. In such cases the thermal breakdown voltage U_b is calculated by the proposed method and compared with its measured value.

Translated by O.M. Blunn

REFERENCES

1. N.P. Bogoroditskii and I.D. Fridberg; *The electro-physical foundation of high-frequency ceramics (Elektrofizicheskie osnovy vysokochastotnoi keramiki)*. Gosenergoizdat (1958).

2. E.A. Gailish; *Zh. tekh. fiz.*, 7, No. 13 (1937).

3. A.P. Aleksandrov *et al.*, *Physics of dielectrics (Fizika die'lektrikov)*, edited by A.F. Val'ter. Gostekhizdat (1932).

4. V.A. Fok; *Trud. LFTL* (sic), 5 (1928).

5. N.P. Bogoroditskii, Yu.M. Volokobinskii and V.N. Tairov; *Bull. Lenin Electrical Engineering Institute*, No. 60, 3, p. 12 (1960).

6. M.A. Mikheyev; *Foundations of heat transfer (Osnovy teploperedachi)*. Gosenergoizdat (1949).

7. M.V. Kirpichev, M.A. Mikheyev and L.S. Eigenson; *Heat transfer (Teploperedacha)*. Gosenergoizdat (1940).

8. P. Schneider; *Practical problems in thermal conductivity* (*Inzhenernye problemy teploprovodimosti*). Foreign Literature Publishing House (1960).

9. V.T. Renne; *Electrical capacitors* (*Elektricheskie kondensatory*). Gosenergoizdat (1959).

10. M.I. Mantrov; *Vest. elektroprom.*, No. 8 (1953).

11. N.P. Bogoroditskii and V.V. Pasynkov, *Radio electronic materials* (*Materialy v radioelektronike*). Gosenergoizdat (1961).

ABSTRACTS FROM PAPERS PUBLISHED IN ELEKTRICHESTVO No.12, 1961

Leading article

The main problems of the electrical engineering industry in the complete electrification of the country. (pp. 2-6).

This article is essentially a statement of the policy of the U.S.S.R. Electrical Engineering Industry and the various tasks which have to be fulfilled in its various branches.

Amplifiers

Pulse-width modulated power amplifiers using switch transistors. (O.A. Kossov *et al.*, (pp. 69-75).

A pulse-width modulator using symmetrical multi-vibrators with a variable phase shift has been patented in the U.S.S.R. as a general-purpose device for controlling the transistors of the output stage of power amplifiers. Junction-type transistors are used in variable power amplifiers with a reversible output on d.c. and a reversible or irreversible output on a.c. Numerous circuit adaptations are considered in detail. It is claimed to be the simplest and most efficient system of its kind.

Communications engineering

A contribution to the analysis of the input impedances of ladder networks. V.S. Davydov, (pp. 44-49).

The input impedances resulting from the switching "on" and "off" of circuit elements are analysed by a simplified mathematical method for circuits with many elements using recurrence relations.

History of electrical engineering

Mikhail Vasil'evich Lomonosov. (pp. 7-9).

The 250th anniversary of the birth of M.V. Lomonosov, scientist, poet, historian and philosopher, is commemorated.

Power systems

A cost analysis of reactive power compensation at industrial undertakings. N.A. Kazak, (pp. 28-31).

The compensation of reactive power by parallel-connected static capacitors is studied as one aspect of the reduction of active power loss in electrical networks. A cost analysis is made to determine the optimum power and point of installation of the capacitors since it is these factors which determine the expedient reduction in reactive power consumption. The proposed method of analysis is mainly applicable to the planning of new networks at industrial undertakings.

Indices of the quality of voltage stabilization in independent power systems. D.V. Vilesov, (pp. 32-36).

Attention is concentrated on qualitative indices for the a.c. networks of ships, locomotives and aircraft, etc., with a view to finding an objective basis for planning the power supply of individual consumers and independent electrical systems as a whole. Steady-state and transient indices of voltage and frequency stability are considered separately by probability methods and integral characteristics (on the assumption that the processes are non-random).

The use of a modelling device for optimum active load distribution in the Karelian power system. N.G. Zaitsev *et al.*, (pp. 80-83).

The Karelian branch of the U.S.S.R. Academy of Sciences has developed an electronic computer for optimizing the distribution of active loads between two power stations. This equipment has been in use since November 1960 on the southern part of the 110 kV Karelian power system (connected to the Leningrad system). Accuracy to within 2-3 per cent is claimed. General details are given.

Rotating machines

The problem of motor reliability. N.A. Tishchenko, (pp. 16-19).

This is the concluding part of an article published in *Elektrichestvo* 11, 1961. Various measures which can be taken to improve the reliability of motors are considered. An appendix contains technical details of Soviet electrical motors.

An exact equivalent circuit and locus diagram for a solid rotor asynchronous machine. V.M. Kutsevalov, (pp. 50-54).

The normal equivalent circuit is not considered accurate in the study of asynchronous machines with solid rotors when the stator winding resistance is large. An exact equivalent circuit is proposed instead, in which the correcting coefficient is a complex quantity. Very accurate current hodographs are derived.

The effect on small asynchronous motors of impedance asymmetry in the stator circuit phases. L.I. Stolov, (pp.76-80).

The effect is considered of the magnitude and character of asymmetry of the stator circuit phase impedances on various characteristics (losses, starting torque and speed), of small asynchronous motors. It is concluded that a saturable reactor in one phase of the stator circuit is sufficient in certain conditions and that an additional inductive reactance in one of the stator phases causes no appreciably increased loss in asymmetrical conditions.

Voltage multipliers

Inhomogeneous ladder networks for stage-type voltage multipliers. G.A. Vasil'ev, (pp. 54-59).

Stage-type voltage multipliers for super-high voltages are regarded as special ladder networks (fourpole meshes). Inhomogeneous ladder networks refer to meshes made up of different sections when the parameters of each section depend on its (ordinal) number. "Matched" networks are considered in particular, i.e. those loaded by their characteristic impedance. Special attention is paid to circuits with a non-decaying voltage and travelling wave stage multipliers at comparatively low frequencies with small capacitors.

Welding

Welding technology today. B.E. Paton, (pp. 9-16).

Welding techniques are being used in Soviet industry on an exceptionally large scale. Various new welding methods are described and photographs of the equipment are given.

ABSTRACTS FROM PAPERS PUBLISHED IN ELEKTRICHESTVO No. 1, 1962

Leading article

The development of power engineering in the light of the decisions of the C.P.S.U. I.A. Syromyatnikov, (pp. 1-6).

An authoritative study is made of long term investment in hydro-electric and coal-burning power station equipment and the national grid to achieve the communist party's programme of complete electrification of the U.S.S.R.

Circuit theory

Analysis of transients in complex Circuit with several non-linear elements. A.F. Berezovskii, (pp. 73-75).

The author combines a graphical-analytical method, based on the substitution of the definite integral by an approximate sum using the trapezoidal formula, with iteration methods, in order to analyse transient behaviour in complex circuits with several non-linear elements. An example is given.

Control engineering

Automation of multi-motor drives. Yu.M. Fainberg, *et al.*, (pp. 25-29).

The author seeks to formulate a general method of selecting the best type of control system to maintain a specified relationship between the speeds of motors in large automated electric drives. A comparative analysis is made of the results of various control systems. The proposed method is illustrated in reference to continuous rolling mills.

A computer study of control system reliability. I.R. Freidzon, (pp. 36-39).

Using the control system of a ship as an example, the author describes a method of analysing the reliability of the control system in its various possible fault conditions by mathematical simulation on a computer. It is proposed to incorporate search elements in control systems which would discover the fault and switch off the system, or eliminate the fault, before damage can be done.

The theory and practice of optimalizing control. A.A. Fel'dbaum, (pp. 39-44).

A general study is made of the criteria of optimalcy and optimalizing control systems.

Impulse testing

A small impulse generator. F.F. Lange *et al.*, (pp. 58-60).

The Lenin All-Union Electrical Engineering Institute has developed a series of three small 1000-1500 kV impulse generators which are of special interest in switchgear testing. They also feature a low internal resistance. Their general details are:

Height for 3 MV, metres		Base dimensions, metres	Energy per unit of volume kW. sec/m3	Voltage gradient, kV/m
1	10.8	0.125	11.1	280
2	3.9	1.15 × 0.57	5.90	770
3	5.85	0.93 × 0.84	3.3	515

Magnetism

The stability of magnetic systems with intra-frame magnets and the calculation of their temperature coefficient. A.V. Mitkevich *et al.*, (pp. 69-73).

To solve the problem of reliability for instruments and electrical gear having permanent magnets, the authors study the relationship between the stability of the gap flux in magnetic systems on the one

hand and the properties of the magnet, the design of the system and the magnetic and temperature stabilization of the system on the other. The article is based on an analysis of eighty systems using magnico magnets and magnico with an 0.5 or 2 per cent titanium content.

Measurement

The measurement of impedance by a "Three meter" system. V.E. Kazanskii, (pp. 81-82).

It is considered that the "two-meter" method of measuring impedance by an ammeter and voltmeter with a correction formula is inapplicable to a.c. circuits. In the proposed "three-meter" system, two ammeters and one voltmeter, or two voltmeters and one ammeter are used, depending on the magnitude of the impedance. The advantage is that the results of the correction formula no longer depend on the impedance of the meters. The system is largely confined to linear impedances.

Power systems

Economic distribution of active power in a mixed power system. I.M. Markovich *et al.*, (pp. 10-11).

A general method is proposed for solving the problem of economic distribution of active power in power systems consisting of coal-burning and hydro-electric power stations with network losses included. The method is based on Lagrange's method of indefinite multipliers.

Determination of the most economical number of connected generator sets. K.A. Smirnov, (pp. 12-15).

The most economical number of connected generator sets in power systems containing coal-burning power stations is considered in the light of changes in network losses, using a method of marginal analysis.

A quantitative estimate of voltage quality in distribution networks. F.F. Karpov, (pp. 16-21).

Using probability methods, a study is made of the duration of deviations from rated voltage in distribution networks. It is considered that the maintenance of continuity for the main consumers at the expense of increased voltage deviations for small numbers of remote non-priority consumers is economically justified from the national

point of view.

The efficiency of series capacitors for the compensation of voltage losses in mine distribution networks. V.G. Bauman *et al.*, (pp. 21-25).

It is argued that the use of series capacitors in large mine networks helps to reduce voltage losses considerably and the system should always be considered.

Rotating machines

Determination of synchronous machine frequency characteristics. N.I. Sokolov *et al.*, (pp. 29-35).

It is considered that the analysis of electromagnetic and electromechanical behaviour has hitherto been based on data corresponding to idealized machines having no more than two discrete rotor circuits along the direct axis and one in the transverse axis. An equivalent circuit is derived for synchronous and asynchronous machines containing many circuits which correctly describes behaviour over a wide range of slip variation. The equivalent circuit can be used for computer studies.

Short-circuit currents in variable speed generators. I.Z. Ageyev, (pp. 45-48).

The author considers (1) the effect of commutating section m.m.f. and brush displacement on the magnitude of the short-circuit current, (2) steady state short-circuit conditions in machines with the full number and half the number of compoles, (3) the characteristics of short circuits in generators without compoles and (4) the tuning of commutation from the short-circuit characteristic.

An electrostatic generator with a rotating cylinder and hydrogen insulation. N.J. Felici, (pp. 63-69).

The author considers that engineering circles in most countries are mistaken in ignoring "electrostatic electromechanics" for which great prospects are claimed. The author follows up articles in the German and French technical press with a detailed survey of electrostatic cylindrical generators using pure hydrogen for use in industry.

Determining the output of motors with a random load. M.A. Dukhovnyi *et al.*, (pp. 75-79).

Probability methods are applied to determine the power of small and medium motors with random fluctuating loads.

Radioactive radiation

Sulphur-cadmium semiconductor γ-radiation detectors. N.G. Drozdov *et al.*, (pp. 49-51).

The authors consider the volt-ampere characteristics, sensitivity, inertial properties and stability of CdS detectors. Their practical use in dosimetry and as γ-relays in automatic control devices appears to be assured in spite of their considerable inertia.

Switchgear

Controlled arresters. S.A. Smirnov *et al.*, (pp. 52-54).

In 1959 the authors patented three types of "triggered" sparkgap which it is claimed can be used for the commutation of large impulse currents at high repetition rates without breakdowns due to the high intensity of the electrical field in the gaps of the discharger in the period between operations. Tests indicate their value in high voltage gear for switching very large currents.

Sparkgap unit for 500 kV magnetic rotating-arc arresters with 100% recovery strength. G.V. Bugkevich *et al.*, (pp. 55-58).

A new sparkgap unit is described for use in magnetic rotating-arc arresters for combined protection from internal surges and lightning strokes on 500 kV transmission lines. These arresters are described in an article translated in this journal from Elektrichestvo 4, 1960. The new improved sparkgap unit has a higher relative recovery strength.

The use of Hall Effect detectors for oscillographing large a.c. currents in switchgear tests. I.B. Bolotin, (pp. 79-80).

Germanium and mercury selenide Hall e.m.f. "pickups" have been

successfully used without capacitors for oscillographing large a.c. currents in laboratory switchgear tests in place of steel- and air-cooled current transformers and shunts.

Traction

The World's longest electrified railroad, Moscow-Baikal. N.A. Lomagin, (pp. 7-9).

General details are given of the recently completed electrified stretch of the Trans-Siberian railway between Moscow and Lake Baikal (approx. 5500 km) with special emphasis on achievements in the electrical construction work.

Revision of the regulations for the corrosion protection of metal structures CN-28-58. D.B. Lomazov, (pp. 60-63).

Plans have been made to revise and enlarge the regulations governing the protection of metal structures from corrosion. The author lists and briefly considers nineteen points which he recommends for further study as regards structures laid underground in electrical traction systems.

ABSTRACTS FROM PAPERS PUBLISHED IN ELEKTRICHESTVO No. 2, 1962.

Capacitors

The reliability of ceramic capacitors of large reactive power. A.T. Alad'ev, (pp. 30-32).

This paper gives the results of Soviet research into the effect of operating conditions and the surrounding medium on the reliability of industrial ceramic capacitors of large reactive power. It is argued that the operational reliability of capacitors can be predicted from the estimated life of the dielectric.

Control engineering

An analysis of schemes with transformer electrical machines by vector diagrams. V.A. Atsyukovskii, (pp.61-63).

The processes taking place in such machines as selsyns and sine-cosine rotary transformers are studied by a combination of vector diagrams. It is shown that a smooth functional relationship can be obtained between the input and output axles of various devices.

Electric furnaces

A method of analysing non-symmetric three-phase circuits in electric arc furnace installations. N.A. Markov *et al.*, (pp. 33-37).

It is considered that the existing graphical-analytical methods of analysing non-symmetric three-phase circuits in electric arc furnaces fail to include the differences in mutual inductance between the individual phases. A general analytic method is proposed on condition that the arc voltage is constant.

Electrical steel

The effect of various elements on the properties of electrical steel. G.A. Garnyk *et al.*, (pp. 71-74).

It has been established that the silicon content of cold-rolled electrical steel can be increased to 6 per cent without it becoming brittle by obtaining the molten steel with an 0.01-0.02 per cent carbon, 0.003 per cent oxygen content and an 0.004 per cent nitrogen content in an induction vacuum furnace. For mass production the molten steel is treated in ladles under vacuum.

Measurement

An oscillographic device for measuring the dynamic magnetization curve of ferromagnetic materials.

Symmetric hysteresis loops are produced on the oscillograph screen by electronic amplitude modulation of the magnetizing sinusoidal current. The brightness of the beam of the oscillographic indicator is modulated and "brightening" pulses are supplied at the instant the current passes through maximum. Accuracy is to within 5 to 6 per cent, but the method is very quick.

Power systems

Special characteristics of automatic field control for generators at stations feeding two power systems. G.V. Mikhnevich, (pp. 1-5).

It is considered that a simple generator-bus equivalent network is inadequate for the study of the stability and quality of transient phenomena in a complex power system in which the generators are equipped with high-response controllers. The results of an investigation of generators operating into two power systems are given.

Reducing the unbalance with two phases open by means of shunt capacitors. N.A. Mel'nikov, (pp. 10-14).

This paper is based on the proposition that the symmetry of a line with two phases open can only be attained by devices which represent an additional load such as the installed banks of static capacitors for compensating the power factor in normal symmetrical conditions.

A mathematical study is made of the limitation imposed by inadequately high negative sequence voltages and currents.

Relays and protection

The principles of earth fault protection responding to transient phenomena. I.N. Popov, (pp. 14-19).

It is considered that earth fault protection utilizing transient electrical quantities is expedient for many electrical systems in which the direction of the fault and the fault sections are determined by the first indications of signal relays which are communicated to the despatcher manually or telemechanically.

Prospects for the application of cybernetics in the theory of the relay protection of power systems. O.V. Mamontov, (pp. 6-10).

The author broadly indicates how methods of engineering cybernetics (as expounded by Wiener and in Automatic Control and Computer Engineering, Ed. V.V. Solodovnikov, currently being published by the Pergamon Institute) can be applied successfully to the formulation of a comprehensive classification and generalized theoretical method of analysis for the electronic protection of power systems. Special amphasis is laid on the theory of games.

Aspects of the behaviour of carrier protection on 400-500 kV lines during transients. S.B. Losev, (pp. 20-26).

After an analysis of primary quantities, the author elaborates on the transient behaviour of Soviet carrier protection for 400-500 kV transmission lines and considers the appropriate type of filter. The use of a "compensation resistance" is advocated with the frequencies transmitted by the tuned circuits of the operating and polarizing circuits of the relays included as well as the capacitive current of the line at supply frequency.

Rotating machines

Variable d.c. machines with permanent magnets and asymmetrical poles. L.M. Polastin *et al.*, (pp. 48-51).

Much scope is claimed for variable d.c. motors and generators with

asymmetrical poles. This claim is based on a series of tests which are described.

The stability of a hydro-electric generator with electric braking. D.E. Trofimenko, (pp. 27-30).

This paper gives an account of analytical investigations into the dynamic stability of a hydro-electric generator with "multi-cycle" electrical braking. Attention is concentrated on the optimum method of controlling the braking for several cycles of swinging. It is claimed that the proposed system is superior to "single-cycle" braking and high-response automatic reclosure.

Hetero-polar polyphase inductor machines. N.N. Levin *et al.*, (pp. 52-55).

Hetero-polar polyphase inductor machines with twin-tooth windings can often be used in electrical drives in synchronous and asynchronous conditions. Special attention is paid to the minimum machine constant.

The heating of solid rotors in synchronous motors on starting. O.V. Livanova *et al.*, (pp. 56-58).

It is calculated by a graphical method that it is safe to start a synchronous motor with a solid rotor at a voltage at least 70 to 80 per cent of the rated voltage. The voltage drop in the reactances of the supply line and transformer is sufficient in some cases for direct starting from the network without special starting reactors.

The e.m.f. due to the leakage fluxes in an armature with double set of brushes. I.M. Sadovskii, (pp. 59-60).

A study is made of the process whereby the e.m.f. is induced in electrical machines with longitudinal and transverse brushes, e.g. amplidynes with a transverse field.

Switchgear

Controlling the damping of the test recovery voltage. S.M. Krizhanskii, (pp. 43-47).

The author considers the main requirements which have to be met in

order to determine the shape of the test recovery voltage curve and compares the conditions of rupturing capacity tests on circuit breakers for various shapes of the curve for a single-frequency recovery voltage. It is argued that data of the conditions of voltage recovery in actual systems are required before any test method can be recommended.

Operating experience with tungsten-based cermet contacts in large circuit breakers. O.K. Teodorovich *et al.*, (pp. 64-68).

The authors strongly advocate the coating or building-up of copper and brass contacts with a tungsten-copper tip. The shape of the circuit-breaker contacts is important and this is illustrated by a drawing.

The volt-ampere characteristics and carrying capacity of non-linear "Tervite" resistors for surge arresters. V.I. Pruzhinina-Granovskaya *et al.*, (pp. 74-77).

This paper describes the electrical properties of a substance called "tervite" which is now being used in place of vylite for the non-linear resistors of surge arresters and combined surge and lightning arresters on super-high voltage transmission lines etc. Tervite features such stability and humidity resistance that it is also used in a.c. and d.c. gear for limiting surges without sparkgaps.

Traction

The design of tramway networks. D.B. Lomazov, (pp. 38-43).

The author reviews the standards laid down for the voltage drop in the rail networks of tramway systems in various countries. It is argued that no general standards can be laid down and a method is proposed whereby the best system for a particular case can be calculated.

ELEKTRICHESTVO

Editor-in-Chief: N. G. DROZDOV

EDITORIAL BOARD

ELECTRIC TECHNOLOGY, U.S.S.R.

1961 VOLUME 4

CONTENTS

Printed in Great Britain by Pergamon Printing & Art Services Ltd., London